NASA CONTRACTOR REPORT

NASA CR159850

(NASA-CR-159850) EXTERNAL FUEL VAPORIZATION STUDY, PHASE 1 (United Technologies Corp.) 133 p HC A07/MF A01 CSCL 21D

N80-25453

Unclas
G3/28 22343

External Fuel Vaporization Study

Phase I Report

By E.J. Szetela
L. Chiappetta

PREPARED BY
UNITED TECHNOLOGIES RESEARCH CENTER
EAST HARTFORD, CT 06108

FOR
NATIONAL AERONAUTICS AND SPACE ADMINISTRATION
LEWIS RESEARCH CENTER

JUNE 1980

NASA CONTRACTOR REPORT

NASA CR159850

External Fuel Vaporization Study

Phase I Report

By E.J. Szetela
L. Chiappetta

PREPARED BY
UNITED TECHNOLOGIES RESEARCH CENTER
EAST HARTFORD, CT 06108

FOR
NATIONAL AERONAUTICS AND SPACE ADMINISTRATION
LEWIS RESEARCH CENTER

JUNE 1980

FOREWORD

This report describes the results of a study of external fuel vaporization for use in advanced gas turbine engines. The effort was conducted at the United Technologies Research Center under sponsorship of the National Aeronautics and Space Administration, Lewis Research Center. The NASA Program Manager was C. E. Baker and the UTRC Principal Investigator was E. J. Szetela. Many consultants participated in this program; in particular, the authors wish to thank H. M. Craig, W. M. Brown, E. F. Cole, D. R. Weisel, G. J. Sturgess, W. B. Wagner, J. M. Tringali, and D. Sadowski of PWA/CPD, J. A. Saintsbury and P. J. Brine of PWA of Canada, Ltd., and R. Conrad of Parker Hannifin Corp.

External Fuel Vaporization Study

TABLE OF CONTENTS

TABLE OF CONTENTS (Cont'd)

External Fuel Vaporization Study

SUMMARY

A conceptual design study was conducted to devise and evaluate techniques for the external vaporization of fuel for use in an aircraft gas turbine with characteristics similar to the Energy Efficient Engine (E^3). In the study, three vaporizer concepts were selected and they were analyzed from the standpoint of fuel thermal stability, integration of the vaporizer system into the aircraft engine, engine and vaporizer dynamic response, startup and altitude restart, engine performance, control requirements, safety, and maintenance.

Three vaporization schemes were investigated. In Scheme 1 a small amount of engine fuel is burned with compressor bleed air in an auxiliary liquid-fueled burner to create hot gas for use on the hot side of a heat exchanger. The fuel is heated as a liquid at high pressure and vaporization is accomplished by flashing across a throttle. In Scheme 2, heat for fuel vaporization is derived from turbine cooling air and the combustor walls. In Scheme 3, an auxiliary burner is used to create a hot gas into which the engine fuel is injected, vaporized, and mixed with the hot gas to produce a very fuel-rich mixture having an equivalence ratio of approximately 10.

The results of the study indicate that Schemes 1 and 2 would offer improvements in performance relative to the baseline E^3 engine; that is, with a fixed engine core size, reductions in specific fuel consumption of nearly one percent, increases in thrust of up to 10 percent, and increases in thrust/weight ratio of over 3 percent were predicted. The use of Scheme 3 would result in a small decrease in engine performance. The use of Schemes 1 or 2 would pose a maintenance problem because of deposits of pyrolysis products on vaporizer internal surfaces. It was calculated that the deposits would have to be removed every 100 hours of operation. Schemes 1 and 3 have auxiliary burners which can be used for ground startup and altitude relight. Fuel vaporization in Scheme 2 on startup can only be accomplished if special components are added for that purpose. The response of Schemes 1 and 3 to demands for power changes is predicted to be reasonably rapid, while the transient response of Scheme 2 appears to be unacceptable. Although the weight of the components in Scheme 1 is predicted to be greater than Scheme 3, and maintenance of Scheme 1 would be more costly because of deposit formation, the current need for reduced fuel consumption and the potential of Scheme 1 to provide substantial improvements in engine performance weighed heavily in the selection of Scheme 1 for detailed study in this program.

LIST OF FIGURES

LIST OF TABLES

INTRODUCTION

Lean premixed/prevaporized (LPP) combustion is a technique for reducing flame temperature and luminosity, thus providing the potential for improving combustor durability, reducing the airflow required for combustor wall cooling, and reducing NO_x emissions. Catalytic combustion promises the same benefits along with the potential of greater combustor stability and additional emissions reductions. A particular problem with LPP or catalytic combustion is the fuel prevaporization requirement. Premixing ducts must be sufficiently long to permit droplet vaporization to occur and at the high pressures and temperatures that exist in high performance engines like the NASA Energy Efficient Engine (E^3), the use of excessively long passages may result in autoignition upstream of the flame stabilizer. A potential solution is to provide a fuel vaporizer which is external to the premixing duct. Thus, premixing ducts need only be long enough to achieve the desired fuel distribution. Heat for the fuel vaporization process can be taken from the combustor inlet air, from the hot products of combustion or from the heat released in a special burner which is fed by a small quantity of engine fuel. The fuel vaporizer can be located outside of the combustor case, or it can be made an integral part of the combustor itself. In any case, an attractive feature of an external vaporizer is that it decouples the fuel vaporization process from the mixing process and permits the use of shorter premixing passages to reduce the problem of autoignition.

A major factor entering the consideration of fuel vaporization is the propensity for solid deposit formation on hot walls in the presence of hydrocarbon fuels. Deposit formation with Jet-A is common above 500 K whereas fuel must be heated to 680 K at some conditions to assure complete vaporization. Deposit formation, deposit removal, and approaches for operating without deposits must all be carefully evaluated in an investigation of external fuel vaporization.

The objective of this study was to select several external vaporizer concepts and conduct a feasibility study using these concepts. The study dealt with problems associated with the thermal stability of the fuel as well as with problems associated with the integration of the entire vaporizer system in the aircraft engine. The results of the study were used to evaluate the potential of external fuel vaporization as applied to LPP or catalytic combustion systems, to identify areas where design data are meager or lacking, and to identify promising directions for future effort.

EXTERNAL FUEL VAPORIZER SCHEMES

During the program, an evaluation was made of three separate concepts, which encompassed basic approaches and alternatives as follows:

	Basic Approach	Alternative
Hardware	All major components separate from the engine	Some components integral with engine components
Fluid State	Two-phase flow in the heat exchanger	Single-phase flow in the heat exchanger followed by flash vaporization
Deposit	Heat exchanger requires frequent cleaning	Potential for vaporization without deposits

The three concepts which were designated Schemes 1, 2 and 3 were devised, investigated, and evaluated during a major portion of the program. The three schemes are represented by the schematic diagrams in Fig. 1. During the evaluation, they were compared in several categories including engine performance, weight, complexity, engine startup, dynamic response during power changes, and maintenance. One scheme was selected for further refinement during the completion of Phase 1 of the program.

The operation of the three schemes will be described in this section together with a brief description of the components and their functions; operating details will be discussed in a later section. The governing premise considered in the design of the hardware is a 100% vaporization of the fuel at the injector inlet because a two-phase fluid at that location could result in phase separation, injector streaking, and hence deterioration of the performance of the main combustor.

Thermodynamics Processes

The fuel vaporization process in a high pressure ratio engine varies with the engine power setting and the selected process (flash vaporization or two-phase heating). The process is illustrated in Fig. 2.

EXTERNAL VAPORIZER SYSTEM CONCEPTS

SCHEME 1 — SEPARATE UNIT — FLASH VAPORIZATION

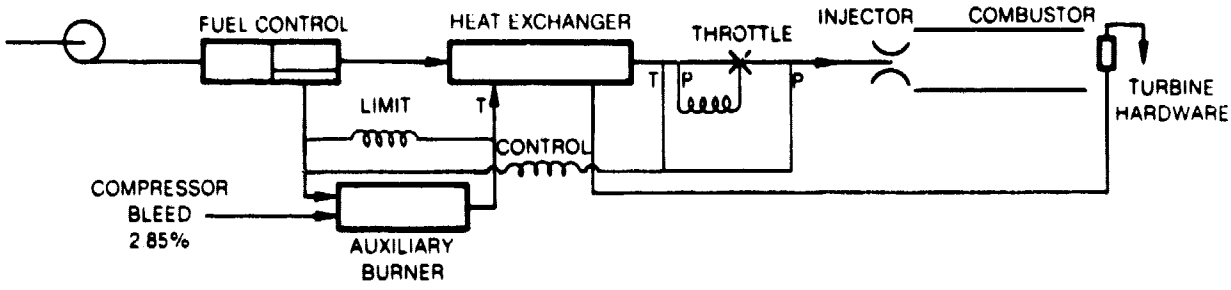

SCHEME 2 — ENGINE HARDWARE UNIT — TWO-PHASE

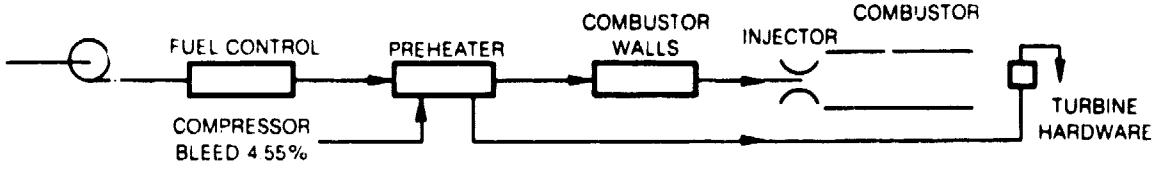

SCHEME 3 — THERMAL OXIDATION GASIFIER — TWO PHASE

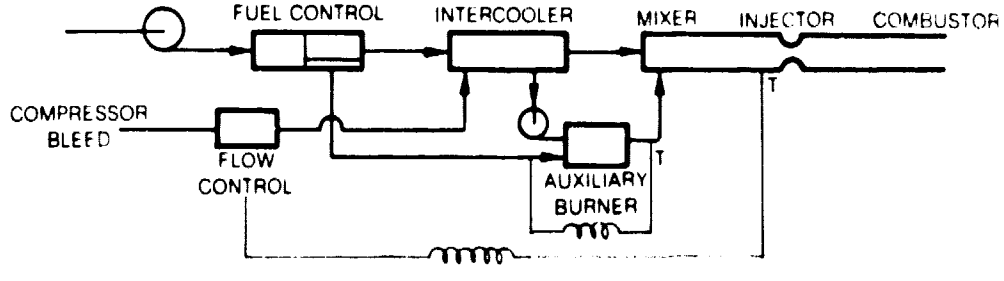

79 11-24-1

FIG. 2

FUEL VAPORIZATION PROCESS

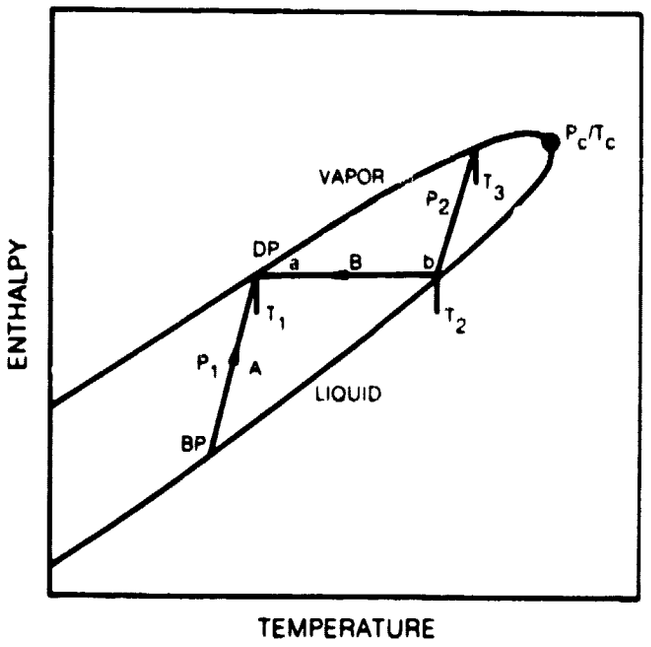

If the fuel injector pressure is P_1, it is necessary to reach the junction of the vapor curve and the constant pressure line P_1 in Fig. 2. This can be accomplished by following path A, which represents two-phase heating, or path B, which represents flash vaporization. Along path A, the fuel is heated first as a liquid until its temperature reaches the bubble point (BP), and then as a two-phase mixture until its temperature reaches the dew point (DP). Along path B, the fuel is heated as a liquid to the junction made by the liquid line and a horizontal line passing through the dew point. This junction defines the required fuel pressure, P_2, and temperature for flash vaporization. After heating, the fuel is passed through a throttling orifice. Throttling with adiabatic conditions is a constant enthalpy process which results in conditions corresponding to point a downstream of the throttle. The pressure drop across the throttle is (P_2-P_1) and the temperature drop is (T_2-T_1).

The example cited is somewhat idealized because the process requires a precise control of conditions at point b. For instance, if the upstream throttle pressure is P_2 and the temperature is between T_2 and T_3, the fuel is in a mixed phase, a condition which is to be avoided by the selection of the flash vaporization process. The two phase state can be avoided throughout the fuel vaporization system by meeting two simple conditions. The fuel will always be a liquid in the heat exchanger if the pressure upstream of the throttle is maintained at P_c (critical pressure) or greater. An exception to this statement is retrograde condensation, a condition described in Ref. 1 which is peculiar to liquid mixtures. Retrograde condensation can be avoided by raising the pressure slightly above P_c. Having met that condition, it is then only necessary to heat the fuel to a temperature T_2 or greater for complete vapor to be specified by thermodynamic equilibrium in the fuel manifold. The special condition where P_2 is equal to or greater than P_c requires that T_2 is equal to or greater than T_c.

If the fuel injector pressure is equal to or greater than P_c, there is no phase distinction between the liquid and vapor in the fuel even if the fuel temperature is less than T_c (see Fig. 2). However, the treatment of phase behavior in the vicinity of critical points given in Ref. 1 indicates that a phase distinction does occur in the presence of a non-condensible gas such as air when the fuel temperature is less than T_c. To eliminate the phase distinction in air, it is necessary to heat the fuel to its critical temperature T_c. Because the pressure in the combustor could be above the critical pressure of the fuel at the engine Sea- vel Take-Off condition (SLTO), which is the external vaporizer design point, the vaporization system was designed to heat the fuel to its critical temperature.

Scheme 1

The vaporization system in Scheme 1 uses a heat exchanger and throttle (Fig. 1). The fuel is in its liquid phase in the heat exchanger where it is heated to a temperature above its dew point. Upon throttling, it is flashed to its vapor state at its dew point. At some conditions, the pressure of the fuel is considerably above its critical pressure because even the burner pressure is above the critical pressure of the fuel. At those conditions, the fuel is heated to its critical temperature and the throttle is kept in a wide-open position.

The heat source in the heat exchanger consists of the products of combustion of a small amount of fuel (a maximum of 1.4 percent of the engine fuel flow), with 2.85 percent of the compressor airflow which is bled from the high pressure exit of the compressor into an auxiliary burner. The hot gas flows in a direction which is opposite to the direction of the fuel (counterflow) for maximum heat exchanger performance. The hot side gas exit temperature is below the compressor bleed temperature and it can be used for turbine cooling.

The main engine fuel control is located in the cold fuel stream where it is minimally affected by the fuel vaporizer. Additional controls are needed as shown. The throttle valve position is adjusted to obtain the proper inlet fuel pressure. The auxiliary burner fuel flow is adjusted to assure that the combination of throttle inlet temperature and throttle exit pressure produces fully vaporized fuel at the fuel injector.

Scheme 2

The vaporizer in Scheme 2 is the main engine combustor wall which is cooled by the fuel undergoing a phase change (Fig. 1). A preheater is used as a supplementary heat source and the compressor bleed air on the hot side of the preheater is sufficiently cooled to improve its turbine cooling capability. The main engine fuel control functions exactly as it does in a conventional engine and no other controls are required for this scheme.

Scheme 3

The fuel is vaporized in Scheme 3 by direct, rapid mixing with a hot gas which consists of the products of combustion produced by an auxiliary burner (Fig. 1). The overall equivalence ratio is maintained considerably above stoichiometric and with proper design, the mixing is sufficiently rapid to promote vaporization. Deposit formation can be minimized or avoided if the residence time in the mixer is minimized. Justification for this premise is the work on partial oxidation of rich mixtures described in Refs. 2 and 3 and the deposit-free vaporization of rich fuel-air mixtures reported in Ref. 4.

Because compressor bleed air is returned to the upstream side of the main combustor, a boost pump is needed to overcome the losses in the bleed flow control, the intercooler, the auxiliary burner, and the mixer. The intercooler is used to reduce the horsepower absorbed in the drive system of the boost pump.

LITERATURE SURVEY

A literature survey was conducted as part of the program in order to obtain the best available information regarding the properties of Jet-A fuel, including thermodynamic and thermal stability data, and heat exchanger design principles covering single phase and two-phase fluids. The literature survey was conducted mainly by computerized retrieval from the files of the Lockheed DIALOG and the Dept. of Energy RECON collections. The DIALOG files that were searched included NTIS, Engineering Index, ISMEC (Institute of Mechanical Engineers), and Chemical Abstracts. A number of bibliographies from documents and text books obtained through the retrieval were also searched. Additional searches were conducted in the published papers of the International Heat Transfer Conference, Advances in Heat Transfer, and the ASME Journal of Heat Transfer. Personal files of UTRC workers in the field of fuel deposit formation were also reviewed. Approximately 3000 citations were examined during the survey and about 150 were found to be informative.

The literature search produced typical properties of Jet-A such as the distillation data and specific gravity. These properties were used in correlation procedures that produced additional fuel properties needed in equations for heat transfer and pressure drop. These equations, which were produced in the search, covered various operational states as follows:

Flow conditions: laminar, transitional, turbulent
Fluid conditions: subcritical, supercritical
Fluid states: liquid, two-phase, vapor

Typical fuel deposit formation rate data at various temperatures were obtained from the literature search. Although velocity, wall material, and fluid state are expected to influence deposit formation, insufficient data exist to quantify the effects of those variables. Also obtained from the survey were air-side properties for tubular heat exchangers, including data for finned tubes and plain tubes in various tube sizes and with various axial and transverse tube spacing.

A summary of the literature survey is included as Appendix A.

FUEL PROPERTIES

The fuel properties that were used in the vaporizer design calculation were either obtained from published sources or calculated by standard procedures. A list of the properties considered and the data source utilized for the various analyses is contained in Table 1 below.

Table 1
FUEL PROPERTY USES AND SOURCES

Property	Use	Reference
Distillation	Identify bubble point and dew point and other property determinations	5 & 6
Enthalpy-Temp Diagram	Determine fuel heating requirements	8 & 9
Specific Gravity	Pressure loss equation and other property determinations	5 & 7
Viscosity	Heat transfer and pressure loss equations	7 & 8
Thermal Conductivity	Heat transfer equations	7 & 8
Specific Heat	Heat transfer and pressure loss equations	7 & 8

This section contains a description of the methods used to obtain the fuel properties together with curves showing the properties that were used in the calculations.

Distillation Data

Three distillation procedures, ASTM D86, TBP (True Boiling Point) and EFV (Equilibrium Flash Vaporization) are described in Ref. 9. They must be used with care because none of them fit the full boiling range in the external fuel vaporization process in which the liquid is in equilibrium with all of the vapor produced in the heat exchanger. ASTM D86 distillation is carried out with continuous removal and condensation of vapor; because the vapor is removed from the system in this method, the final boiling point is of no value to the external fuel vaporization problem. A TBP distillation is performed with physical separation of a large number of fractions and neither the initial nor the final boiling point are pertinent. A EFV distillation is done with liquid in equilibrium with vapor but the initial boiling point is in error because it is not measured until considerable

vapor has been produced. A plausible approach to obtaining boiling point data for the external fuel vaporization process is the use of ASTM D86 for the initial boiling point, sometimes called the bubble point, and EFV for the final boiling point, or dew point.

ASTM D86 distillation data obtained from Ref. 1 for Jet-A at one atmosphere are shown in Fig. 3. The maximum, average, and minimum temperature curves at one atmosphere are representative of 30 samples of fuel. The average curve was converted using procedures found in Ref. 6 to an EFV curve which is shown in Fig. 4. Ref. 7 contains a procedure for extrapolating EFV curves obtained at one atmosphere to higher pressures and this procedure was used to obtain the remainder of the curves in Fig. 4. The procedure used to extrapolate the one atmosphere ASTM D86 curves higher pressures was formulated from the methods of Ref. 9.

The data points at the extreme left ends of the curves in Fig. 3 are considered to represent the bubble points of the fuel. (The bubble point, which is usually referenced as a temperature, is also called the vapor pressure when reference is made to the pressure.) The data points at the extreme right ends of the curves in Fig. 4 are considered to represent the dew points of the fuel. The bubble points and dew points are shown in Fig. 5.

Enthalpy-Temperature Diagram

The boundary of the enthalpy-temperature diagram shown in Fig. 6 is a composite of vapor enthalpy and liquid enthalpy curves calculated by the procedures contained in Ref. 7. The liquid enthalpy curve is in agreement with the data contained in Ref. 8. The curves intersect at the critical point of 21.7 atm and 680 K which was calculated by the methods of Ref. 7.

Two other sources were used to derive critical values. It was found that the method of Ref. 10 gave a 1.5 atm higher pressure and a 6 K lower temperature than the method of Ref. 7 while the method of Ref. 11 gave a 0.3 atm lower pressure and an identical temperature. The constant pressure vaporization lines were constructed by connecting with a straight line each bubble point on the lower liquid line to its corresponding dew point on the upper vapor line. These lines represent the thermodynamic path for a constant pressure vaporization process. These lines were subdivided into fraction of vapor quality shown in Fig. 6 by a graphical process in which the data of Fig. 4 and 5 are used to obtain the "true" curve in Fig. 7. The "true" curve of temperature vs. percent vaporized is arbitrarily assumed to have the same general shape as the EFV curve and the bubble point (BP) is assumed to be equal to the initial point of the ASTM D-86 curve

FIG. 3

ASTM D86 DISTILLATION FOR JET-A FUEL

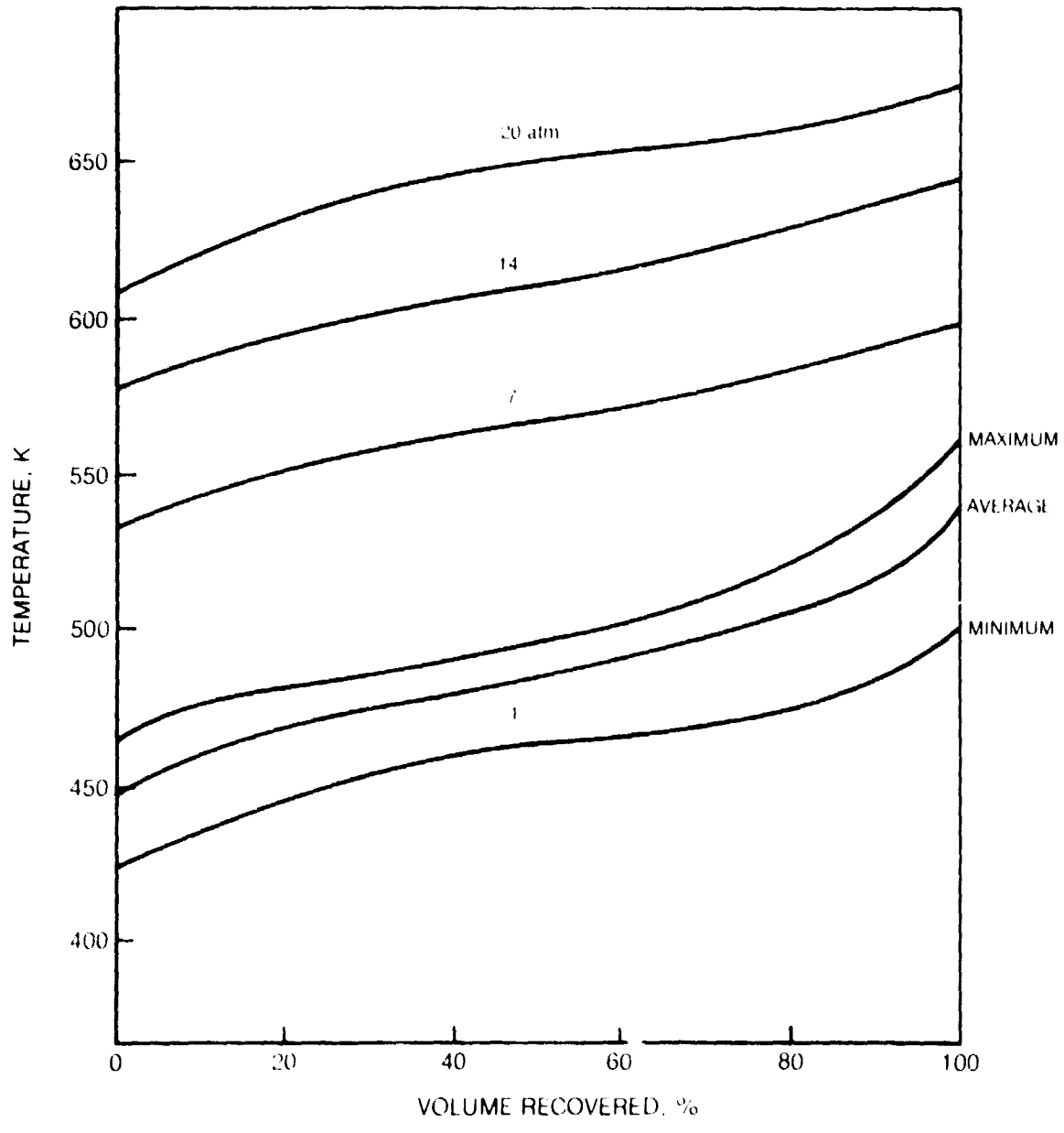

80-2-71-6

FIG. 4

EQUILIBRIUM FLASH DISTILLATION FOR JET-A FUEL

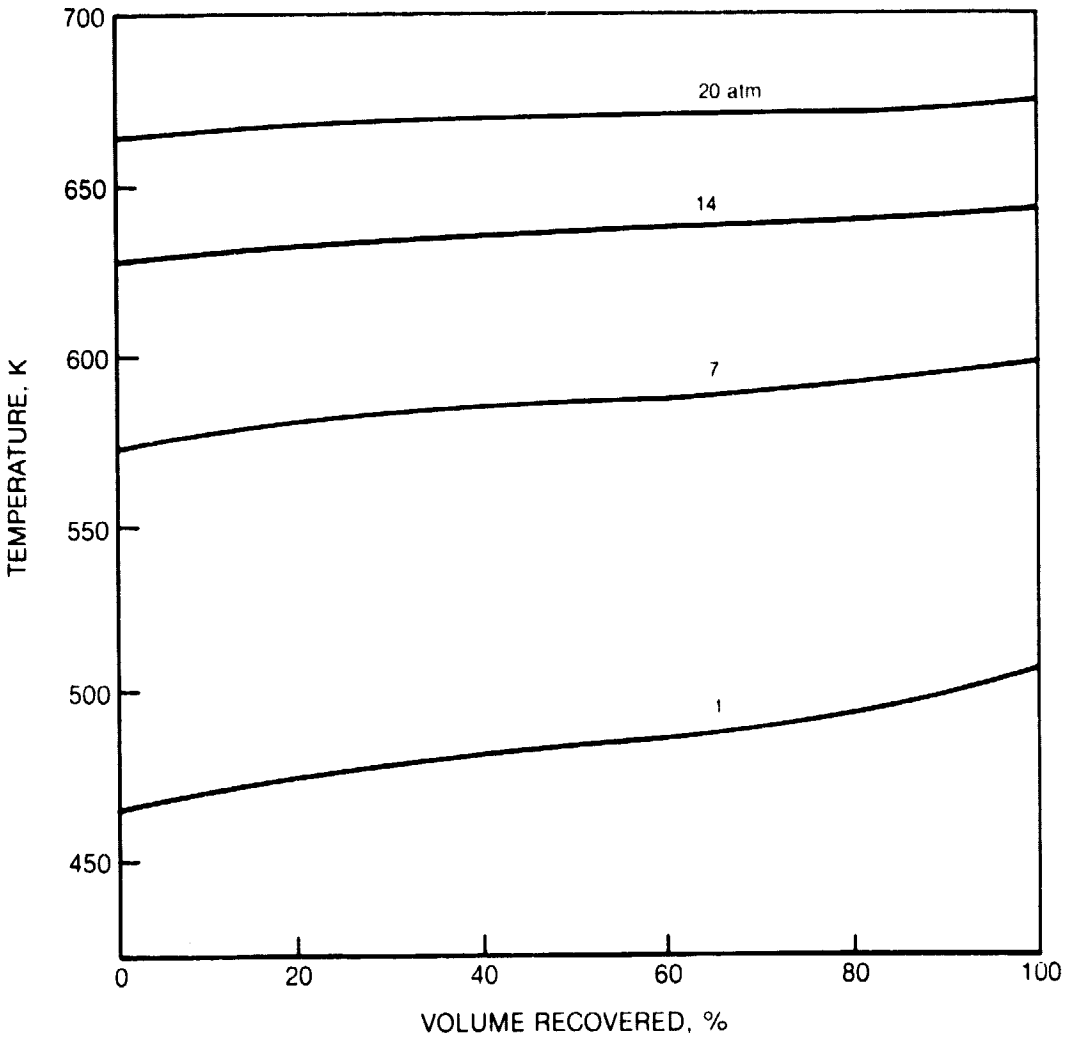

80-2-71-7

FIG. 5

BUBBLE POINT AND DEW POINT OF JET-A

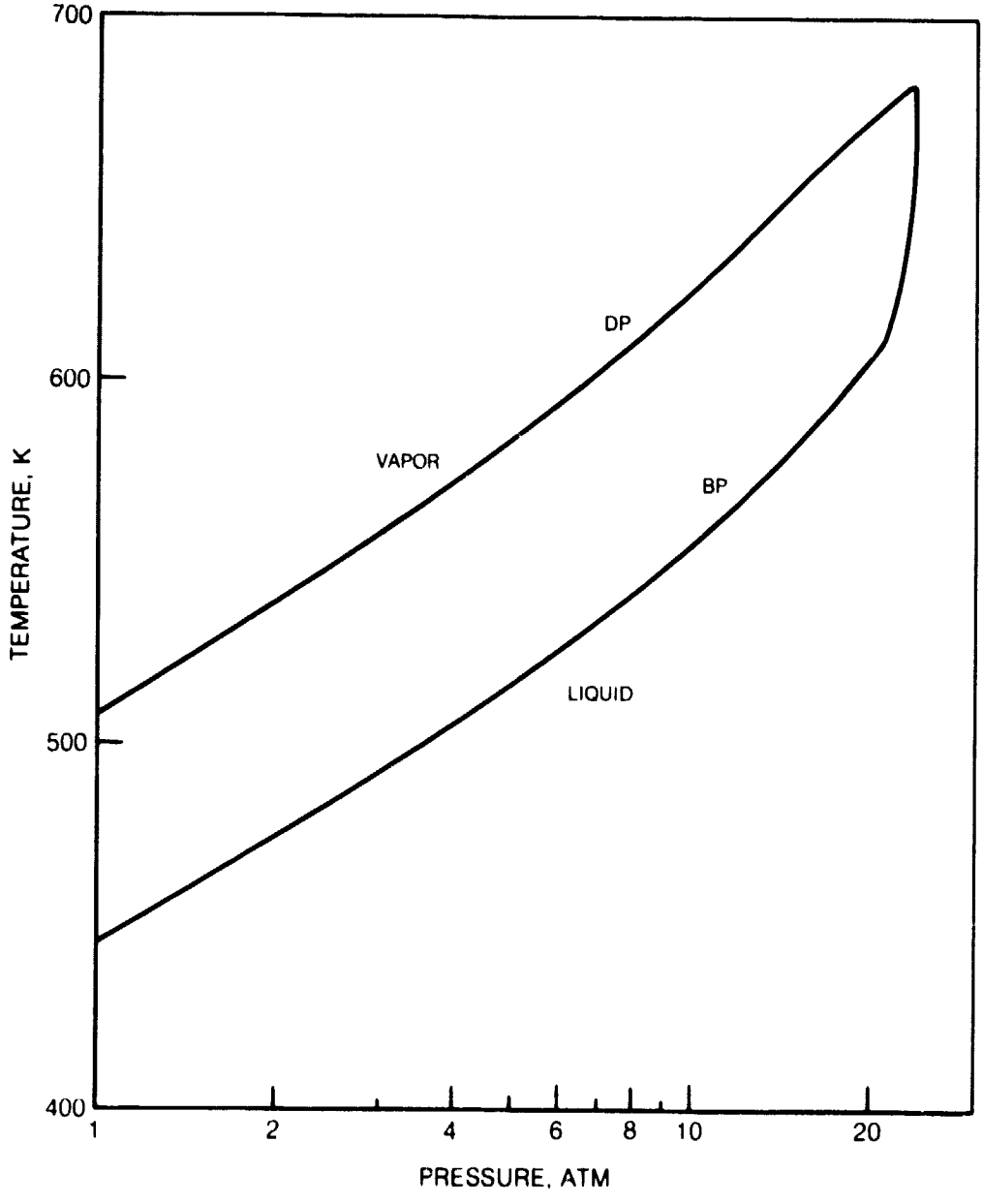

80-2-71-19

FIG. 6

ENTHALPY OF JET-A FUEL

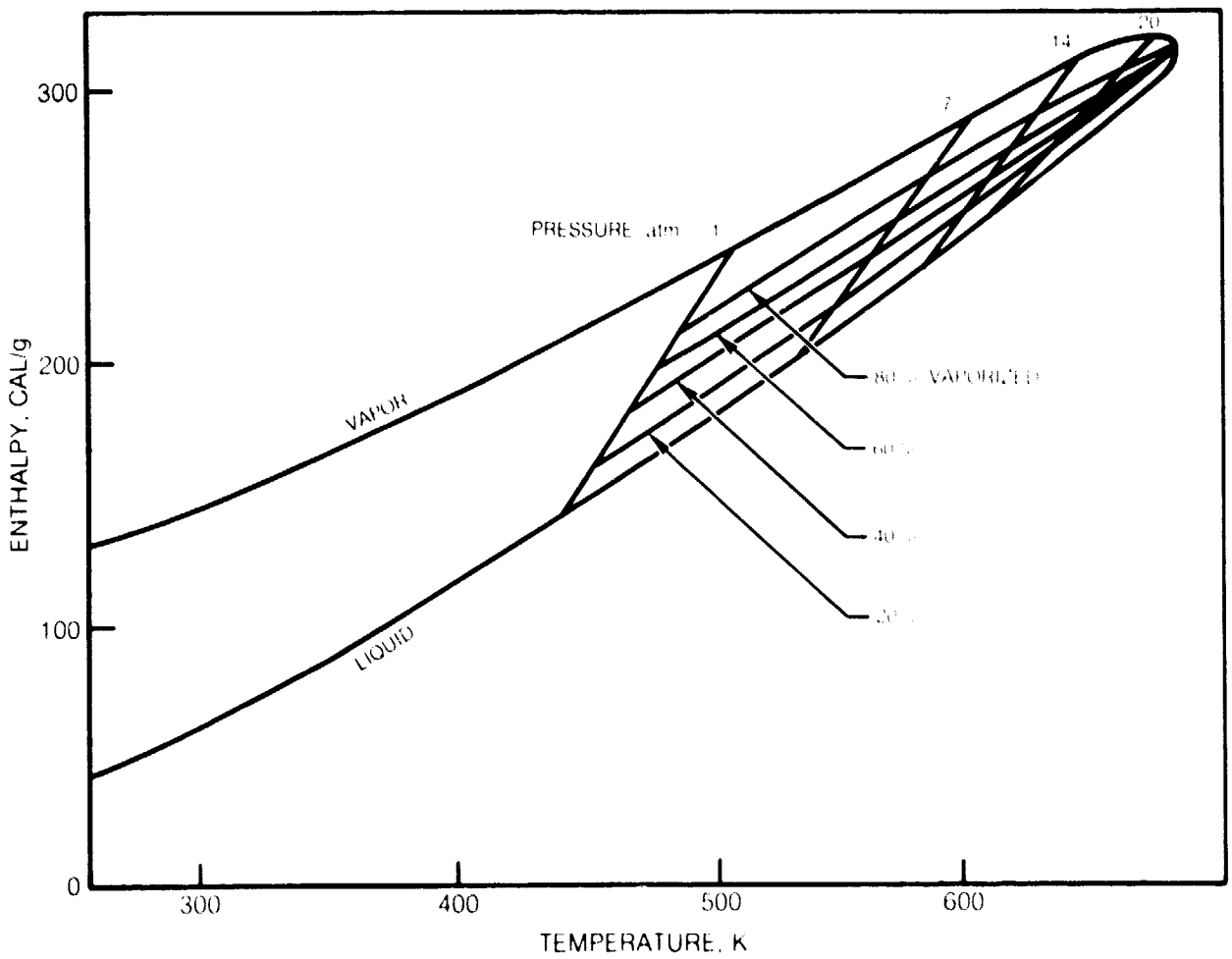

80-2-71 8

FIG. 7

BOILING CURVE DEFINITION

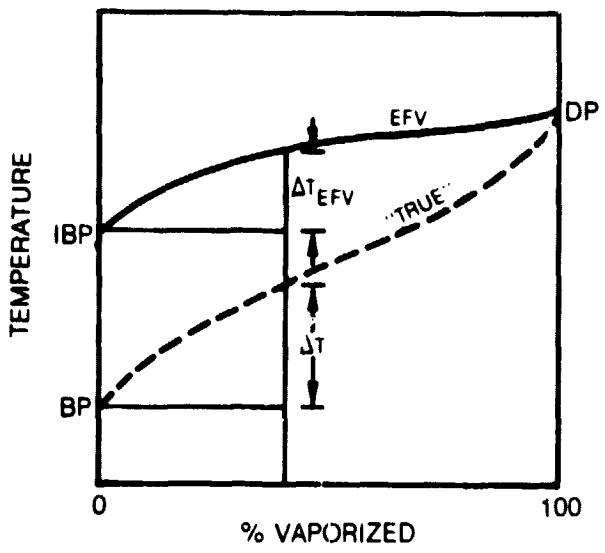

The "true" curve is constructed by assuming that the temperature at each point can be obtained by equating two ratios as shown below:

$$\frac{\Delta T}{\Delta T_{EFV}} = \left[\frac{T_{DP} - T_{BP}}{T_{DP} - \left(T_{IBP}\right)_{EFV}} \right] \qquad (1)$$

Other Properties

All other properties were calculated using the procedures in Ref. 7. Specific gravity curves for the fuel liquid and vapor are shown in Fig. 8. The liquid specific gravity was found to be in close agreement with data in Ref. 5, 6, and 8; however, comparative vapor data were not found. Viscosity data for liquid and vapor are shown in Fig. 9. Liquid viscosity data shown here agree up to a temperature of 475 K with data in Ref. 6 and 8. Above that temperature, only data from Ref. 8 were available and the curve in Fig. 9 was higher by approximately 25 percent. Thermal conductivity variations for liquid and vapor are shown in Fig. 10. Since liquid data do not agree among Refs. 6, 7, and 8, the lowest values of thermal conductivity were used in design calculations in order to make the results conservative. The vapor curves are in agreement with data in Refs. 6 and 8. Specific heat curves for the liquid and vapor are shown in Fig. 11. Liquid specific heat data agree up to a temperature of 425 K with data in Ref. 8. Above that temperature, the curve in Fig. 11 becomes progressively lower than the data in

FIG. 8

SPECIFIC GRAVITY OF JET-A

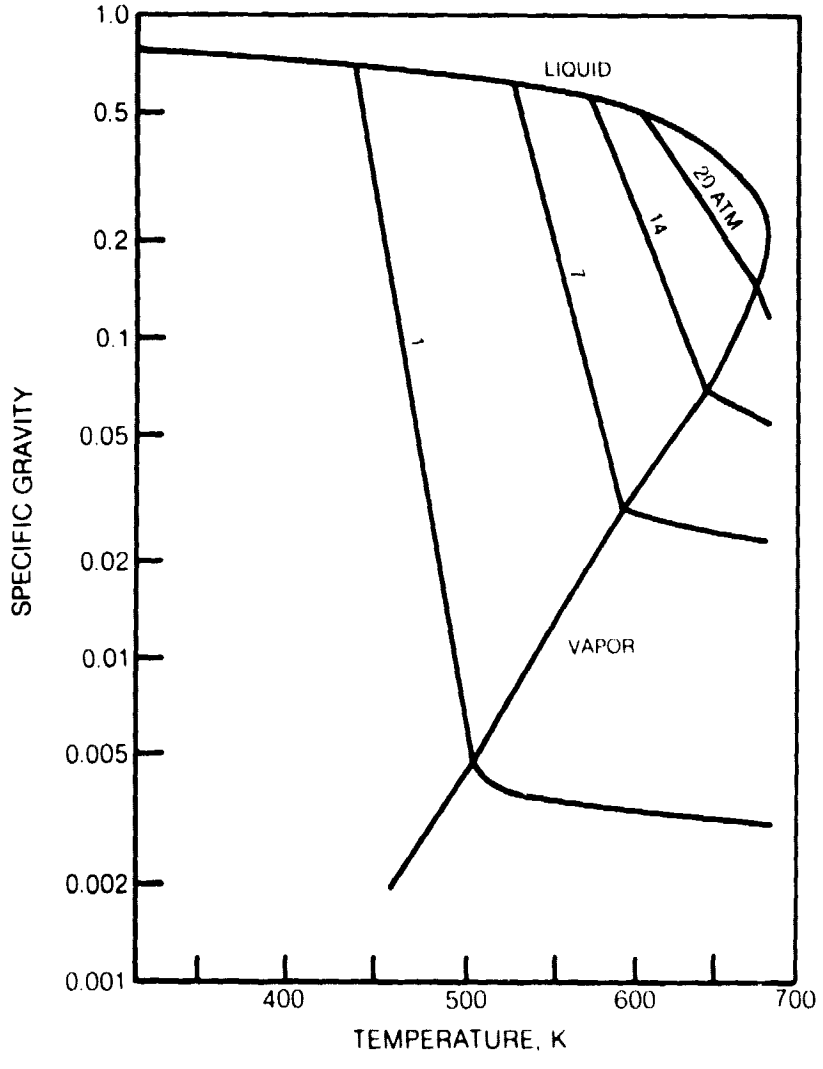

80-2-71-9

FIG 9

VICOSITY OF JET-A

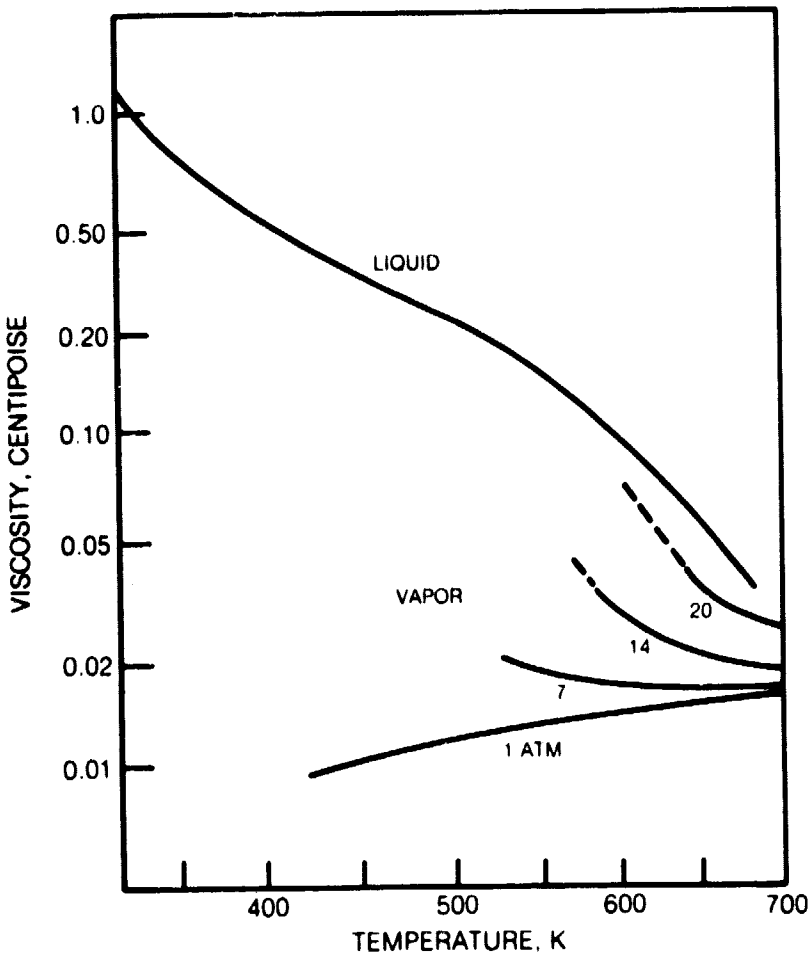

80-2-71-10

FIG. 10

THERMAL CONDUCTIVITY FOR JET A

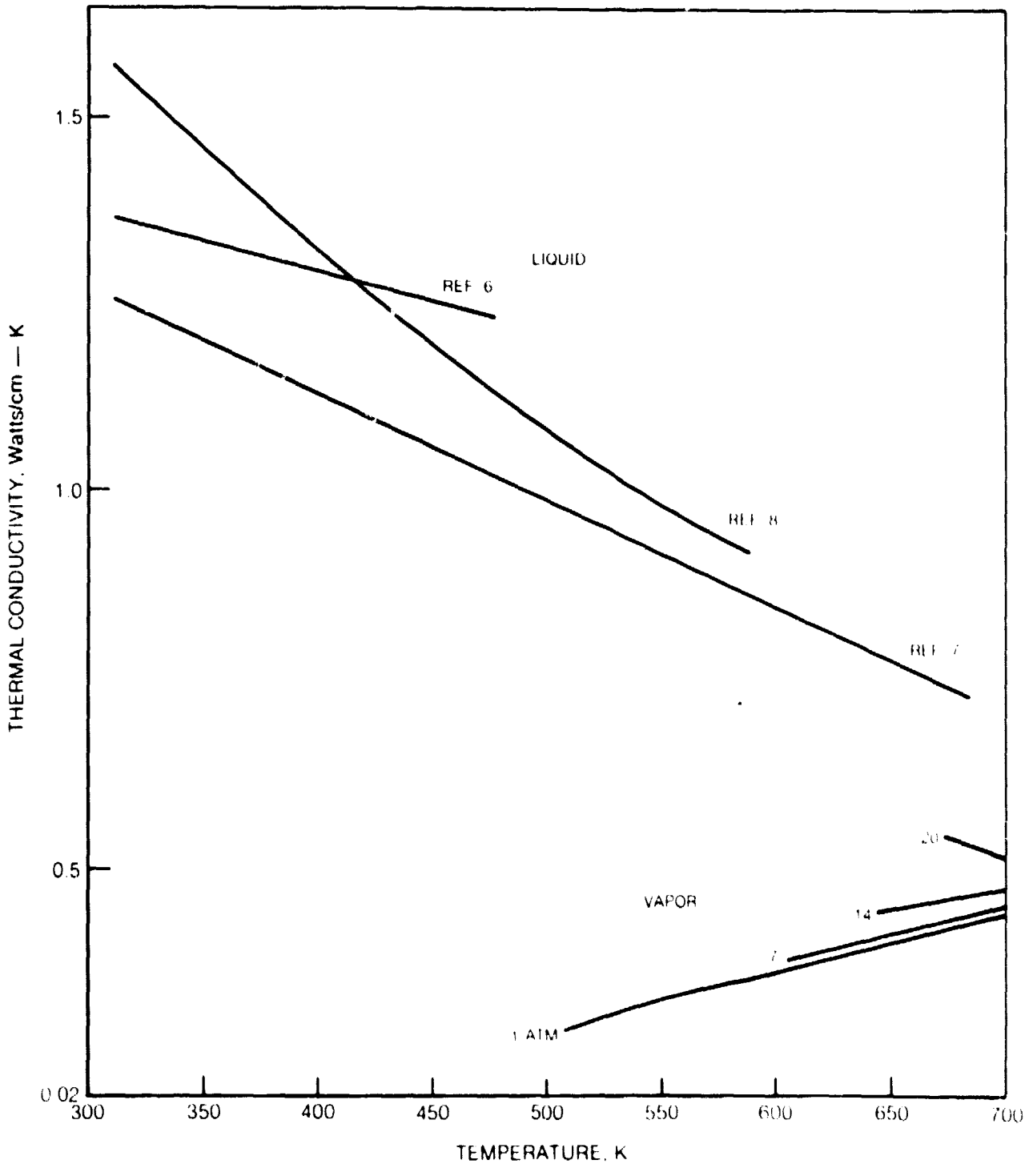

80-2-71 11

FIG. 11

SPECIFIC HEAT OF LIQUID JET-A

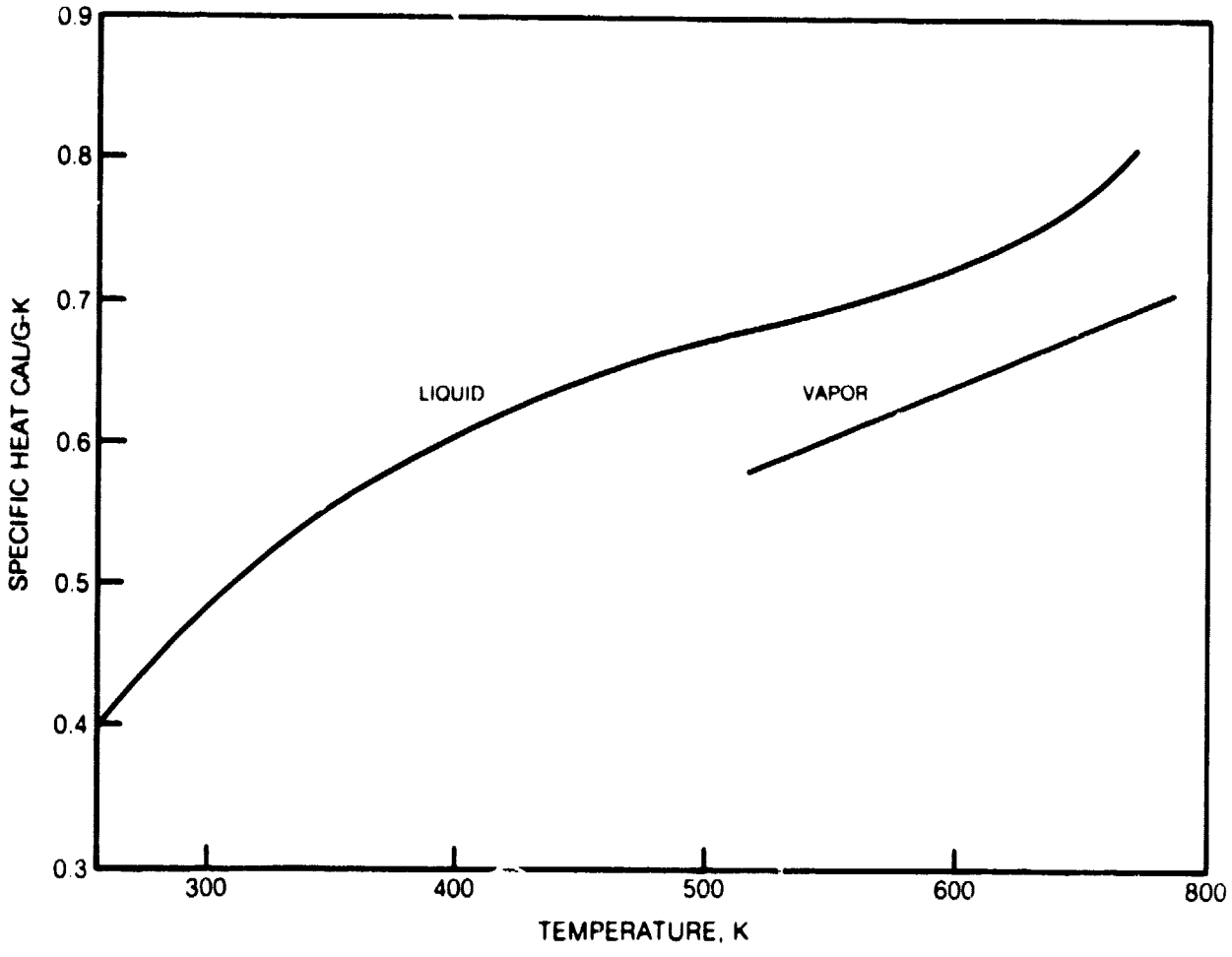

80-2-71-12

Ref. 8 until at 590 K it is 25 percent lower. The vapor curve agreed with the data in Ref. 6 but it was 25 percent lower than the data in Ref. 8.

The specific heat of either liquid or vapor is represented by the slope of the tangent to the curves of the Enthalpy-Temperature diagram in Fig. 6. Straight lines were used to represent the vaporization process; therefore, a constant specific heat can be used in the product C_p $(T_{DP}-T_{BP})$ to represent the energy added to the fuel in the vaporization process. The use of specific heat to represent enthalpy changes in the liquid, in the two-phase mixture, and in the vapor simplified the calculations, therefore, an effective specific heat was derived for vaporization. The results are shown in Fig. 12.

Deposit Formation

Relationships between deposit formation rate and temperature were found in data contained in Ref. 4 and they were used to derive the curve marked Standard in Fig. 13 which was used in heat exchanger design. The rate values were converted to thickness by assuming that the specific gravity of the deposits is unity and the time between cleaning is 100 hours. The equivalent peak value of deposit thickness is 0.02 cm. The monotonic and modified curves were used to improve convergence in the iteration during transients as discussed in a later section of this report.

FIG. 12

EFFECTIVE SPECIFIC HEAT OF JET-A DURING VAPORIZATION

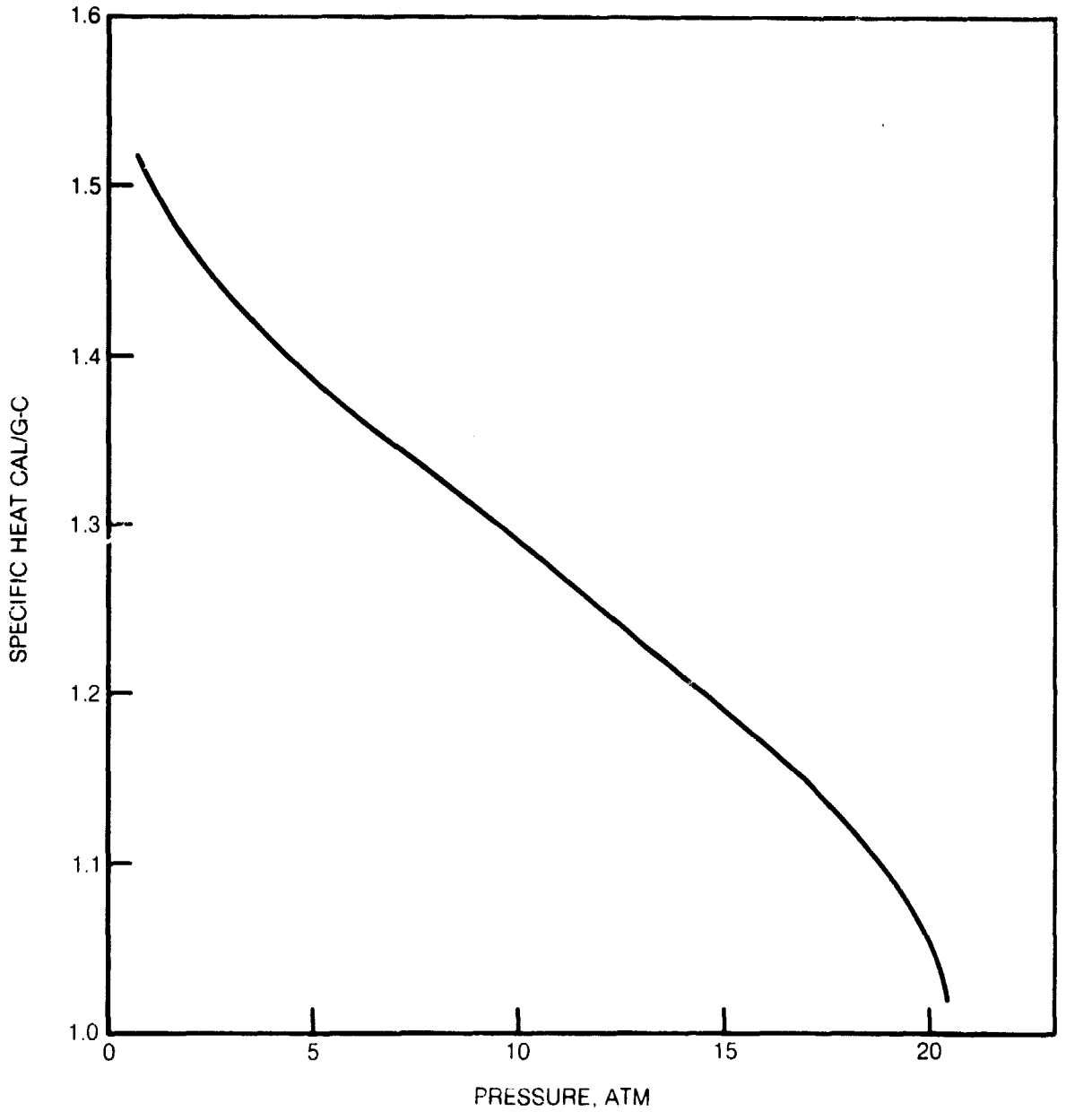

80-2-71-13

FIG. 13

VARIATIONS OF DEPOSIT RATE VS TEMPERATURE

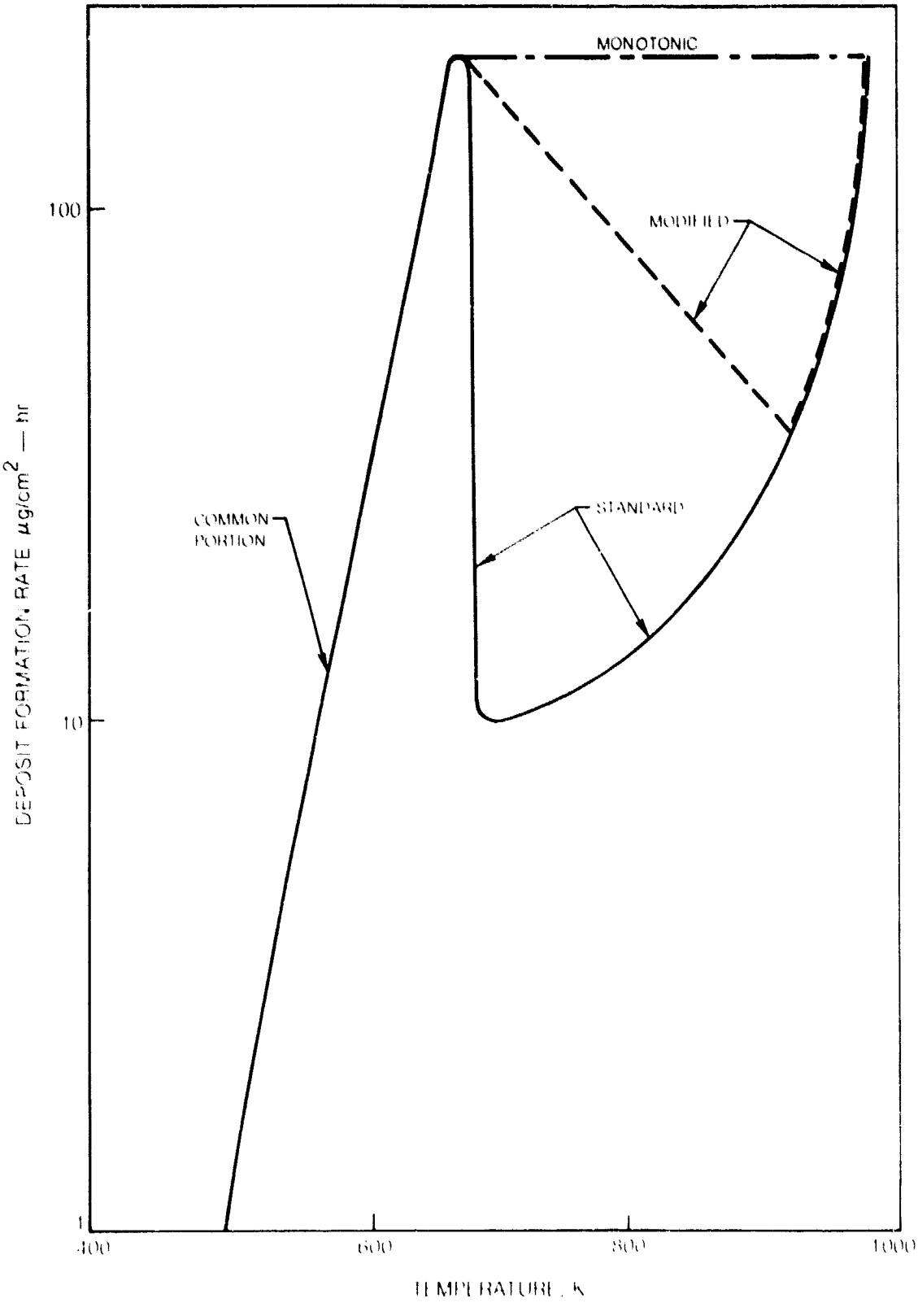

RO 1 3 1

HEAT EXCHANGER DESIGN DATA

Heat transfer and pressure loss calculations require the use of correlating equations or curves for the determination of heat transfer coefficients and friction factors for the two fluids at various conditions as follows:

Fuel:	Liquid, supercritical
	Liquid, subcritical
	Two-phase
	Vapor
Air:	Gas

This section contains the equations and curves used in the calculation of heat transfer coefficients and friction factors.

Fuel

It was found in the heat exchanger calculations that it was beneficial to maintain turbulent flow wherever the fuel was a liquid. Therefore, only two conditions were required for liquid fuel; turbulent supercritical (pressure above the critical pressure) and turbulent subcritical. The heat transfer in supercritical flow was calculated by the following equation which was found in Ref. 12.

$$Nu_w = 0.003354\ Re_w^{0.951}\ Pr_w^{0.435} \left(\frac{\rho_w}{\rho_B}\right)^{0.38} \tag{2}$$

The heat transfer in subcritical flow was calculated by the following equation which was found in Ref. 8.

$$Nu_B = 0.0046\ Re_B^{0.927}\ Pr_B^{0.628} \tag{3}$$

The friction factor for frictional pressure loss calculations was obtained from the smooth-tube curve on standard Moody charts (Ref. 13) with the following correction for non-isothermal flow:

$$f = f_{iso} \left(\frac{\mu_w}{\mu_B}\right)^{0.14} \tag{4}$$

In two-phase flow, the method suggested in Ref. 14 was used to calculate the heat transfer coefficient. Two terms are employed, the first term describing simple convection and the second describing the phase change. The equation is shown below.

$$h = 0.023 \frac{K_B}{D} Re_B^{0.8} Pr_B^{0.4} F + \quad (5)$$

$$0.00681 \left(\frac{K_{L_B}^{0.79} \, Cp_{L_B}^{0.45} \, \rho_{L_B}^{0.49} \, g^{0.25}}{\sigma_{L_B}^{0.25} \, \mu_{L_B}^{0.29} \, H^{0.24} \, \rho_V^{0.24}} \right) \left(T_W - T_{SAT} \right)^{0.24} \left(P_{SAT} - P_{SAT_B} \right)^{0.75} S$$

F is a function of X which is defined as follows:

$$\overline{X}^2 = \left(\frac{Re_V^m}{Re_L^n} \right) \left(\frac{C_L}{C_V} \right) \left(\frac{\rho_V}{\rho_L} \right) \left(\frac{1-x}{x} \right)^2 \quad (6)$$

where X is the quality of the vapor and m, n, C_L, C_V, and an additional constant N are defined in Table 2.

Table 2

DEFINITION OF CONSTANTS IN EQ. (5)

Liquid Vapor	Turbulent Turbulent	Laminar Turbulent	Turbulent Laminar	Laminar Laminar
m	0.25	0.25	1.0	1.0
n	0.25	1.0	0.25	1.0
C_L	0.079	16	0.079	16
C_V	0.079	0.079	16	16
N	4.0	3.5	3.5	3.0

S depends on F and Re_L as shown in Fig. 14.

Two-phase flow pressure loss is the sum of momentum loss and friction loss according to Ref. 15. Momentum loss can be calculated as follows:

$$\left(\frac{\Delta P}{\Delta Z} \right)_{mom} = \frac{G_T^2}{g} \left[\frac{(1-x)^2}{(1-\alpha)\rho_L} + \frac{x^2}{\alpha \rho_V} \right] \quad (7)$$

where

$$\alpha = \left[\left(\frac{\rho_V}{\rho_L} \right)^{2/3} \left(\frac{1-x}{x} \right) + 1 \right]^{-1} \quad (8)$$

FIG. 14

RELATION BETWEEN BOILING PARAMETERS S AND F

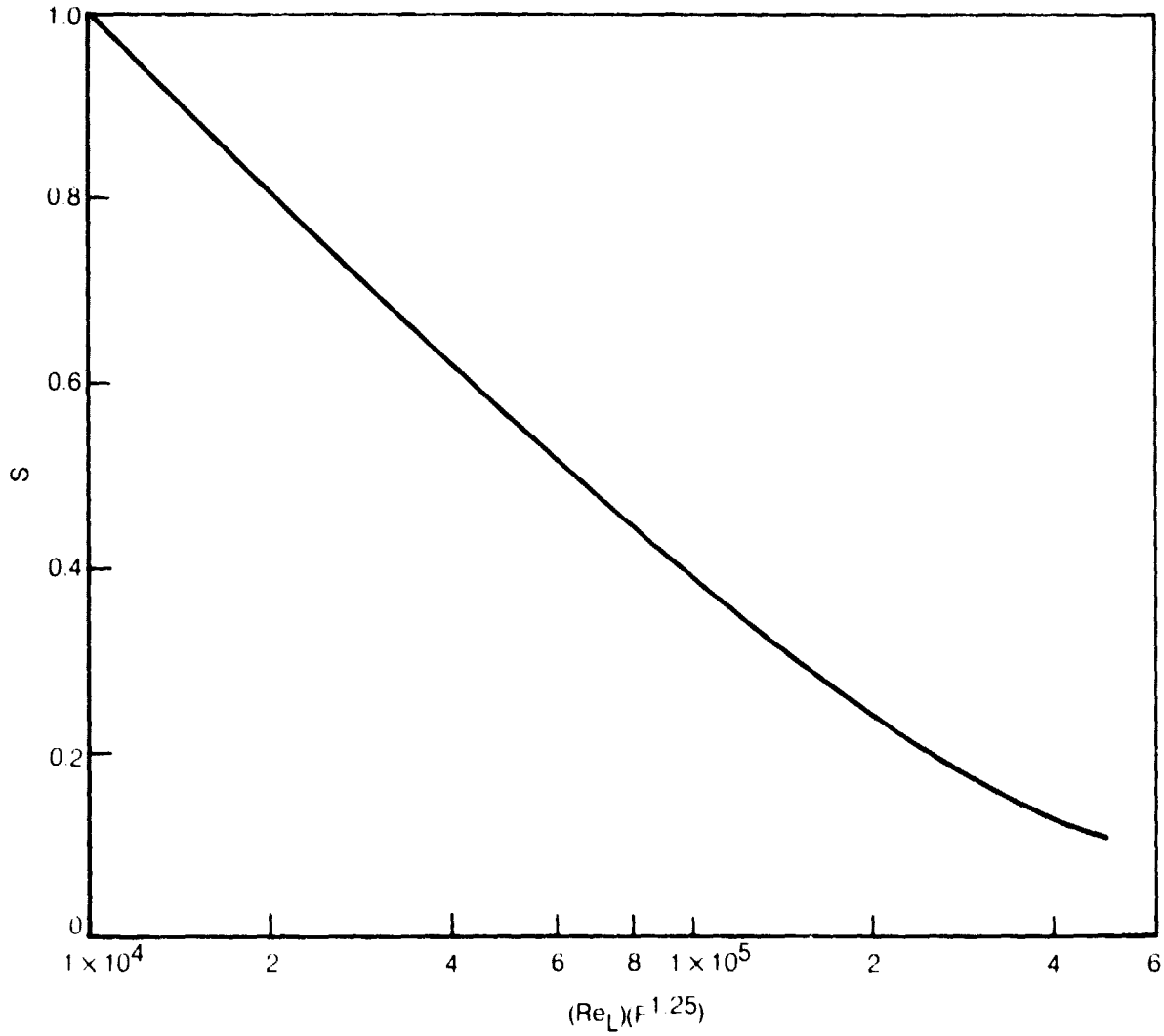

80-2-71-20

Two-phase friction loss is related to single phase friction according to Ref. 14 as follows:

when

$$\overline{X} > 1 \qquad \Delta P = \Delta P_L \left[1 + \left(\frac{1}{\overline{X}}\right)^{2/N}\right]^N \tag{9}$$

when

$$\overline{X} < 1 \qquad \Delta P = \Delta P_V \left[1 + (\overline{X})^{2/N}\right]^N \tag{10}$$

In these equations, ΔP_L and ΔP_V are calculated as if the liquid fraction or the vapor fraction fills the entire flow space. The liquid friction factor was described previously. For the vapor in two-phase flow or at 100% quality, the friction factor is calculated by methods obtained from Ref. 16. Heat transfer coefficients for the fuel vapor at 100% quality were also obtained from the data in Ref. 16.

The air side heat transfer coefficients and friction factors were obtained from Ref. 16 for the finned-tube and plain-tube geometries that were used in the heat exchanger calculations. The characteristics of these geometries will be described in a later section. The air properties used in these calculations were obtained from tables contained in Ref. 17.

ENGINE OPERATING CONDITIONS

The external fuel vaporization concepts were designed for the cycle and performance parameters anticipated for the Pratt & Whitney Aircraft version of the Energy Efficient Engine (E^3), currently being developed under a contract with NASA. The E^3 is configured as a high bypass ratio (6.5:1) engine in the 190,000 Newton Thrust Class, with a pressure ratio of approximately 38:1 at the cruise design point. Representative operating conditions for the E^3 at the design points of the takeoff/landing cycle and for maximum rated cruise are consistent with the conditions used in Ref. 18. They are listed in Table 3.

Table 3

REPRESENTATIVE OPERATING CONDITIONS FOR THE ENERGY EFFICIENT ENGINE

	Ground Idle	Approach	Max Cruise	Sea-Level Take-Off
Combustor Inlet Temperature (K)	473	621	754	810
Combustor Inlet Pressure (atm)	4.4	11.7	13.8	31.2
Air Flow Rate (kg/sec)	14.0	31.6	31.7	70.2
Combustor Exit Temperature (K)	815	1118	1533	1611
Combustor Exit Pressure (atm)	4.1	11.0	13.1	29.5
Fuel Flow Rate (kg/sec)	0.13	0.43	0.74	1.68
Overall Fuel-Air Ratio	0.009	0.0137	0.023	0.0240

ANALYTICAL PROCEDURES

Analytical procedures were required for the design of the auxiliary combustor and main heat exchanger in Scheme 1, the preheater and vaporizing, fuel-cooled combustor walls in Scheme 2, and the intercooler, auxiliary combustor, and mixer in Scheme 3. It was found that a hand calculation was adequate for the design of the auxiliary combustor using the curves contained in Ref. 18. For the mixer, a UTRC computer program described in Appendix B supplied the required design data. The heat exchangers presented a special problem because: the fuel was either a supercritical fluid or a two-phase mixture; fuel deposits, which are a function of wall temperature, often control the rate of heat transfer; and fuel properties used in the heat transfer equations are strong function of bulk temperature, wall temperature, and fuel pressure.

A computer program was devised for the design of the heat exchangers that were included in the three schemes. The program was relatively simple in execution, but complex in the input format and the manipulation of input parameters. An iteration procedure was used to obtain the temperature distribution through the heat exchanger. At times, the procedure failed to result in convergence. Problems with convergence were usually associated with gradients such as the deposit formation rate (which will be discussed in a later section) or the variation in the hot-to-cold temperature difference found in high-effectiveness cases.

Details of the calculation procedures are discussed in Appendix B.

COMPONENT DESIGN

Preliminary calculations indicated that SLTO is the design condition for all components. The reason lies in the use of a portion of the engine airflow to heat the engine fuel flow in all components. Although the air is used differently in each scheme, the magnitude of the fuel flow relative to the air flow is a major consideration, and the fuel-air ratio is highest at SLTO. All of the components were designed at that condition and checked at the other conditions listed in Table 3.

Scheme 1

As shown in Fig. 1, the main components of Scheme 1 are the heat exchanger and the auxiliary burner. Other components include the throttle valve and the associated piping for fuel and air distribution.

Heat Exchanger

To design the heat exchanger, three cores (tube arrangements) with the characteristics shown in Table 4 were selected from Ref. 16.

Table 4

HEAT EXCHANGER CORE CHARACTERISTICS

Core No.	1	2	3
Tube dia., cm	1.64	0.965	0.965
Fin dia., cm	2.85	2.34	None
Heat transfer area/total volume, m^2/m^3	269	535	211
Fin spacing, cm	0.363	0.291	None
Free flow area/frontal area	0.449	0.524	0.200

The heat exchanger flow arrangement was cross-counterflow as shown in Fig. 15. A large number of fuel passes was chosen to maintain a high fuel velocity in order to produce a high fuel-side heat transfer coefficient. High fuel velocity can be attained because the fuel is pumped as a liquid and fuel-side pressure loss in the heat exchanger does not create a significant penalty.

FIG. 15

CROSS-COUNTER FLOW ARRANGEMENT

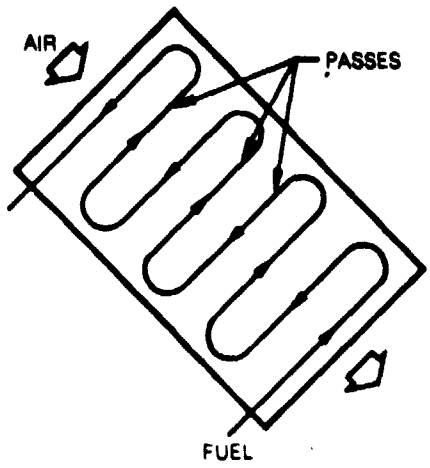

With each heat exchanger core, various combinations of heat exchanger length, width, and depth were selected and the computer program was used to determine the fuel exit temperature and air-side pressure loss. The inlet air temperature was fixed at 1255 K which was found in preliminary calculations to represent a reasonable compromise between obtaining a compact heat exchanger size and a need for high temperature materials. The compressor bleed airflow was fixed at 2.85 percent because it was found in preliminary calculations that, at the resulting outlet temperature, the exit airflow is suitable for turbine cooling.

The results of the heat exchanger calculations are shown in Figs. 16 and 17. It was found that both Cores 1 and 2, which contain finned tubes, gave nearly identical heat exchanger volumes. Plain tubes appear to be more favorable for this application, partly because of the compactness of Core 3 (surface area/unit volume), and partly because the tubes contain only prime surfaces as opposed to fins which are secondary surfaces of less than 100 percent efficiency. The air-side pressure drop for the core of the final design is one percent of the air pressure and the fuel-side pressure drop is 12 atm. An exploded view of the heat exchanger is shown in Fig. 18 and the overall dimensions are shown in Fig. 19. Tapered air manifolds are used to produce uniform distribution of air across the 0.61 m span at the inlet and exits ends of the heat exchanger. Fuel is transferred between passes (tubes) by a connecting groove in a plate that covers the ends of the tubes.

FIG. 16

FUEL EXIT TEMPERATURE VS VOLUME

SCHEME 1

SLTO

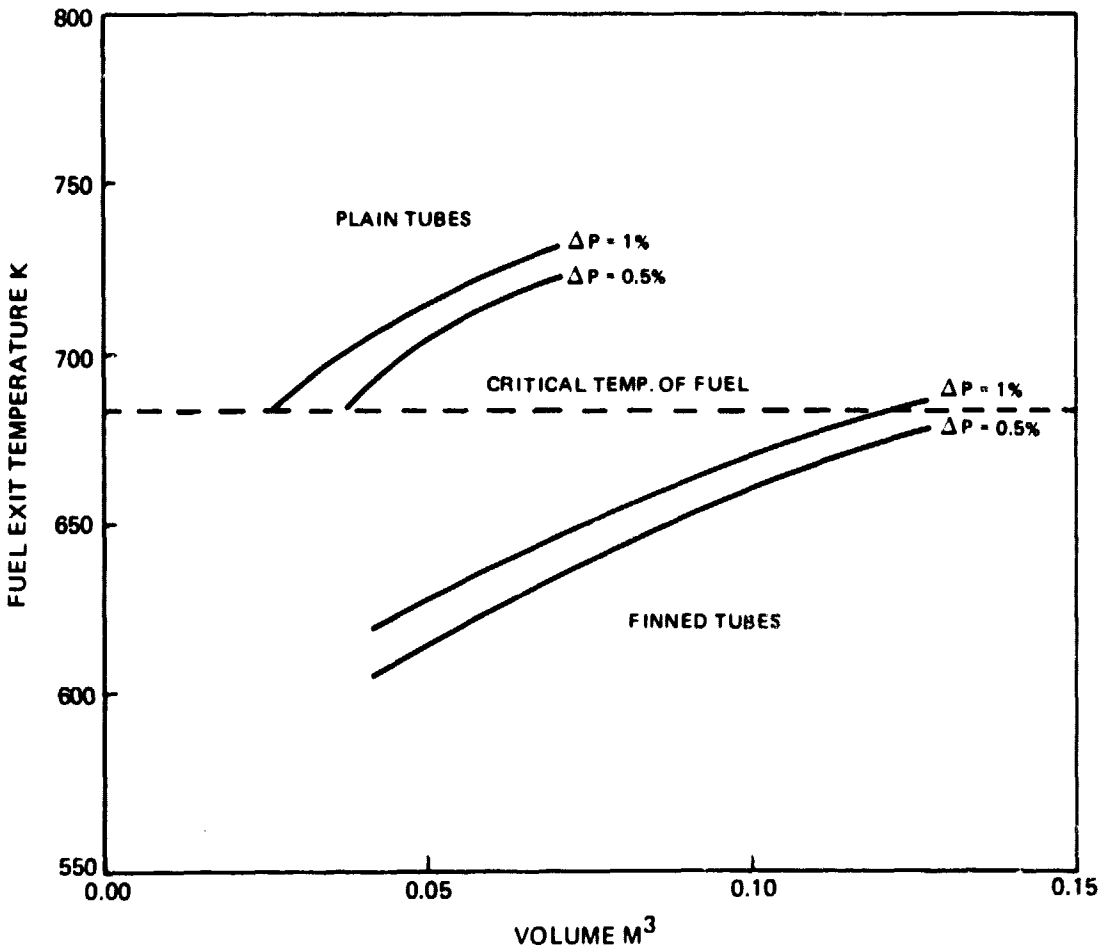

79 08 17 1

FIG. 17

HEAT EXCHANGER VOLUME VS AIRFLOW

SCHEME 1
SLTO

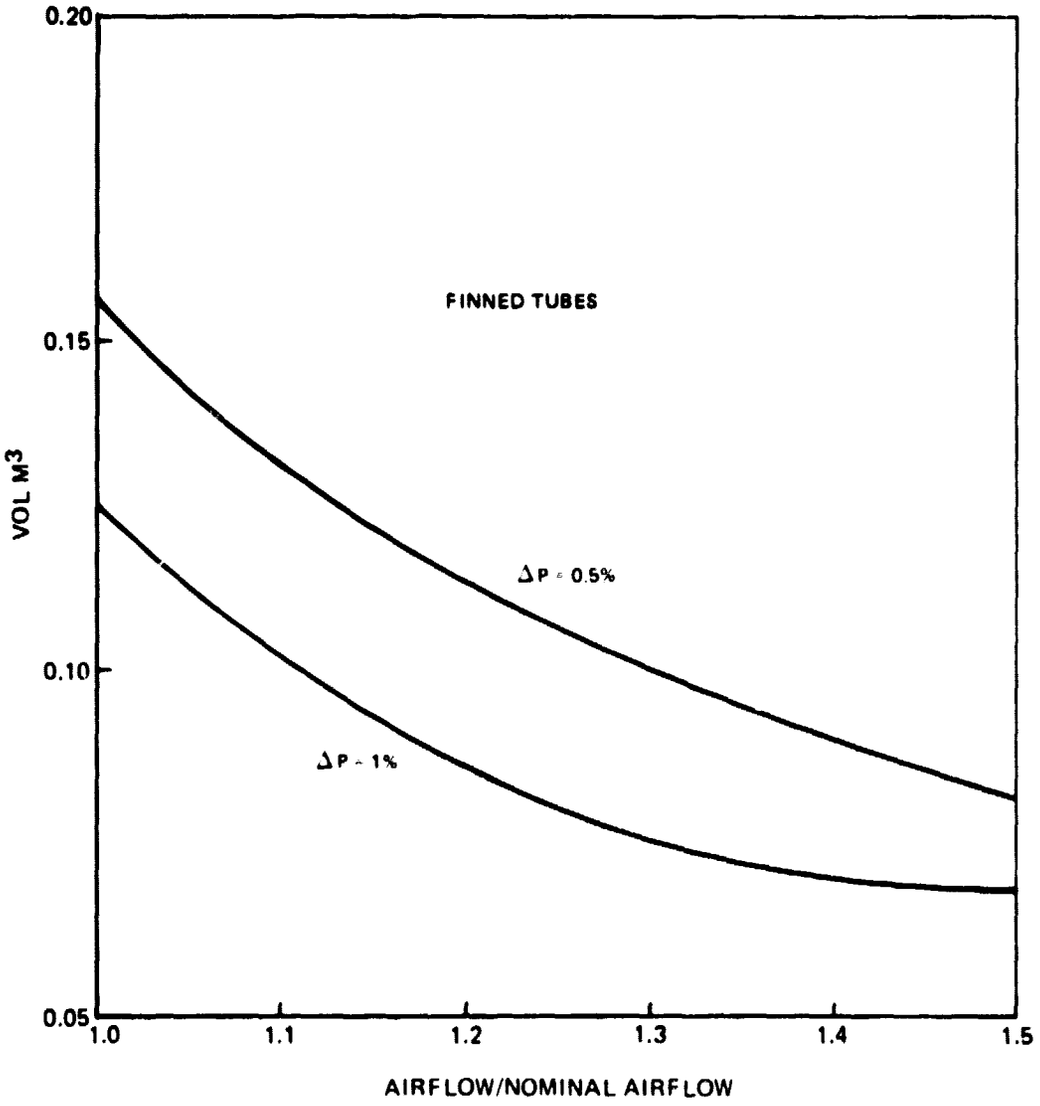

79-08 17 2

FIG. 18

VAPORIZER DETAILS

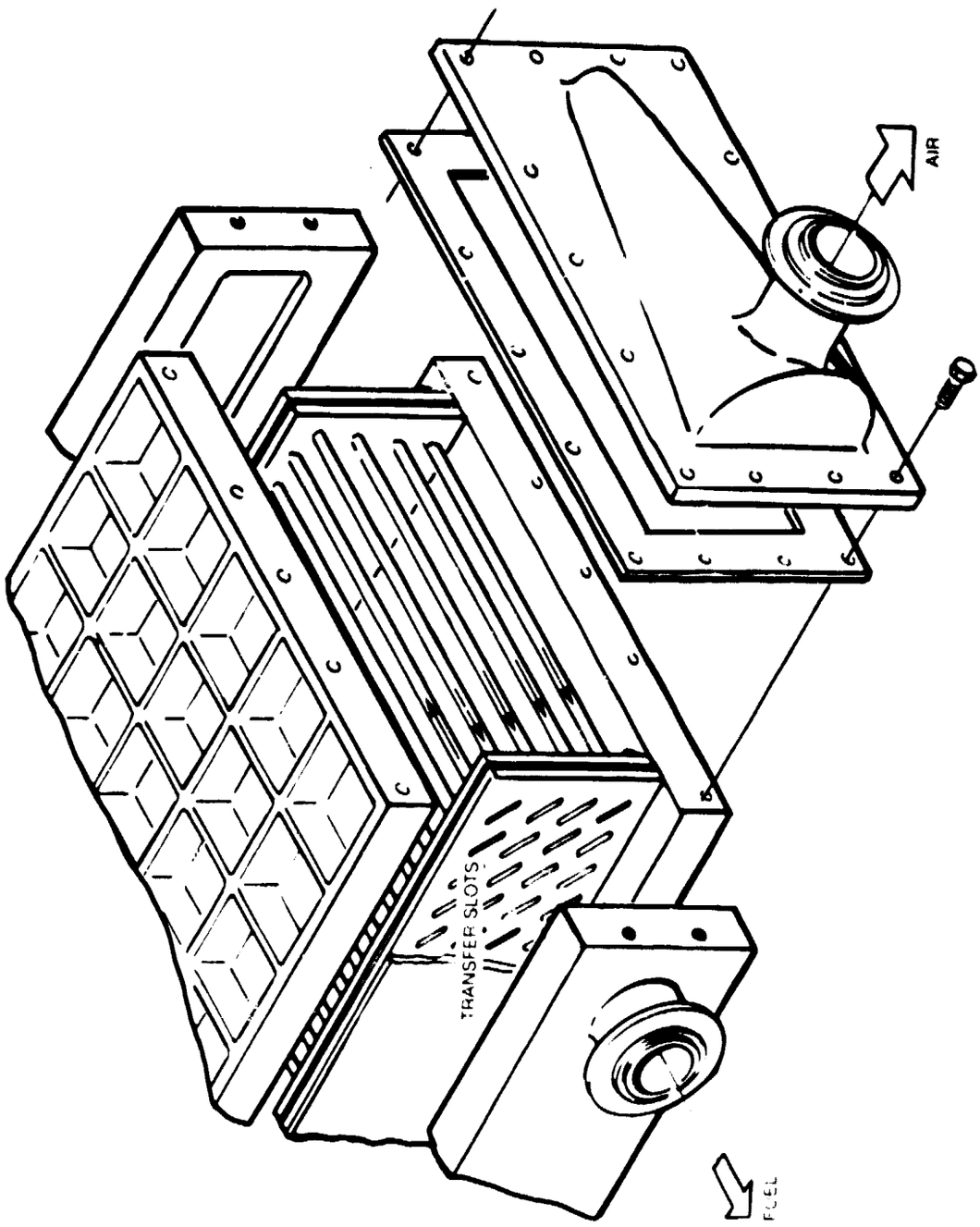

80--2-71 2

FIG. 19

SCHEME 1 HEAT EXCHANGER DIMENSIONS

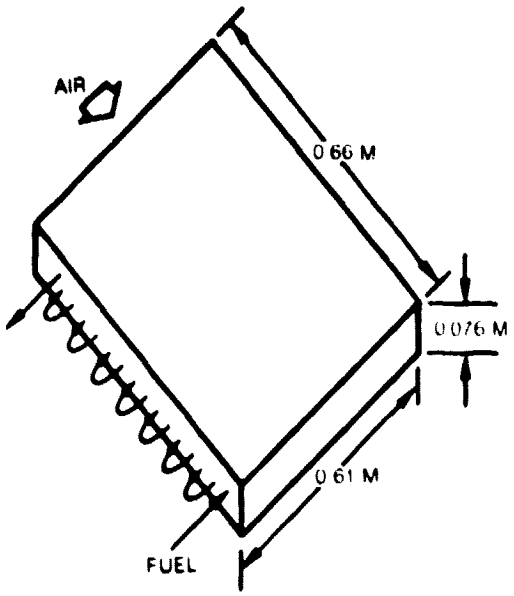

Auxiliary Burner

The auxiliary burner was designed by selecting conservative operating parameters from Fig. 20 which is a smoothed version of the data found in Ref. 19. The design parameters include a velocity of 22 m/sec, a volumetric space heating rate of 27×10^6 kcal/m^{-3} atm, and a dome height (combustor diameter) of 9.4 cm. The combustor length was chosen to be 19 cm which includes a 20 percent safety factor over the value determined from the design parameters. Figure 21 shows the details of the combustor including the fuel injector.

The fuel flow requirements of the auxiliary burner vary with the engine operating conditions as shown in Table 5.

The fuel flow range in the first four columns indicates that between SLTO and Idle, the turndown ratio is 3.2. If this was the entire operating range, it could be achieved with a simplex (single orifice) pressure atomizer. However, the required operating range in turndown ratio extends to 66 if the altitude relight fuel flow is included. The auxiliary burner must operate with good efficiency at altitude conditions to facilitate the supply of vaporized fuel to the main engine combustor at restart. These operating conditions were discussed with an atomizer manufacturing representative who felt that a duplex (dual orifice) pressure atomizer can be used over the entire fuel flow range. Discussions were also held with combustor design engineers of P&WA of Canada, Ltd., builders of small gas turbines, who felt that an aerating atomizer can be used to cover the operating range of the

SPACE HEATING RATE FOR GAS TURBINE COMBUSTORS

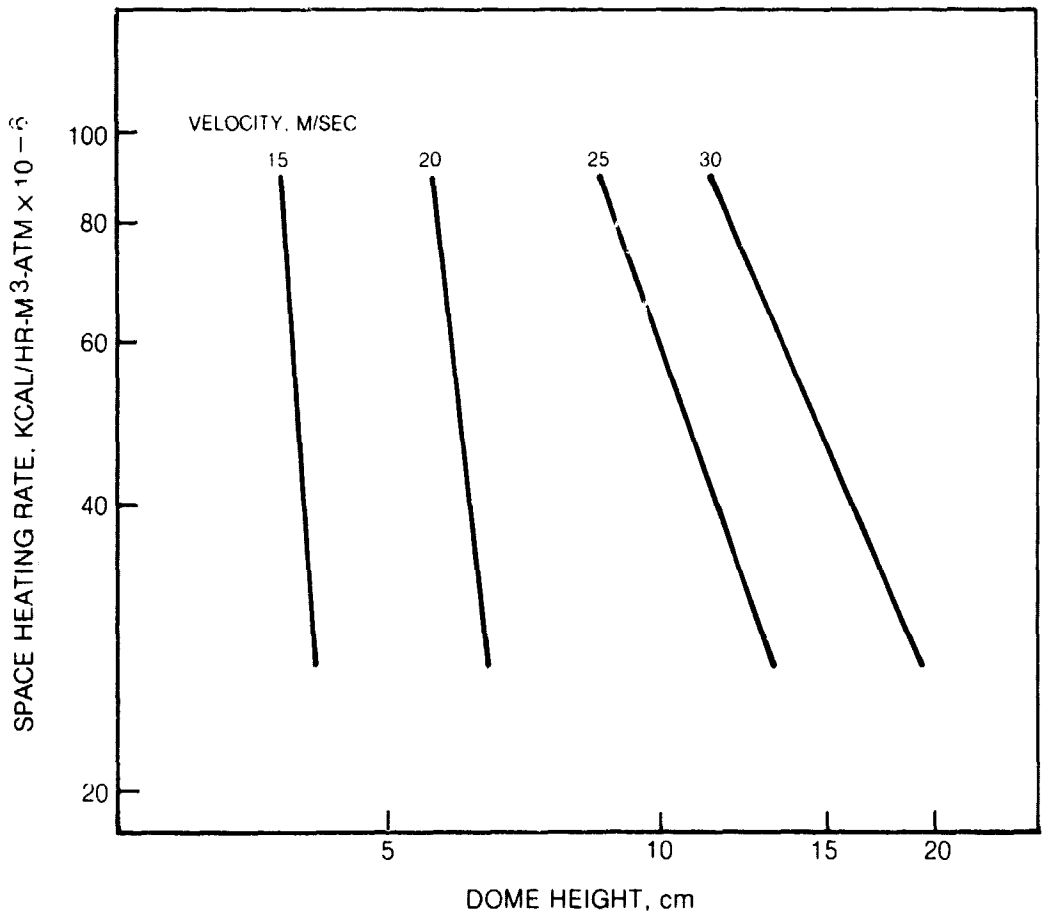

80-2-71-22

AUXILIARY BURNER USED IN SCHEMES 1 AND 3

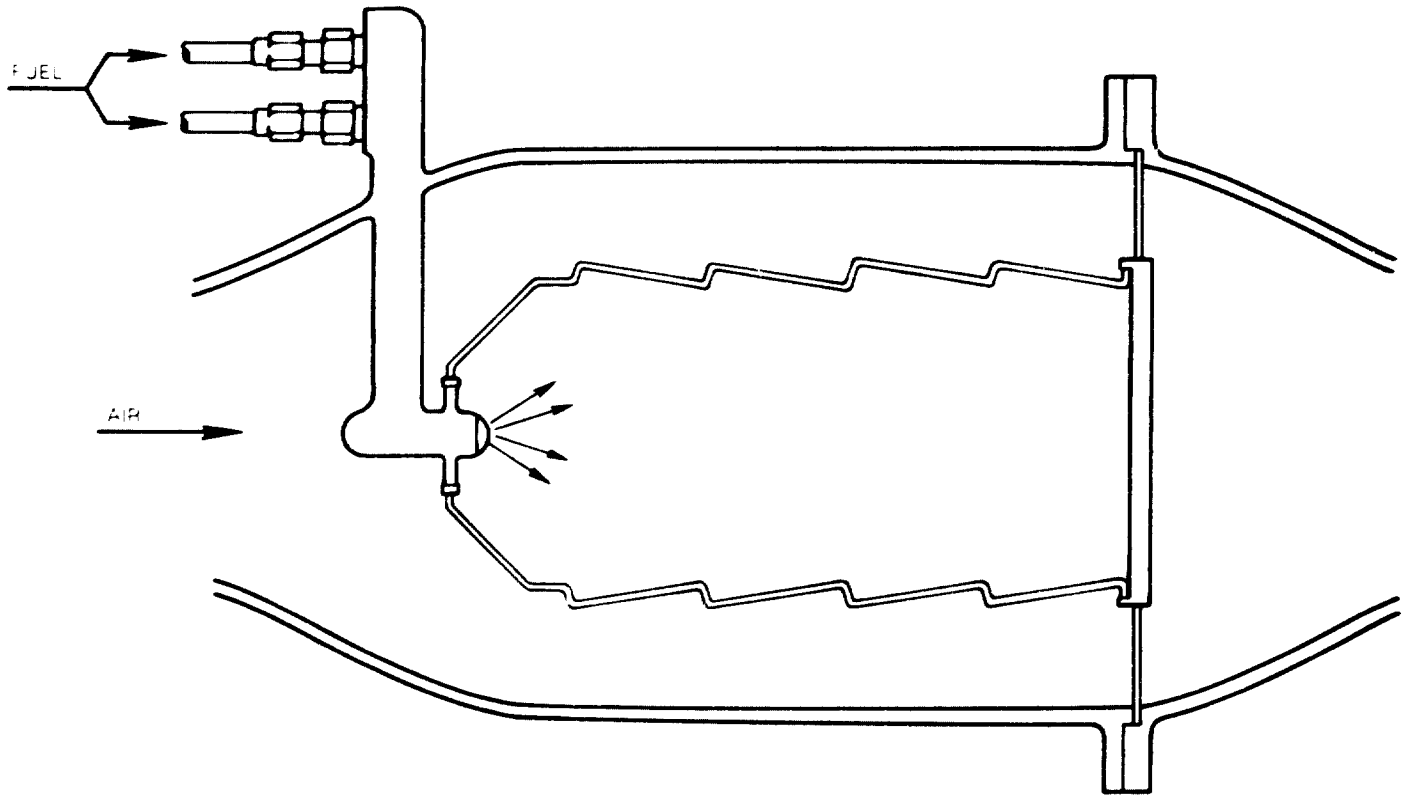

80-2-71-21

FIG. 21

Table 5

AUXILIARY BURNER OPERATING CONDITIONS

	SLTO	Cruise	Approach	Idle	Altitude Relight
Inlet Pressure, atm	31.1	13.8	11.7	4.4	0.24
Inlet Temperature, K	810	754	621	473	251
Airflow, Kg/sec	2.00	0.92	0.90	0.41	0.013
Design Exit Temperature, K	1255	1145	1145	1145	1255
Corresponding F/A	0.012	0.011	0.014	0.018	0.028
Corresponding Fuel Flow, Kg/sec	0.0239	0.0101	0.0125	0.0074	0.00036

burner. They also felt that a special pressure atomizer should be used for altitude startup, and that the low fuel flow associated with that condition will cause difficulties with the design of the special atomizer.

Valves and Piping

Additional components that require consideration include the main engine fuel control, the throttle valve, and the inlet and exit pipes on the air and fuel sides of the vaporizer.

Engine Fuel Control

In current aircraft engines, the fuel is maintained in a liquid state in the fuel control. Fuel is metered in response to a change sensed in engine parameters such as shaft speed. The schematic diagrams in Fig. 1 show the location of the fuel control which assures that metered fuel is always in a liquid state. Additional functions are added to the fuel control such as metering of the auxiliary burner fuel flow which is controlled by vaporizer exit parameters and limited by the auxiliary burner exit temperature. However, the added fuel control functions can be provided with conventional approaches, particularly in cases of steady-state or minor fuel flow changes. Major changes in operating conditions such as rapid acceleration and deceleration will be discussed in a later section.

Throttle Valve

The throttle valve is a variable restriction which offers a negligible resistance to flow when the compressor discharge pressure is high enough to require that the fuel pressure is above its critical value (21.8 atm). At lower values of fuel pressure, the throttle restriction results in the pressure drop (P_2-P_1) that is needed along path B of Fig. 2. It is expected that the throttle valve in the engine will have the fluid-flow characteristics of a sharp-edged orifice in order to have the pressure drop occur rapidly. A rapid pressure decrease is needed to prevent the existence of any intermediate fluid states between liquid

and vapor. The equivalent of a tortuous passage such as exists in a needle valve might contain a two-phase fluid which could produce vapor-lock phenomena and flow instabilities.

At high engine fuel flow such as SLTO, the pressure in the fuel manifold is at or above the critical pressure of the fuel; there can be no two-phase flow in either the heat exchanger or the manifold and the throttle remains completely open. At lower engine fuel flow where the manifold pressure is reduced below the critical pressure of the fuel, a pressure drop is required across the throttle valve and the throttle is partially closed. As the engine fuel flow (and manifold pressure) is further reduced, the throttle valve pressure drop increases and the throttle area decreases.

Although the valve is located in a region where deposits will form on the walls along the fuel path, the throttle valve should not be impeded in its function because it is not required to close tightly. The valve is not required to seal internally, but it must seal the fuel from leaking externally over a possible operating range of 490 to 940 K and at pressures to 35 atm.

More discussion of the operation of the throttle valve is contained in a later section.

Fuel and Air Piping

The air-side pipe size was selected to have an internal diameter of approximately 5 to 6 cm to assure that the overall air-side pressure loss conforms with the value of 8 percent used in the engine performance calculations.

The vaporizer air manifold is semicircular and is tapered to produce uniform flow within the heat exchanger. The overall air pressure loss is the sum of the increments listed in Table 6.

Table 6

AIR PRESSURE LOSS (PERCENT)

Compressor Exit to Auxiliary Burner	0.8
Auxiliary Burner	4.0
Vaporizer (including manifolds)	2.5
Vaporizer Exit to Turbine	0.3
Total	7.6

The fuel-side heat exchanger pressure loss is 12 atm which is considered to be acceptable from the standpoint of the fuel pump. The fuel system piping was selected to assure uniform flow in the fuel injectors by making the pressure loss in the fuel injectors the dominant fuel-side pressure loss. The fuel manifold and the lines feeding the injectors have a velocity head which is 0.1 times the

velocity head in the injector ports. The fuel manifold has a 3 cm diameter at the inlet and tapers to the diameter of the injector feed lines which are 0.5 cm in diameter.

Engine Components

Consideration was given to the design requirements of the vaporized-fuel injectors and the vaporized-fuel combustor in the engine because both components have an impact on the vaporizer design. The fuel injector affects the throttle exit pressure which determines the dew point of the fuel at any operating condition. The combustor may have either single or multiple stages and the number of stages affects the fuel distribution system.

The vaporized fuel injector is considered to be a closed hemispherical passage with four drilled holes on its periphery. The fuel passage is surrounded by an annular air passage which has a venturi shape as shown in Fig. 22 to suppress flashback. It was assumed that if the combustor has a single stage, two circumferential arrays having twenty injectors in each array would be used. A third array was added for a dual stage combustor as shown in Fig. 23.

Calculations were made to determine port size as a function of injector pressure drop and the results are listed in Table 7.

Table 7

INJECTOR PORT SIZE

Pressure Drop, %	Hole Size, cm
1	0.160
10	0.094
20	0.079
50	0.063

Discussions with P&WA engineers revealed that the anticipated circumferential variation of burner inlet total pressure is close to one percent and a portion of this variation might be felt at the discharge of the injector. To assure uniform fuel flow at the injector exit, the pressure drop should be at least 10 times the variation in injector pressure. The corresponding injector size is 0.094 cm. Deposit data obtained in the program described in Ref. 20 indicated that deposit formation in the fuel ports should be much less than the maximum thickness of 0.02 cm anticipated in the heat exchanger; therefore, the selected port size might be acceptable. An injector pressure drop of 10 percent was used to determine the throttle exit pressure.

In a single stage combustor, it can be assumed that the equivalence ratio in the combustion zone is maintained at a constant value and that the airflow into the dilution zone is varied to obtain the required overall equivalence ratio at

FIG. 22

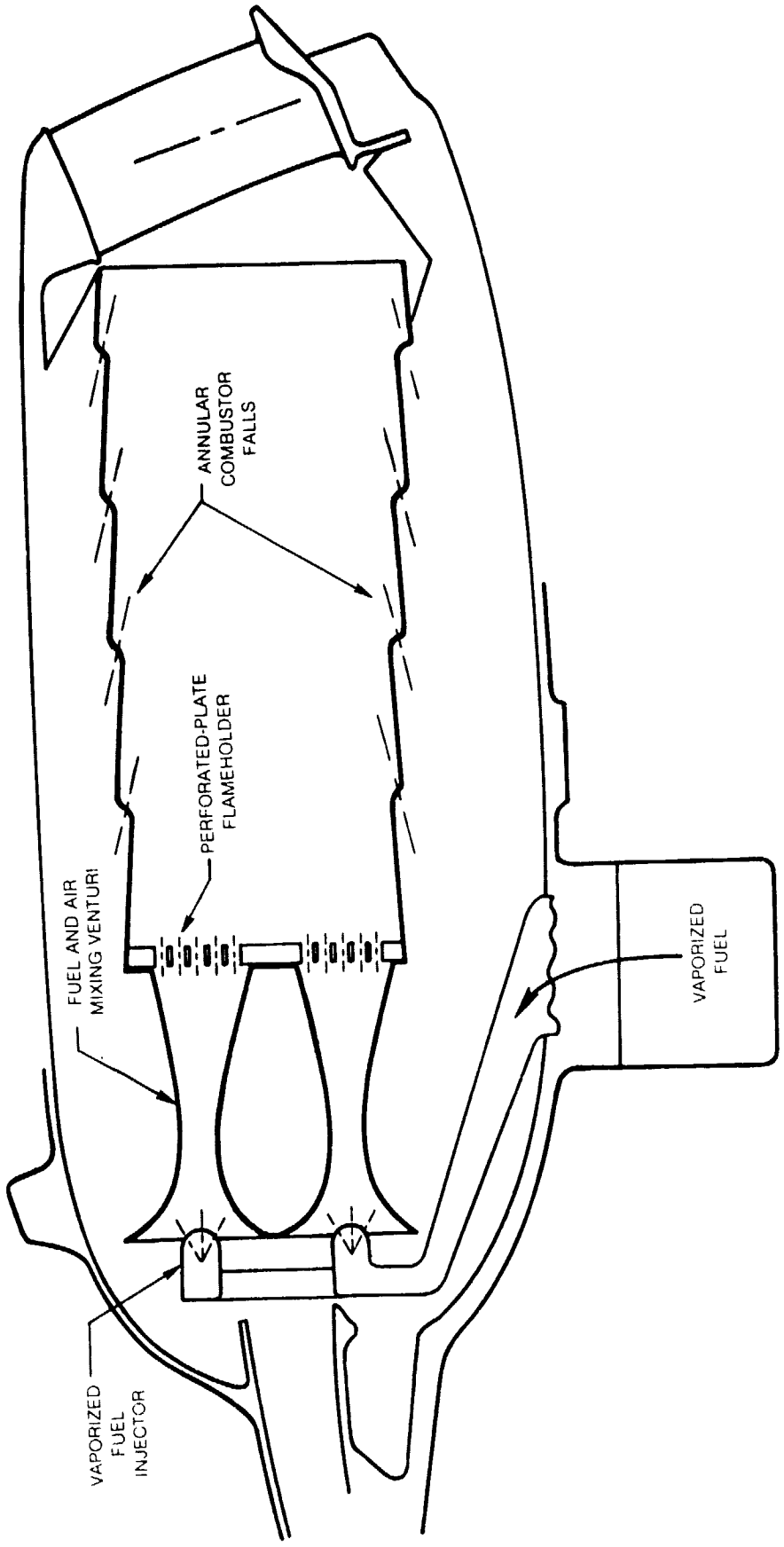

VAPORIZED FUEL INJECTOR AND PERFORATED-PLATE FLAMEHOLDER

79-09-17-10

FIG. 23

TWO-STAGE BURNER CONCEPT

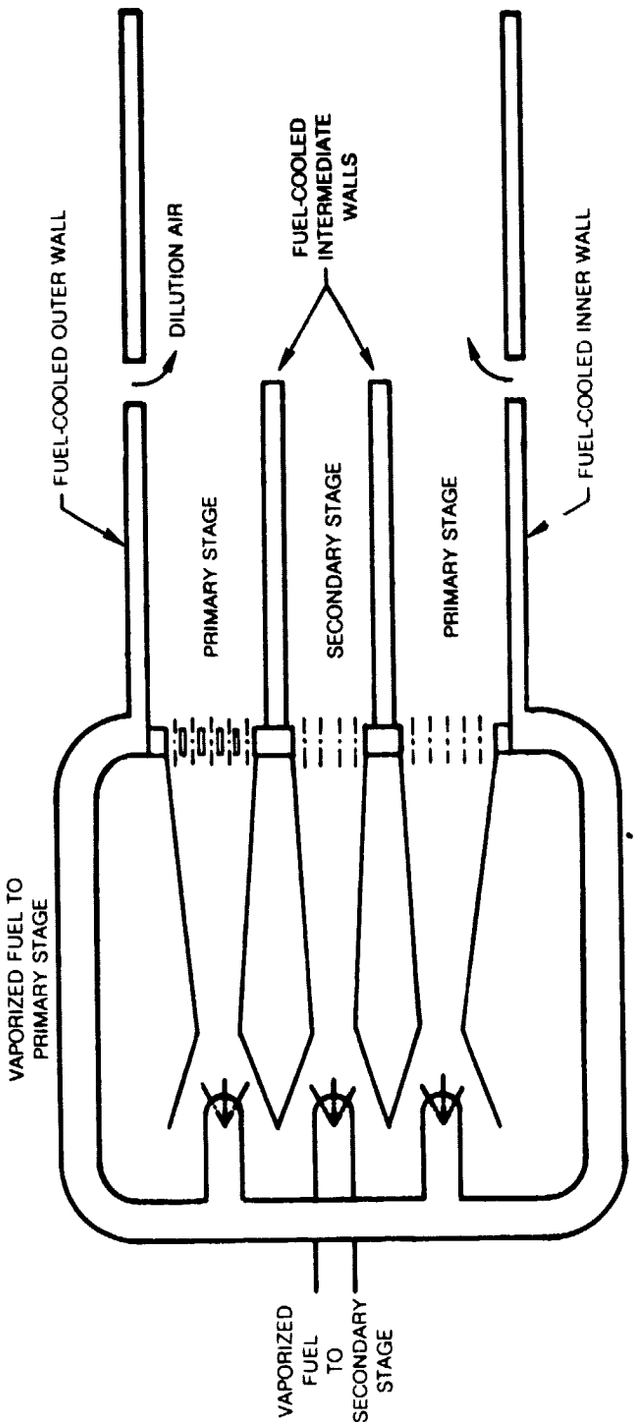

79-09-17-8

individual engine operating conditions. An alternative approach that does not involve air flow variation and the implied variable area combustor hardware is the use of staged combustion zones. In the two-stage combustor that was considered in this program, the fuel flow schedule was manipulated to assure that the highest equivalence ratio did not exceed the value selected on the basis of wall temperature considerations and that the lowest equivalence ratio was sufficient to maintain high combustion efficiency. Two fuel flow schedules, as shown in Fig. 24, were considered. The solid line is based on setting the maximum equivalence ratio in the primary (continuous flow) stage and secondary (interrupted flow) stage at 0.6 for the control of combustor wall heat transfer and the emission of NO_x. The lowest equivalence ratio can be made as high as possible if the minimum value is the same for both stages. A value of 0.36 was found to satisfy the E^3 engine operating conditions found in Table 3. The dashed line is based on setting the maximum equivalence ratio in the secondary stage at 0.6 to control wall heating and NO_x emission at SLTO and allowing the higher value in the primary stage at part power. Pertinent conditions resulting from the use of these different fuel flow schedules are shown in Table 8.

Table 8

EQUIVALENCE RATIO IN STAGED COMBUSTOR

Schedule (Fig. 24)	1 (solid)	2 (dashed)	3 (not shown)
Maximum in Primary	0.6	0.8	1.0
Maximum in Secondary	0.6	0.6	0.6
Minimum in Both Stages	0.36	0.42	0.46

Steady-State Operation

A schematic diagram of the component arrangement for operation with either a single stage or dual stage combustor is shown in Fig. 25. Also shown are the steady-state operating parameters for the four engine operating conditions which include SLTO, cruise, approach, and idle. Transient operation and altitude relight are discussed in later sections. In the dual stage combustion concept, it is desirable to split the vaporizer into a dual stage unit, which can be a single component, because the fuel must be metered as a liquid. If only one vaporizer was used, it would be necessary to split the flow in a location where the fuel is hot and apt to leave deposits. A split compressor bleed flow is allowed because the air flow splitter is located on the downstream, or cool side, of the vaporizers.

The first set of values in Fig. 25, labeled Compressor Discharge, were taken directly from anticipated E^3 conditions in Table 3. The next set, labeled Vaporizer Inlet, includes the air temperature which was selected for this study on the basis of heat exchanger durability. The design value of 1255 K represents the highest temperature where nickel-based alloys (such as Hastelloy X), still have a reasonable strength. The temperature was reduced to 1144 K at other conditions to obtain a reasonable long-time creep strength. The off-design temperatures can be reduced further, if desired, because the assumption of constant heat exchanger inlet temperature produced a higher fuel temperature than required.

FIG. 24

TWO-STAGE COMBUSTOR FUEL FLOW

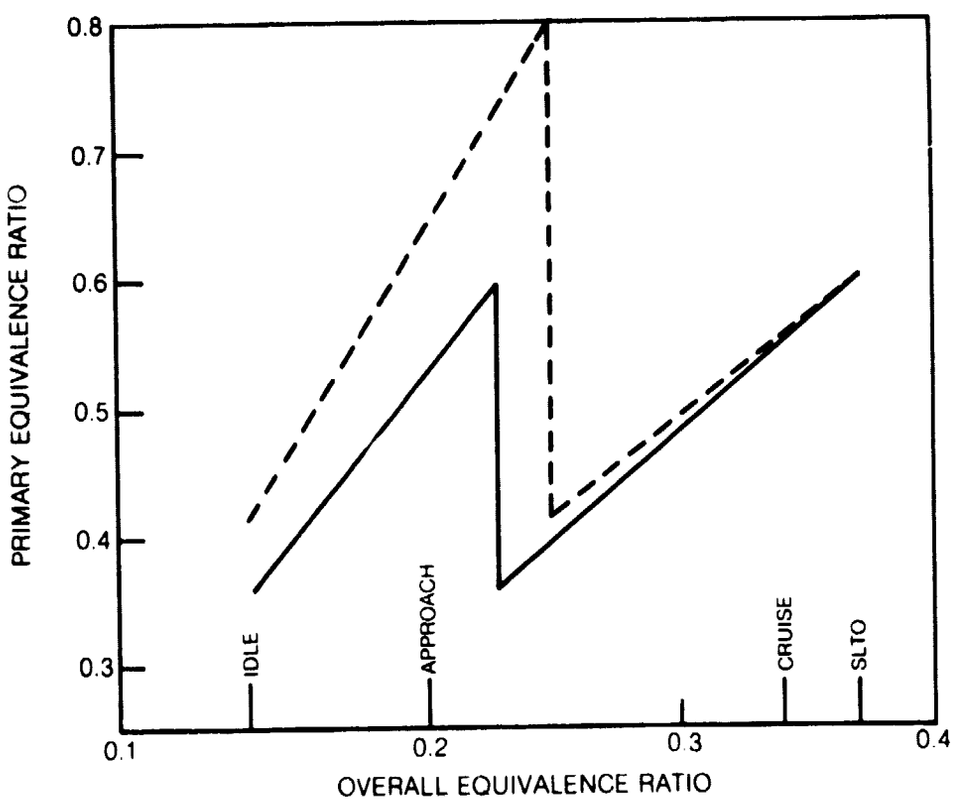

80-2-71-14

EXTERNAL VAPORIZER — FUEL SYSTEM DIAGRAMS

SCHEME 1 — FLASH VAPORIZATION

SINGLE STAGE COMBUSTOR

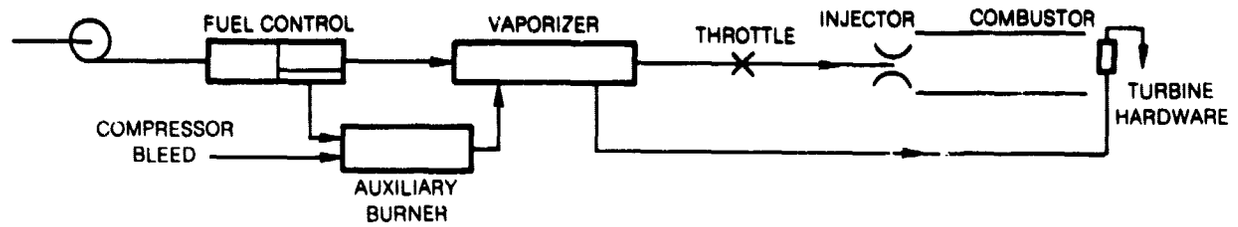

DUAL STAGE COMBUSTOR

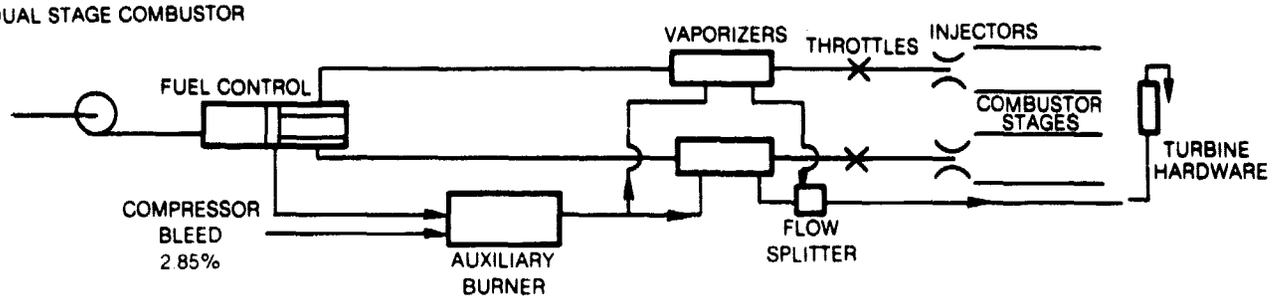

	SLTO	CRUISE	APPROACH	IDLE
COMPRESSOR DISCHARGE				
PRESSURE ATM	31.1	13.8	11.7	4.4
TEMP K	810	754	621	473
VAPORIZER INLET				
AIR TEMP K	1255	1144	1144	1144
FUEL TEMP K	311	311	311	311
THROTTLE INLET				
MINIMUM PRESSURE ATM	34.6	21.8	21.1	20.7
SELECTED PRESSURE ATM	34.6	21.8	21.8	21.8
MINIMUM TEMP K	683	683	678	636
CALCULATED TEMP K	683	694	789	939
THROTTLE EXIT				
PRESSURE ATM	34.6	16.0	12.6	4.7
TEMP K	683	685	785	939
DEW POINT K	683	661	644	594
INJECTOR ΔP %				
SINGLE STAGE	10	10	7	4
DUAL STAGE	10	10	17	9
BLEED AIR TO TURBINE				
PRESSURE ATM	29.1	12.9	10.9	4.1
TEMP K	487	367	478	348

79-10-23-1

The throttle inlet and exit conditions are shown in the data listed in Fig. 25 at the four engine conditions. The throttle inlet minimum pressure is the "idealized" pressure called P_2 in Fig. 2 (p. 4) except for SLTO where it is equal to compressor discharge pressure plus injector pressure drop. At other conditions, the minimum pressure is equal to the critical pressure at Cruise and only slightly lower pressures at Approach and Idle. The selected pressure at SLTO is set at injector inlet conditions at SLTO and at the critical pressure at the other three conditions. At SLTO and Cruise, the minimum temperature is the critical temperature. At Approach and Idle, the minimum temperature corresponds to point b in Fig. 2. The calculated throttle inlet (vaporizer exit) temperature at SLTO is equal to the minimum required temperature because SLTO is the vaporizer design point. At all other (off-design) conditions, the calculated throttle inlet temperature which was obtained in the output of the heat exchanger computer program is above the minimum value.

The throttle exit pressure listed in Fig. 25 is equal to the compressor discharge pressure plus injector pressure drop. The exit temperature was determined from thermodynamic considerations, e.g., Fig. 2 (p. 4). At SLTO the throttle is wide open and there is no temperature drop. At the other conditions, the temperature drop across the throttle is quite small, as would be expected from the increasing level of throttle inlet temperature; a higher temperature brings the fuel vapor closer to an ideal gas which has no temperature drop during throttling (Joule-Thompson coefficient = zero, Ref. 21). It can be seen that the throttle exit temperature at off-design conditions exceeds the minimum required (dew point) temperature which is point a on Fig. 2.

It might appear that the throttling process does not involve much flash vaporization because at high engine power (Cruise) the operating conditions (P_1 and P_2) are near the tip of the dome in Fig. 2 and at low power (Idle) the calculated temperature indicates that the fuel is in the vapor state upstream of the throttle. However, the design work accomplished on the vaporizer system to date must be considered as preliminary; as the design more closely approaches a hardware stage, other operating conditions will be investigated and other operating modes might be selected for the conditions that have been examined. As previously stated, the table in Fig. 25 shows that the vaporizer inlet (auxiliary burner exit) gas temperature is constant at three of the engine power settings. A lower gas temperature might be desirable at lower fuel flow to reduce the vaporizer wall temperature. It will be shown later that metallurgical considerations favor low wall temperature. If a lower gas temperature were assumed, the calculated throttle inlet fuel temperature would be closer to the minimum temperature.

The injector pressure drop values are different for the dual stage combustor than the single stage. It was assumed that the dual stage has 50 percent more injectors than the single stage. For the same pressure drop, therefore, the dual stage injectors have a 10 percent smaller diameter. The dual stage injectors have a higher pressure drop at Approach and Idle because 1/3 of the ports are closed.

It can be seen that the vaporizer exit temperature, which is labeled Bleed Air to Turbine, is considerably below Compressor Discharge temperature. This is the result of cooling with fuel along the counterflow paths in the heat exchanger.

The combination of low temperature and high pressure make the air a better coolant than conventional cooling air bled directly from the compressor. The result is improved engine performance which will be discussed in a later section.

Scheme 2

As shown in Fig. 1, the main components of Scheme 2 are a preheater and the vaporizer. The preheater extracts heat from compressor bleed air and the vaporizer is integral with the walls of the engine combustor.

Preheater

The design of the preheater followed the same methods described previously for the heat exchanger in Scheme 1. The three heat exchanger cores which included two with finned tubes and one with plain tubes were used in calculations of outlet fuel temperature for various combinations of length, width, and depth. The compressor bleed airflow was fixed at 4.55 percent because, at the resulting outlet temperature, the exit airflow is suitable for turbine cooling.

The heat exchanger calculations showed that the two cores containing finned tubes gave nearly identical heat exchanger volumes. Plain tubes appear to be more favorable for this application. The air-side pressure drop for the core of the final design is 1.6 percent of the inlet pressure. The fuel-side pressure drop is 4 atm which is a small fraction of the capability of standard engine fuel pumps. The overall dimensions of the heat exchanger are shown in Fig. 26. The results of the heat exchanger calculations are shown in Fig. 27.

FIG. 26

SCHEME 2 PREHEATER DIMENSIONS

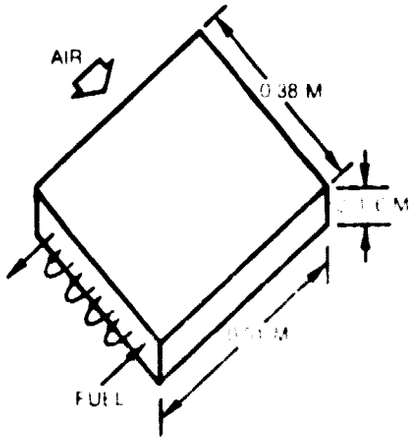

FIG. 27

PREHEATER EXIT TEMPERATURE VS VOLUME

SCHEME 2

ENGINE IDLE CONDITION

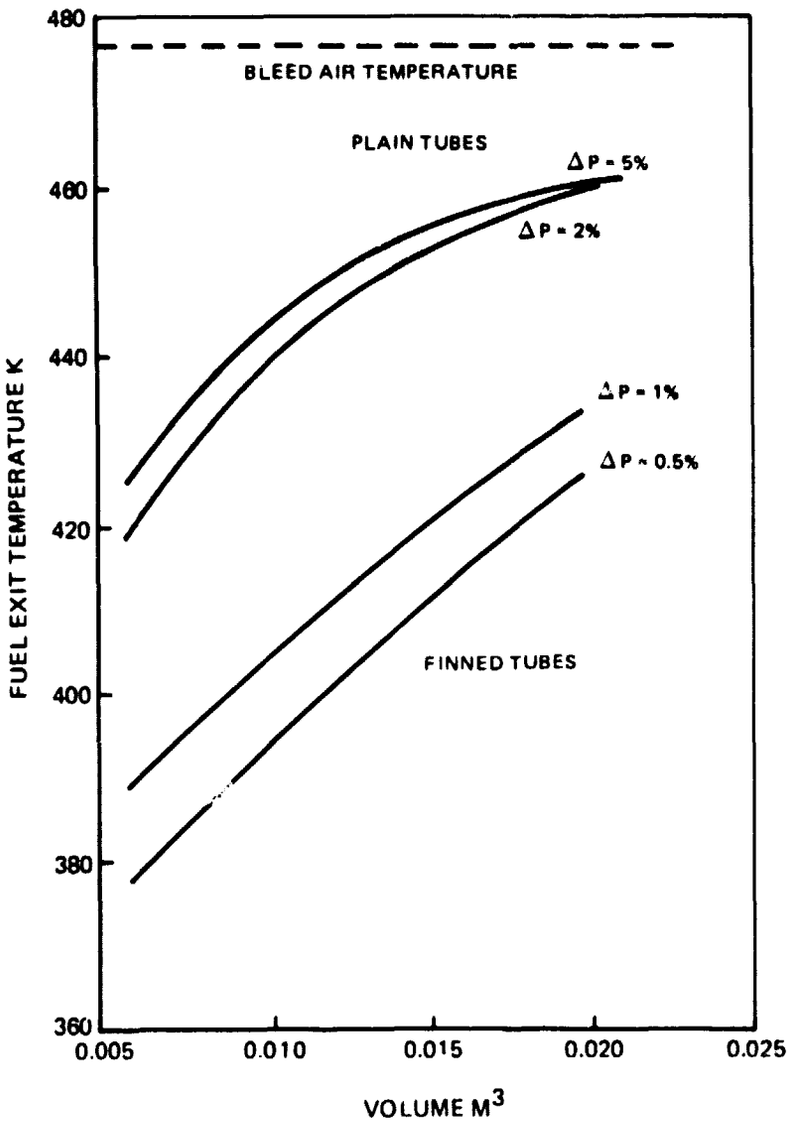

79-08-17-3

Vaporizer

Vaporization of the fuel takes place within the cooling channels of a fuel-cooled main engine combustor. Combustor wall cooling was examined for two versions of an LPP combustor, i.e., a single stage, and a dual stage. The single stage combustor requires variable dilution airflow which is controlled to maintain an equivalence ratio of 0.6 in the burning zone. The dual stage operates on the primary stage at low fuel flow and on both primary and secondary stages at higher fuel flow. In the dual stage, the equivalence ratio was assumed to vary linearly between a minimum of 0.36 and 0.60 as shown in Fig. 24. As the overall equivalence ratio is increased above 0.26, the secondary stage is turned on, the primary equivalence ratio is reduced, and both stages operate at the same equivalence ratio.

A conceptual representation of the two-stage combustor is shown in Fig. 23. The fuel flows circumferentially along the combustor wall in a rectangular channel which has a radial dimension of 0.63 cm and an overall axial dimension of 1/2 of the axial length of the wall. The channel has a number of radial partitions to produce suitable structural rigidity. The fuel paths are shown in Fig. 28. The fuel enters the inlet distribution manifold through the burner case near the aft end of the combustor, flows circumferentially again to the collector manifold. It can be seen in Fig. 28 that the fuel channels of intermediate and inner walls are fed from the forward end of the combustor to the first passage where the circumferential flow begins.

Steady-State Operation

A schematic diagram of the component arrangement for operation with either a single stage or dual stage combustor is shown in Fig. 29. Also shown are the steady-state operating parameters for the four engine operating conditions which include SLTO, cruise, approach, and idle. Transient operation and altitude relight are discussed in later sections.

In the dual stage combustion concept, it is desirable to locate the fuel control for metering the primary and secondary fuel flow in a deposit-free environment. Therefore, the preheater was split into a dual-stage unit (Fig. 29), which can be a single component with two sets of passages. Each stage supplies fuel to portions of the combustor walls which are dedicated to the vaporization of fuel feeding the primary and secondary injectors. When only the primary fuel is flowing, the intermediate wall between the primary and secondary combustion zones (Fig. 23) is cooled by fuel flowing in passages on the primary side. There are also passages on the secondary side of the intermediate walls for cooling with fuel when the secondary stage is active. All of the compressor bleed air is used in a single preheater during primary-only operation. When the secondary fuel is turned on, the flow splitter is actuated to split the bleed air between the two preheaters; secondary fuel leaving the second preheater is fed to fuel passages on the secondary side of the combustion zone.

The combustor wall temperature along the fuel path varies as the fuel temperature increases. Calculated wall temperatures at the four E^3 engine operation conditions are listed in Table 9.

FIG. 28

SCHEMATIC REPRESENTATION OF FLOW IN FUEL-COOLED COMBUSTOR WALLS

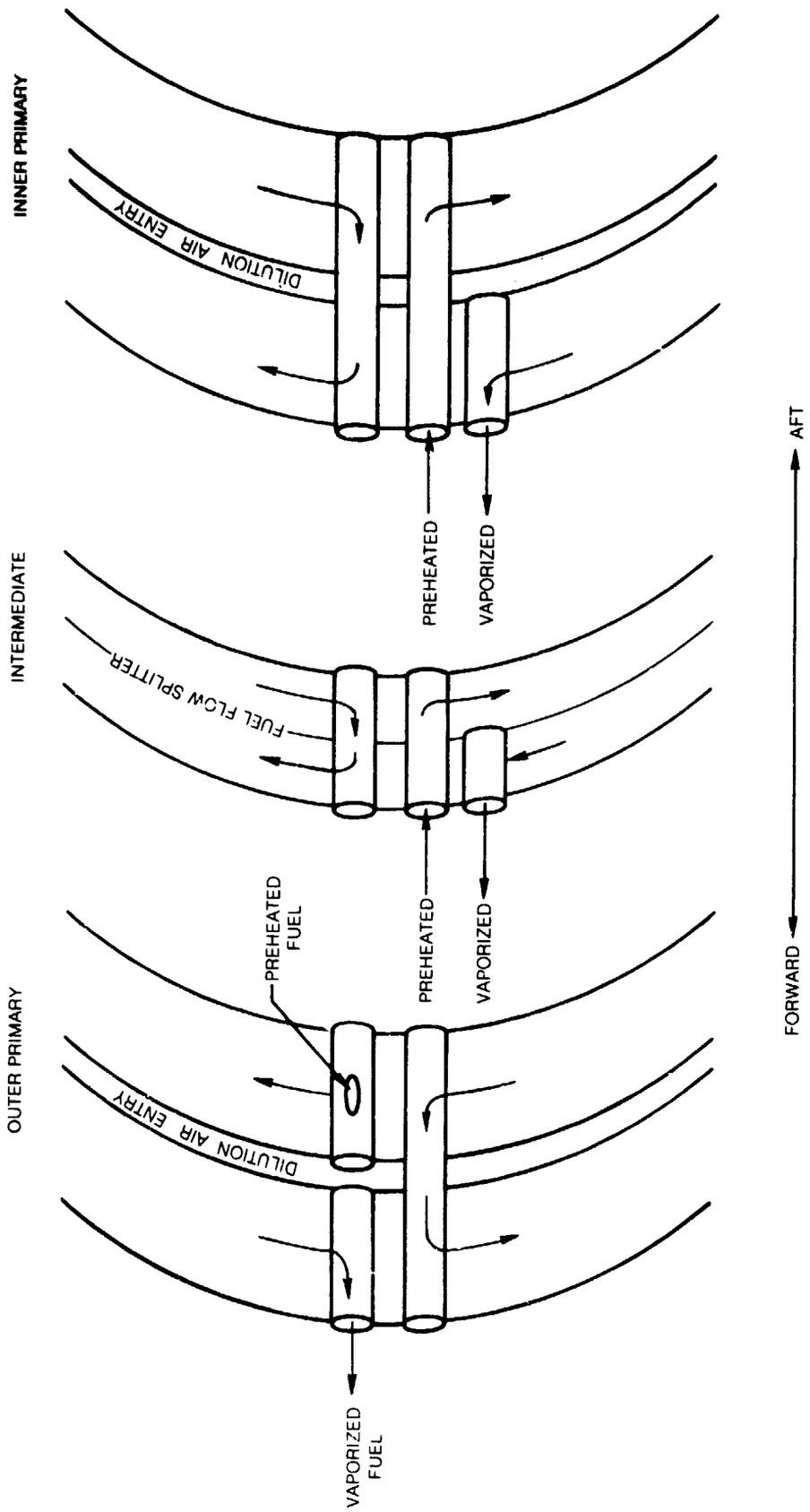

79-09-17-9

FIG. 29

EXTERNAL VAPORIZER — FUEL SYSTEM DIAGRAMS

SCHEME 2 — TWO-PHASE

SINGLE STAGE COMBUSTOR

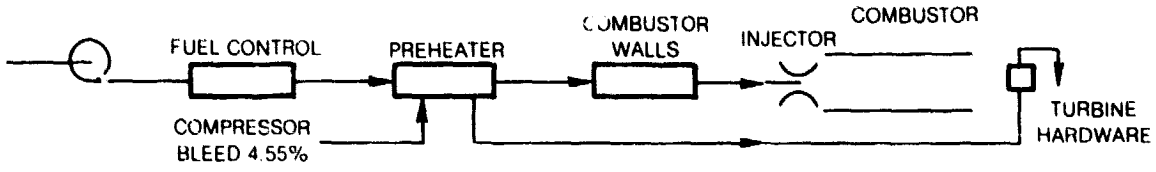

DUAL STAGE COMBUSTOR

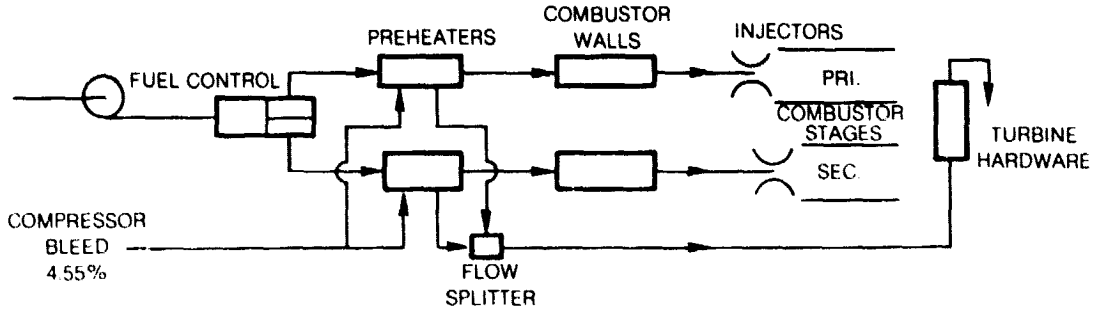

	SLTO	CRUISE	APPROACH	IDLE
COMPRESSOR DISCHARGE				
PRESSURE ATM	31.1	13.8	11.7	4.4
TEMP K	810	754	621	473
PREHEATER DISCHARGE				
FUEL TEMP K	560	565	546	453
AIR TEMP K	489	439	446	406
INJECTOR INLET				
FUEL PRESSURE ATM	34.6	17.0	12.7	4.8
FUEL TEMP K	698	688	679	652
DEW POINT K	683	661	644	594
INJECTOR PRESSURE DROP %				
SINGLE STAGE	10	10	8	8
DUAL STAGE	10	10	16	16

79-10-23-2

Table 9

COMBUSTOR WALL TEMPERATURE, K

SLTO	765 - 1070
Cruise	630 - 760
Approach	610 - 770
Idle	570 - 800

The potential use of the turbine inlet guide vane walls as sources of heat was also investigated as an alternative to cooling the combustor walls. It was found that although the surface area of the vanes is only about one-fifth of the combustor surface area, the gas-side heat transfer coefficients at the vane surfaces produce a much greater heat flux in the turbine inlet guide vanes. It was found that the existing E^3 surface area would yield about half of the heat required for fuel vaporization. An extension of the vanes approximately 7.6 cm along the engine axis into the combustor would be necessary to supply all of the heat. To use this approach, however, the fuel passage size must be kept very small in order to produce the high fuel side heat transfer coefficients needed to offset the high gas-side coefficients. Calculations based on a passage size of 0.5 cm resulted in a wall temperature of 1480 K which is considered to be excessive.

The performance of the components in Scheme 2 at four E^3 engine conditions is shown in Fig. 29. A comparison of the second group of data with the first group indicates that the compressor bleed temperature is decreased by 330 K in the preheater. Therefore, the bleed flow leaving the preheater is valuable for turbine cooling. The third group of data indicate that the fuel temperature leaving the combustor wall cooling passages is always higher than the minimum temperature required for complete vaporization.

Scheme 3

As shown in Fig. 1, the main components of Scheme 3 are an intercooler, a pump, an auxiliary burner, and a mixer. The mixer is the fuel vaporizer in which fuel is sprayed into preheated air at an equivalence ratio much greater than stoichiometric. The preheated air is the vitiated product of the auxiliary burner. Because this air is returned to the main engine combustor, the air pressure must be boosted by the pump to make up the loss in the auxiliary burner. The intercooler is used to cool the bleed air in order to minimize the pump size and horsepower requirement.

Mixer-Vaporizer

The design of the mixer-vaporizer is based on the concept that fuel and heated air at an equivalence ratio considerably above stoichiometric (7-13) can be mixed rapidly enough to produce a homogeneous, vaporized mixture without reaching chemical equilibrium. Although the temperatures associated with chemical equilibrium are acceptable, soot can be produced in considerable concentrations (as shown in Fig. 30). Local conditions must also be considered because locally, the

FIG. 30

CARBON FORMATION AND TEMPERATURE AT EQUILIBRIUM

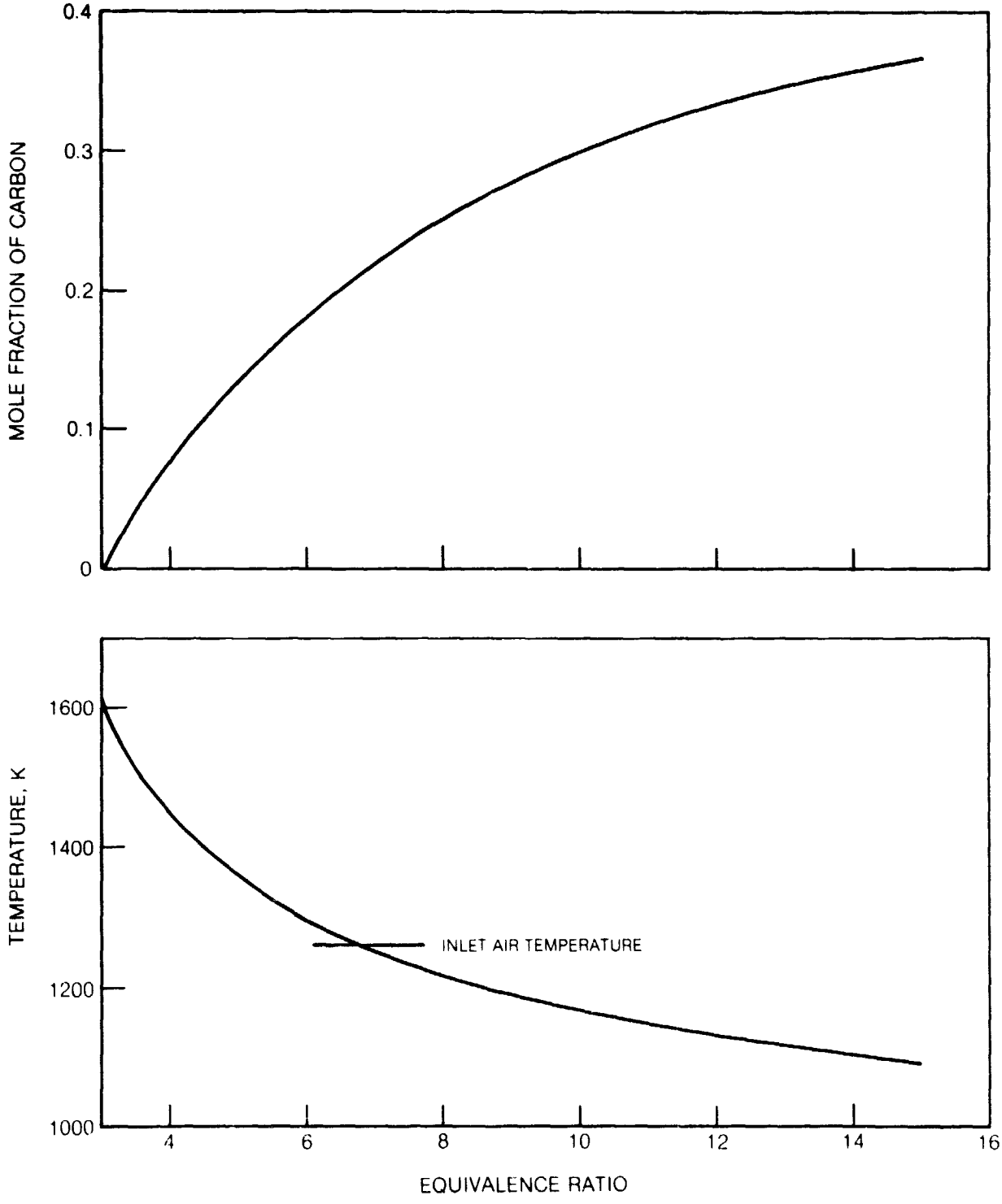

80-2-71-15

vapor fuel-air ratio encompasses the entire range from zero to the final rich value including stoichiometric. Autoignition in the region near stoichiometric must be avoided because severe overheating could result. Mixer-vaporizers have been in limited use in aircraft engines, but experience to date has been with units producing in the order of 15 percent vaporized fuel while the unit in Scheme 3 is expected to produce 100 percent vaporization. There is some evidence to support the possibility that air can be added to the fuel during the vaporization process without producing soot. Data were reported in Ref. 3 from experiments in which air was added to fuel over a range of equivalence ratio from 15 to 30. The fuel was vaporized in electrically heated tubes without the formation of soot deposits.

The mixer-vaporizer is a round, constant-area duct. The fuel is fed into the duct with a uniform distribution of small droplets and the length of the duct is calculated to provide sufficient residence time for complete fuel vaporization. Length and residence time are a function of droplet size, inlet temperature, mixer diameter (gas velocity), and hot gas flow. Design calculations were made at SLTO for a range of these parameters and the effect of inlet temperature is shown in Fig. 31, the effect of diameter is shown in Figs. 32 and 33, and the effect of hot gas flow is shown in Fig. 34. It can be seen that length and residence time are strong functions of droplet size and it will be important to produce droplets in the order of 50 μ diameter. The inlet air temperature was chosen to be 1255 K in order to permit use of high-temperature nickel-based alloys like Hastelloy X. The duct diameter was chosen to be 8.9 cm.

It was found that unlike Schemes 1 and 2 where bleed airflow was held constant, the required length for mixing and residence time in the mixer were essentially constant when the bleed velocity instead of the airflow was held constant at all of the E^3 conditions. A summary of mixer operation at the four engine conditions is contained in Table 10.

Table 10

PERFORMANCE OF 8.9 cm MIXER

	SLTO	Cruise	Approach	Idle
Inlet Gas Velocity, m/sec	37	37	37	37
Air Flow, %	2.86	2.75	2.39	1.95
Mixer Length, cm for Droplet Sizes:				
50μ	7.0	7.0	7.0	5.7
75μ	12.0	13.3	14.6	14.6
120μ	29.3	30.5	31.8	36.9
Residence Time, msec for Droplet Sizes:				
50μ	3.8	4.1	3.5	3.4
75μ	7.7	8.4	7.3	7.4
120μ	17.8	18.8	16.5	18.2
Exit Temperature K	735	745	845	885

MIXER LENGTH VS. INLET GAS TEMPERATURE

12.7 cm MIXER DIAMETER
3.7% OF ENGINE AIRFLOW

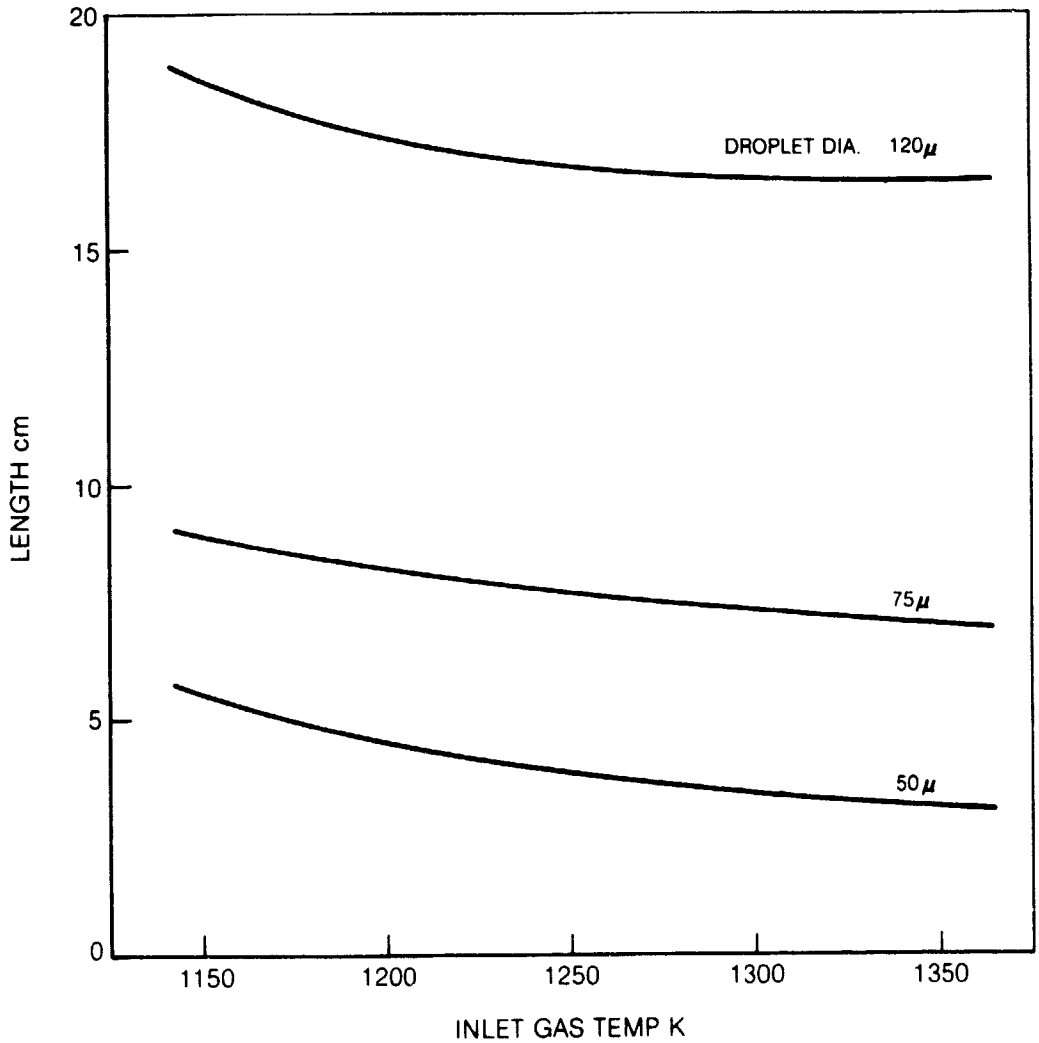

79-09-17-4

FIG. 32

MIXER LENGTH VS. DIAMETER

1250K INLET GAS TEMP.
3.7% OF ENGINE AIRFLOW

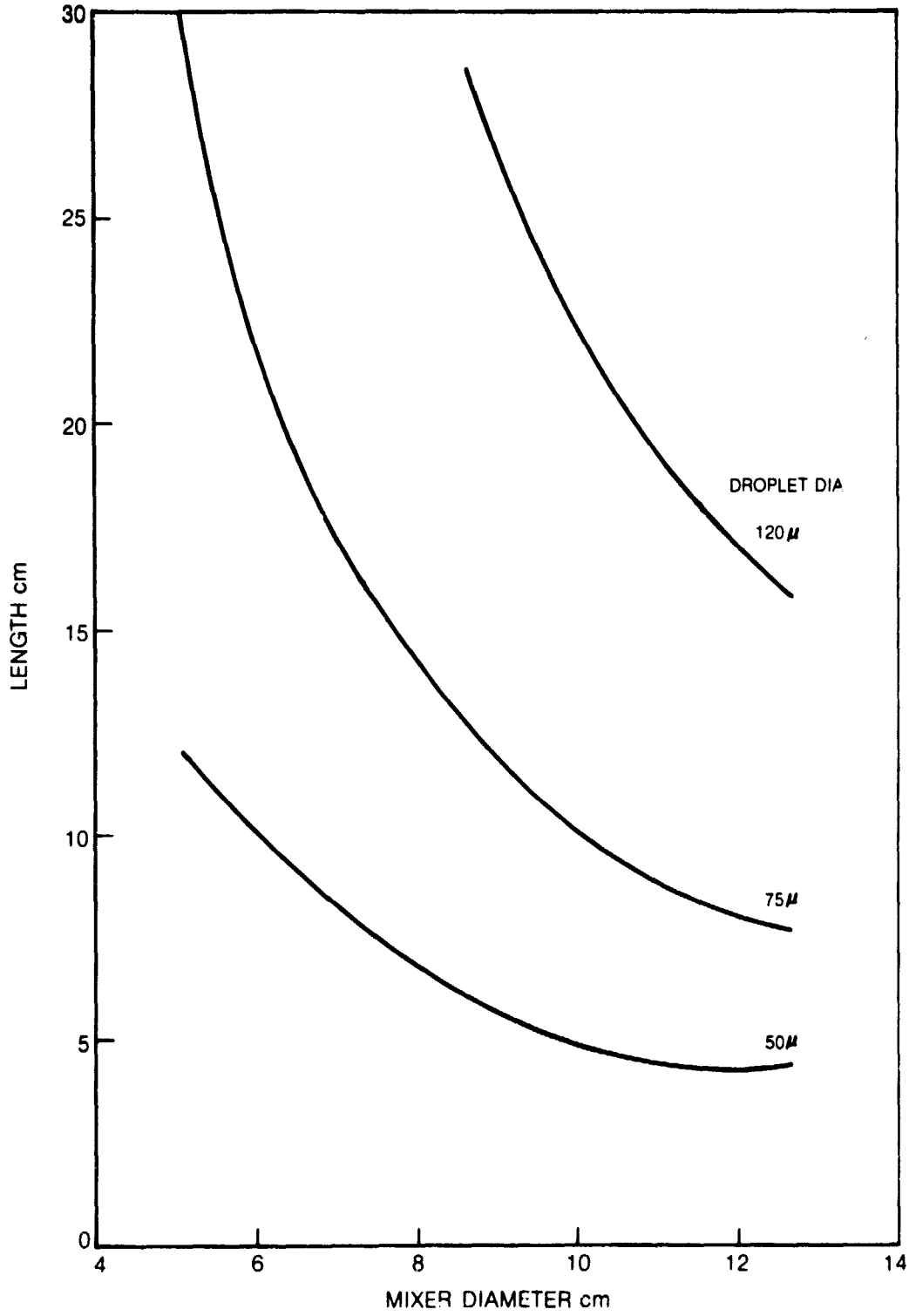

79-09-17-3

FIG. 33

RESIDENCE TIME IN MIXER

1250K INLET GAS TEMP.
3.7% OF ENGINE AIRFLOW

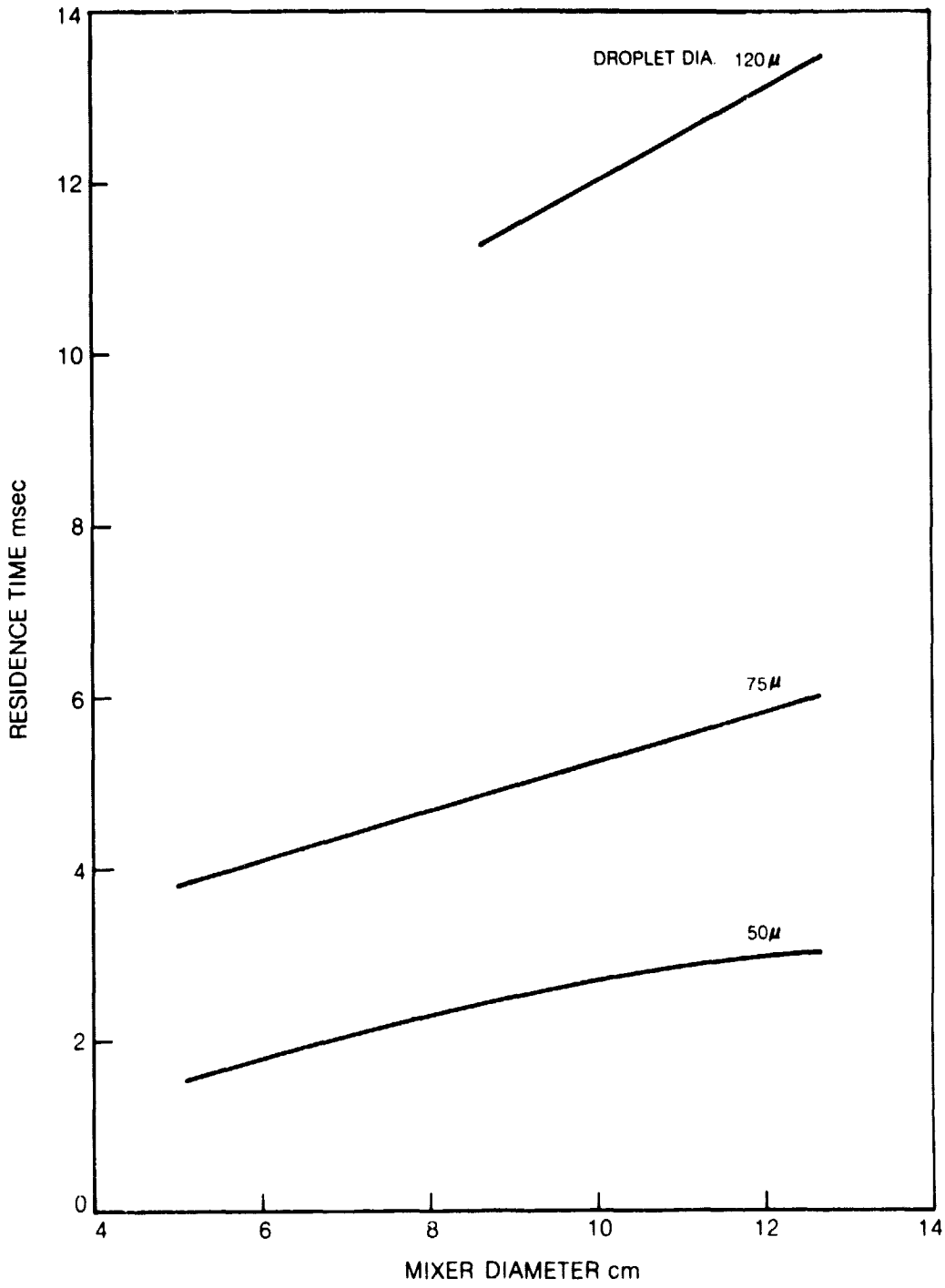

79-09-17-2

FIG. 34

MIXER LENGTH AND RESIDENCE TIME

8.9 cm MIXER DIAMETER
1250K INLET GAS TEMPERATURE

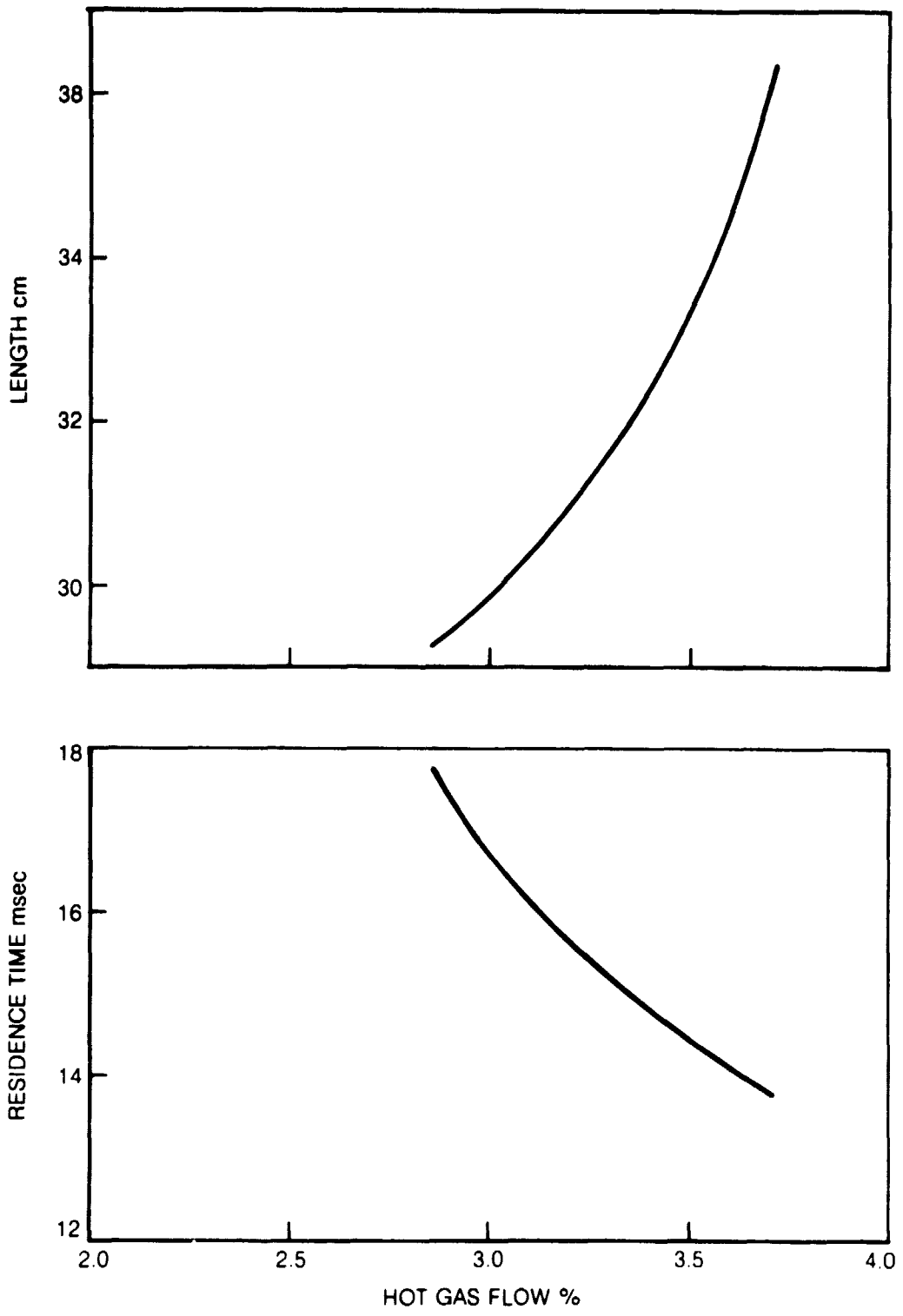

79-09-17-1

Auxiliary Burner

The auxiliary burner airflow and exit temperature in Scheme 3 is the same as in Scheme 1. Therefore, the auxiliary burner diameter was selected to be 9.4 cm and the length, 19 cm. The altitude relight conditions are also the same for Scheme 3 as they are for Scheme 1; therefore, a dual-orifice pressure atomizer can be used to satisfy all of the operating conditions.

Air Pump

The bleed air pump is a scaled version of a centrifugal air compressor produced by the Hamilton Standard Division of United Technologies for aircraft cabin air conditioning. For the purpose of analysis, it was assumed to operate at 24,000 rpm, which is considered to be within the state-of-the-art in gearbox design. The impeller diameter and the required drive horsepower are shown for the two intercoolers and for no intercooler in Fig. 35. These results are based on a bleed airflow of 3.7 percent. Airflow has a direct effect on required horsepower and a small effect on impeller diameter, as shown in Fig. 36.

Intercooler

The intercooler analysis was based on the use of plain tubes which were found to result in compact heat exchangers in Schemes 1 and 2.

Two sizes of intercoolers were analyzed, and the results of the analysis are shown in Table 11. The analysis accounts for the deposit thickness that is expected to be present on the intercooler walls after 100 hours.

Table 11

INTERCOOLER PERFORMANCE ANALYSIS

	Intercooler 1	Intercooler 2
Core Volume, m^3	0.0046	0.0019
Exit Air Temp., SLTO, °K	610	710
Exit Fuel Temp., SLTO, °K	450	385
Fuel Deposit Thickness, mm		
SLTO	0.03	0.009
Cruise	0.003	0.001
Approach	0.001	0.0005
Idle	None	None

Intercooler 1 might be capable of several thousand flights between cleaning. Intercooler 2 can be used almost indefinitely without cleaning.

FIG. 35

BLEED PUMP IMPELLER DIAMETER AND DRIVE POWER

3.7% OF ENGINE AIRFLOW
6% VAPORIZER SYSTEM PRESSURE LOSS

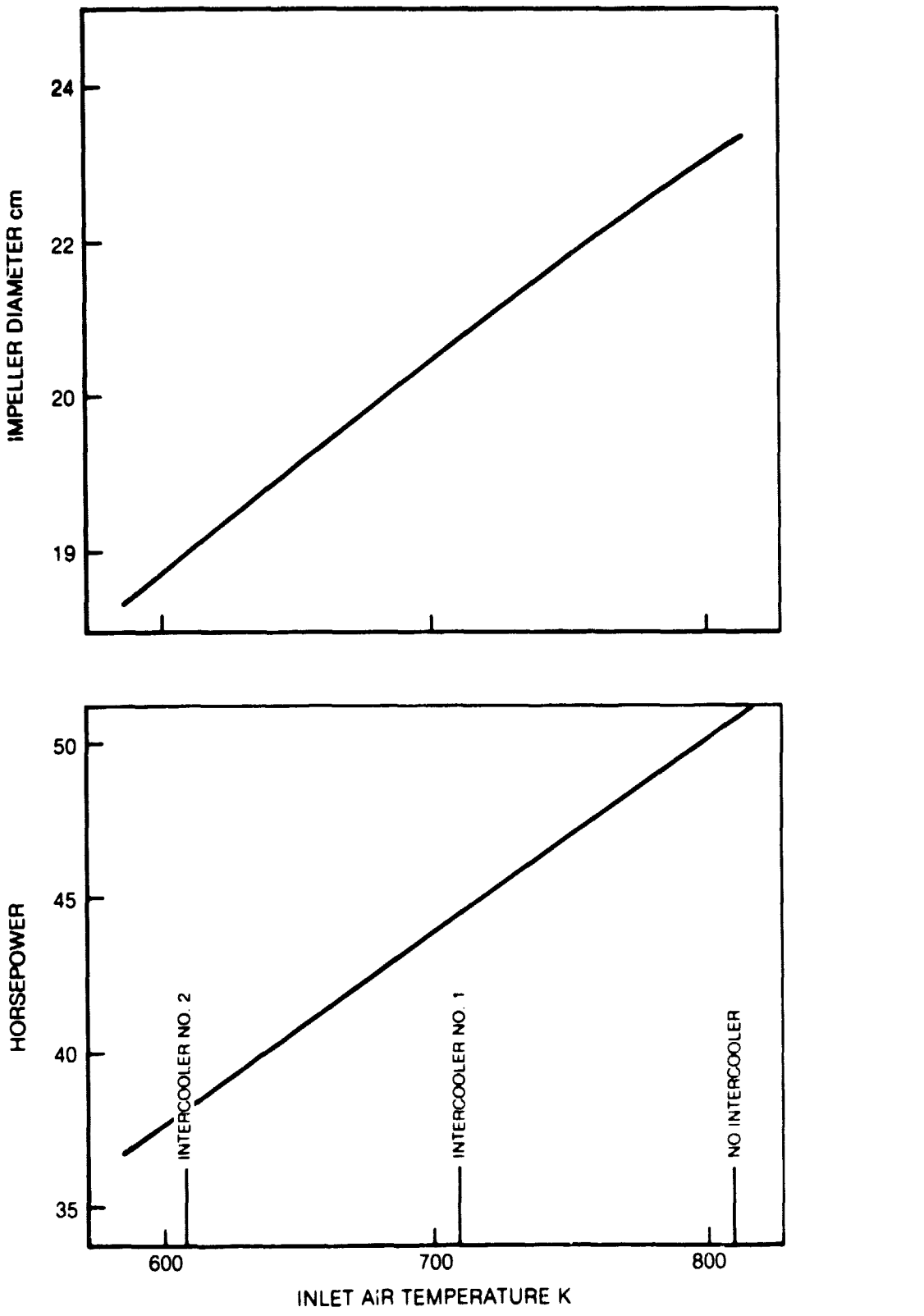

79-09-17-7

EFFECT OF GAS FLOW ON BLEED PUMP POWER AND SIZE

INTERCOOLER NO. 1

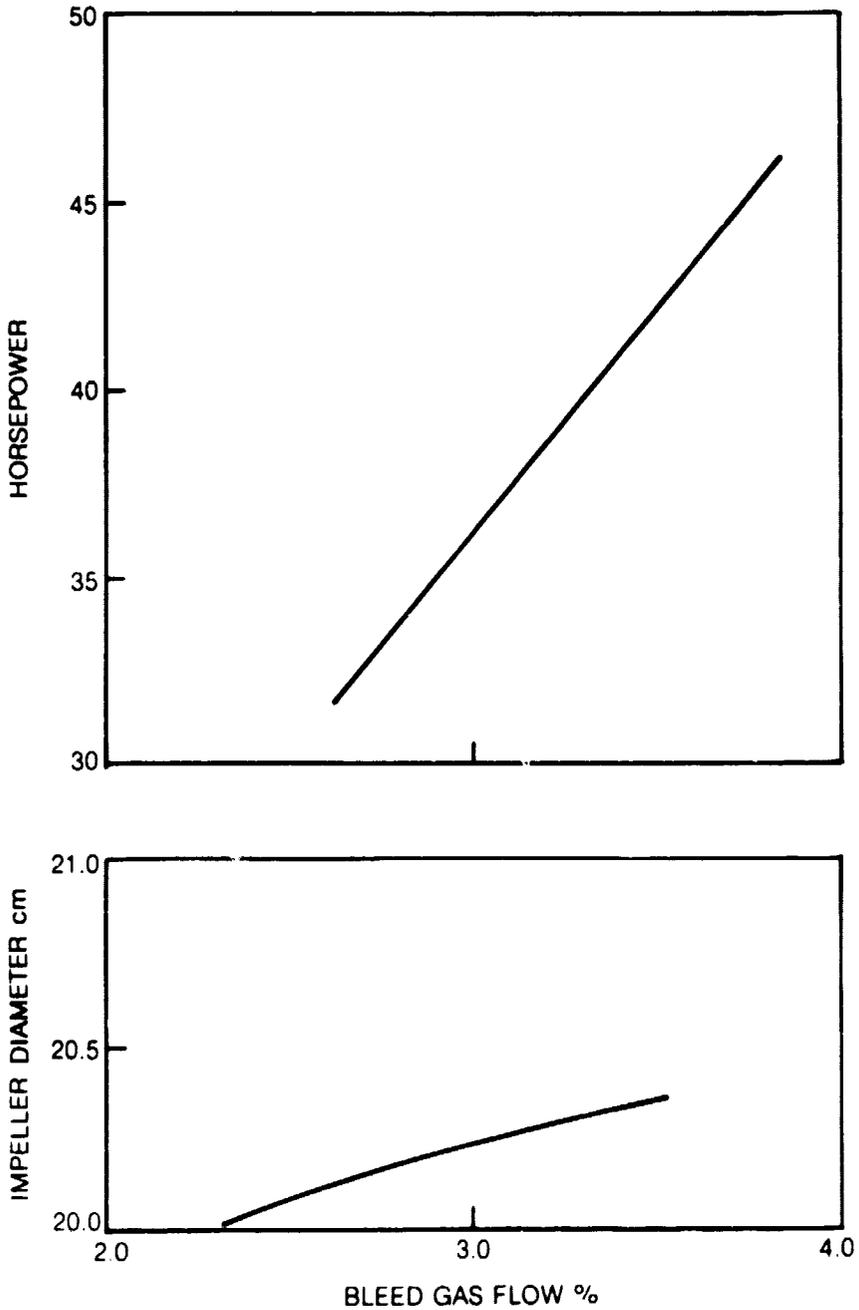

79-09-17-5

Steady-State Operation

It can be seen in Fig. 37 that the component arrangement with a dual stage combustor includes a single intercooler and pump. This arrangement is possible by assuming that the intercooler will not foul the fuel control which allows metering the fuel to the two combustor stages at a point downstream of the intercooler. Two mixers are required because a flow splitter would contain recirculation regions where deposits would form.

The second set of values in Fig. 37, which are intercooler discharge temperatures, refer to the performance anticipated with Intercooler 2. The airflow rates shown in the third set of values are based on a constant velocity of 37 m/sec. Other velocities can be used to alter the equivalence ratio since it is believed that the equivalence ratio can affect the tendency to form soot.

EXTERNAL VAPORIZER — FUEL SYSTEM DIAGRAMS

SCHEME 3 — THERMAL OXIDATION GASIFIER — TWO PHASE

SINGLE STAGE COMBUSTOR

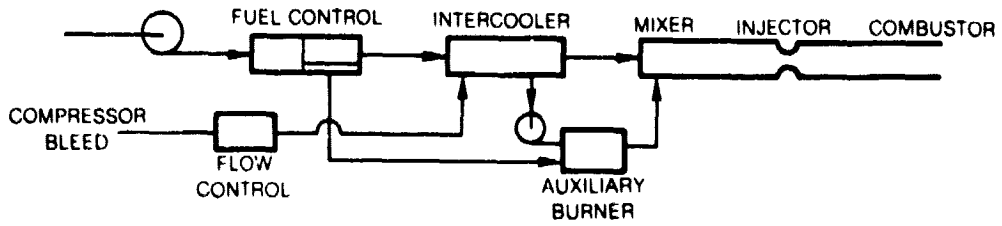

DUAL STAGE COMBUSTOR

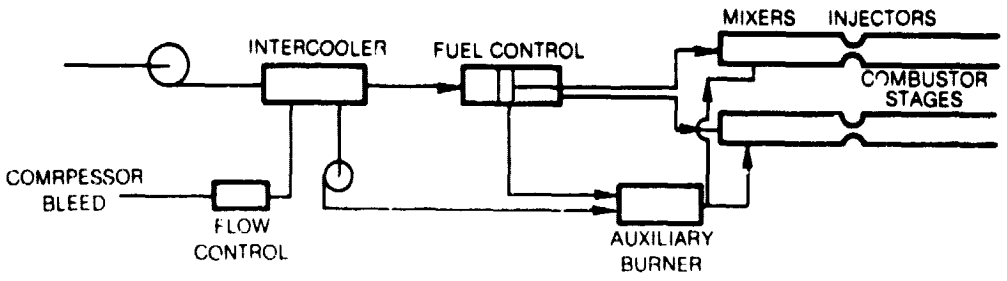

	SLTO	CRUISE	APPROACH	IDLE
COMPRESSOR DISCHARGE				
PRESSURE ATM	31 1	13 8	11 7	4 4
TEMP K	810	754	621	473
INTERCOOLER DISCHARGE				
FUEL TEMP K	385	394	[illegible]	358
AIR TEMP K	709	643	[illegible]	489
AUXILIARY BURNER				
AIRFLOW % OF ENGINE	2 9	2 8	2 4	2.0
DISCHARGE TEMP K	1255	1255	1255	1255
MIXER				
EQUIV RATIO	12 6	12 5	8 5	6 9
RESIDENCE TIME msec	1 7 8	1 8 0	1 5 1	1 4 4
EXIT GAS TEMP K	735	747	845	883
INJECTOR PRESSURE DROP %				
SINGLE STAGE	10	10	6	5
DUAL STAGE	10	10	14	10

79-10-23-3

PACKAGING

The relative shapes of the engine compressor and burner cases and the fan duct usually create a space for packaging engine components such as the gearbox, fuel control, fuel pump, oil cooler, oil tank, fuel lines, bleed ducts, etc. Although this space in production engines does not leave room for large additional components such as the heat exchangers and auxiliary burners described in this report, major modifications in development engines could create the necessary space. Assembly drawings of the E^3 engine indicate that external fuel vaporization components can fit around the high compressor and burner cases if space is allowed for them while packaging other components. Artistic views of the component arrangements for the three Schemes are shown in Figs. 38 to 40.

FIG. 38

SCHEME 1 PACKAGING ARRANGEMENT

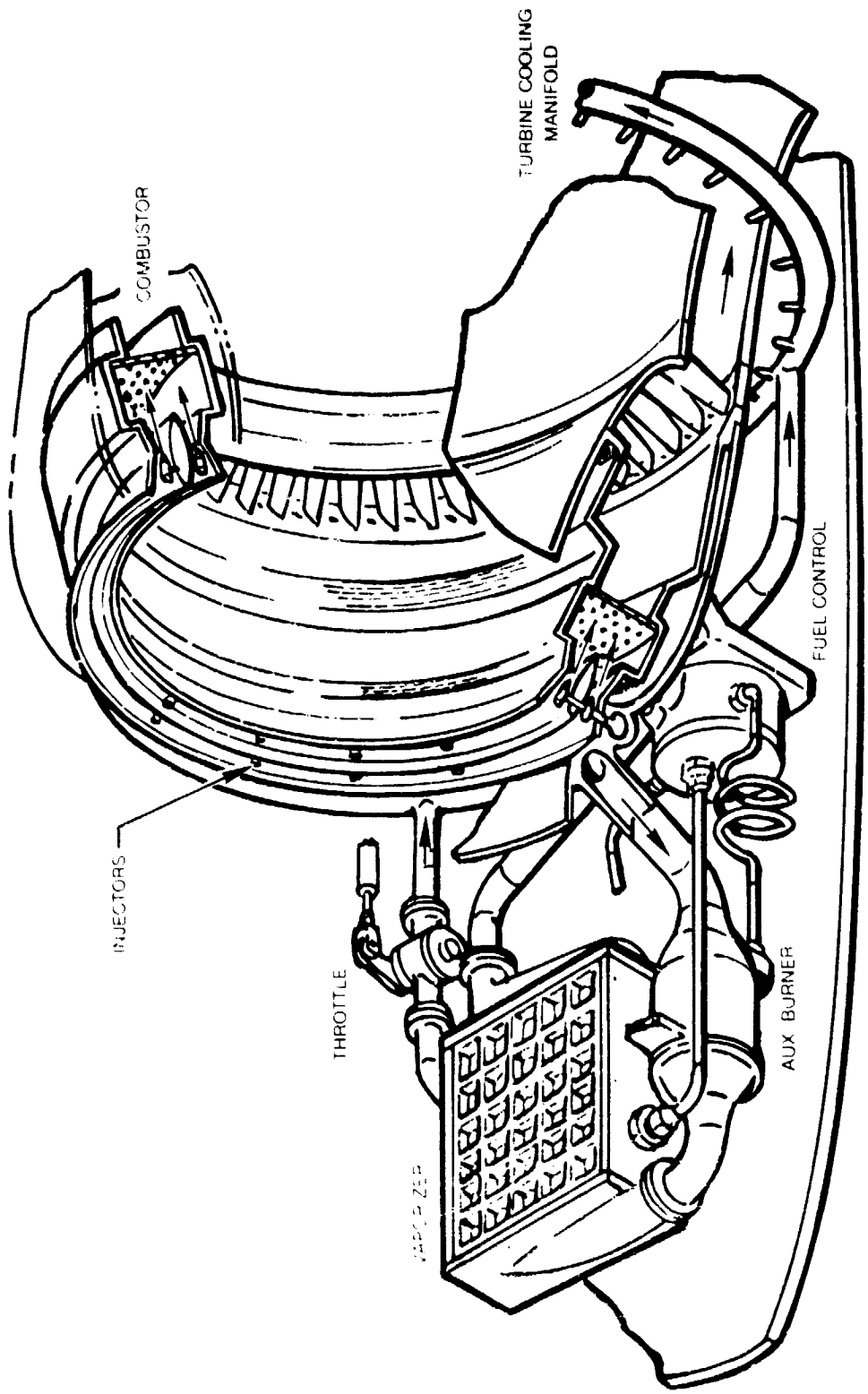

80 2 71 3

FIG. 39

SCHEME 2 PACKAGING ARRANGEMENT

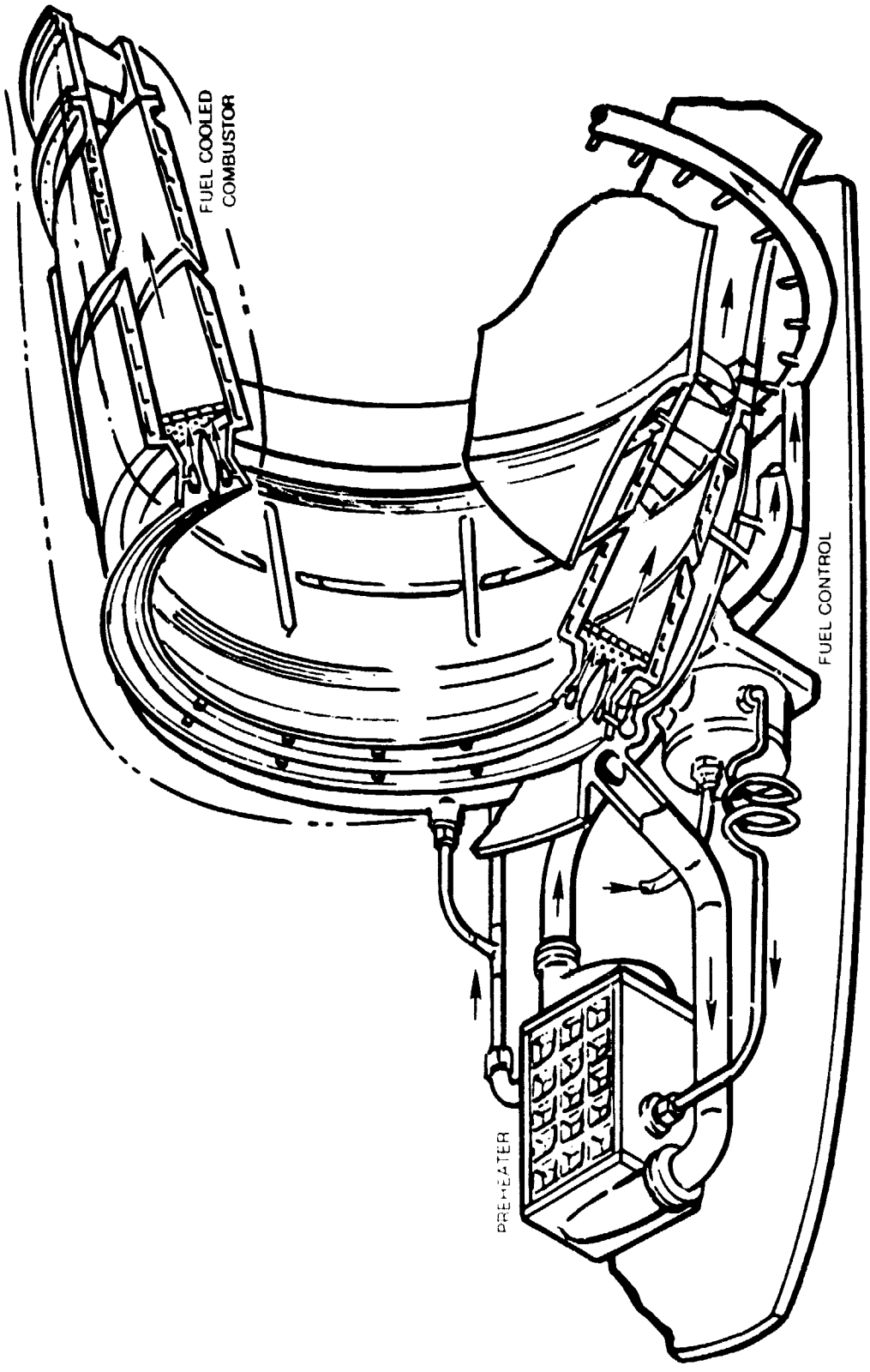

80-2-71-4

FIG. 40

SCHEME 3 PACKAGING ARRANGEMENT

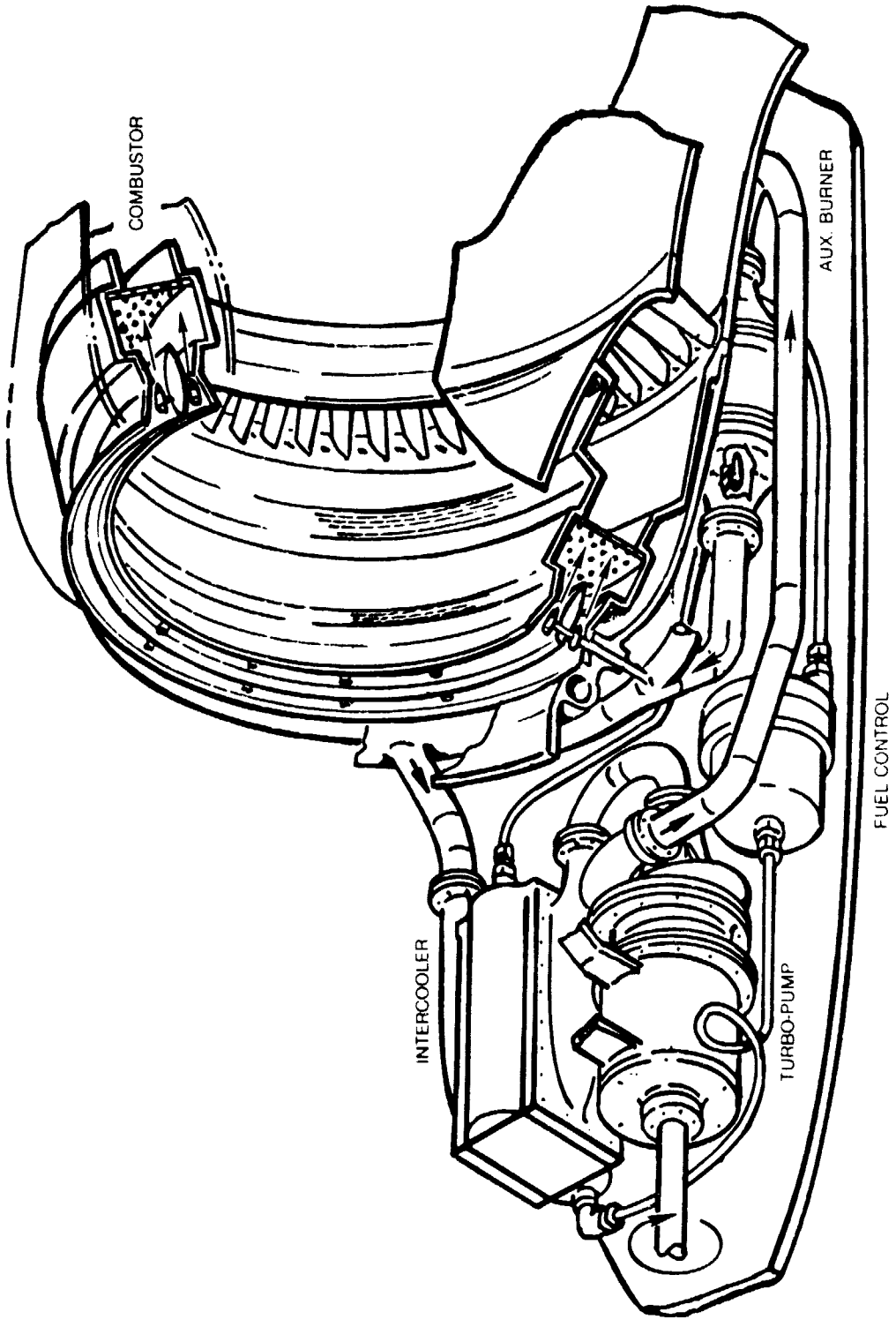

80-2-71-5

WEIGHT

Weights of the components of the three schemes were estimated in order to provide input for the ranking of the individual schemes. In two of the three schemes, the heat exchanger is the heaviest component and the heat exchanger shell weight is more than twice the tube weight. The reason for this lies in the rectangular cross section of the heat exchanger. Since the shell is a pressure vessel that is exposed to 31 atm at SLTO, the rectangular shape is not structurally ideal for this purpose. The rectangular shape was chosen because it is a straightforward way of attaining the multipass cross-counterflow arrangement that results in a minimum heat exchanger volume. Further detailed design effort might produce a heat exchanger flow arrangement with a lighter shell.

The estimated weights of the components are listed in Table 12.

Table 12

ESTIMATED FUEL VAPORIZATION SYSTEM WEIGHTS, Kg

Scheme 1		
Vaporizer Tubing	23.0	
Vaporizer Shell	72.7	
Vaporizer Manifolds	2.5	
Auxiliary Burner	3.8	
Connecting Lines	2.8	
Total		105
Scheme 2		
Preheater	36.0	
Added structure in combustor	24.5	
Connecting Lines	2.6	
Total		63
Scheme 3		
Intercooler	13.2	
Air Pump	30.0	
Combustor	3.6	
Mixer	1.5	
Connecting Lines	4.0	
Total		52.3

ENGINE PERFORMANCE

Engine performance was evaluated with the assumptions that the cooled air leaving the heat exchanger in Schemes 1 and 2 was effective in reducing overall turbine cooling airflow requirements. Scheme 3 had no redeeming features to offset the effect of the air pump power requirement. In evaluating engine performance, the core size and airflow were essentially unchanged and the fan size was revised for a different airflow. Two approaches concerning the cooling airflow were taken. In the first approach, the total turbine cooling airflow was reduced and the combustor exit temperature was held constant. In the second approach, the total turbine cooling airflow was held constant and the combustor exit temperature was allowed to increase.

Reduced Turbine Cooling Flow

The use of precooled turbine cooling air with a constant engine core size permits the reduction of total cooling air flow. Cooling flow is ultimately mixed with the main core flow resulting in a loss of turbine efficiency. Less cooling flow results in less turbine efficiency loss and a reduction in specific fuel consumption. Less cooling flow results in an increase in available turbine power which can be used to increase the air flow through the fan. More fan flow results in more thrust. Table 13 contains a summary of the changes in engine operating parameters and performance.

Table 13

PERCENT CHANGES IN PERFORMANCE WITH REDUCED TURBINE COOLING FLOW

Scheme	1	2	3
Design			
Turbine Cooling Air	- 2.1	- 2.9	None
Bypass Ratio	+ 1.9	+ 2.8	None
Turbine Efficiency	+ 0.25	+ 0.35	None
SLTO			
Thrust	+ 2.0	+ 2.5	- 0.30
Specific Fuel Consumption	- 0.25	- 0.50	+ 0.10
Max Cruise			
Thrust	+ 1.4	+ 2.1	- 0.1
Specific Fuel Consumption	- 0.30	- 0.50	None

Increased Combustor Exit Temperature

Precooled turbine cooling air with a constant engine core size permits an increase in combustor exit temperature if the total cooling air flow remains constant. Higher combustor exit temperature increases the overall cycle efficiency which results in an increase in available power. The power can be used to increase the airflow through the fan and more fan flow results in greater thrust. In the E^3 engine which incorporates a single stage turbine operating at a supersonic Mach number, the higher combustor exit temperature reduces the expansion ratio and increases turbine efficiency. The result is a reduced engine specific fuel consumption. Table 14 contains a comparison between the effects of reduced turbine cooling flow vs. increased combustor exit temperature on an engine with a Scheme 1 fuel vaporization system.

Table 14

COMPARISON BETWEEN TWO DESIGN APPROACHES

Design	Reduced Cooling Flow	Increased Exit Temperature
Turbine Cooling Air, %	- 2.1	None
Combustor Exit Temperature, K	None	+ 80
Bypass Ratio, %	+ 1.9	+ 12
SLTO		
Thrust, %	+ 2.0	+ 10.3
Specific Fuel Consumption, %	- 0.25	- 0.9
Max Cruise		
Thrust, %	+ 1.4	+ 10.3
Specific Fuel Consumption, %	- 0.30	- 0.5

It can be seen that both approaches result in an increase in thrust. The thrust change in the second approach is substantial, and the corresponding weight change (for the fan) is much smaller. As a result, allowing an increase in the combustor exit temperature results in a 3.3% reduction in thrust/weight ratio. A more substantial engine study in which the core size of the engine is varied would show that the thrust/weight ratio and thrust can be traded against the weight penalty of the Scheme 1 external fuel vaporization system.

TRANSIENT RESPONSE

An external fuel vaporization system can affect both the acceleration and deceleration characteristics of an engine because the temperature of the heat exchanger varies with changes in engine flows and temperatures. Discrete increments in time are required to vary the heat exchanger temperature. To distinguish whether the time increments have a deleterious, beneficial, or inconsequential effect on the engine would require the addition of a heat exchanger performance algorithm to the engine transient response calculation. The scope and scheduling constraints of the present program dictated the need for an alternative approach to judge the relative effect of the three schemes and the possible impact on the external fuel vaporization system on engine response.

The method employed in the transient response evaluation was to examine in detail the critical components of each of the three schemes during acceleration from idle to SLTO. The internal engine parameters during a normal transient for a typical modern jet engine were normalized and divided into several time increments. These parameters included fuel flow, equivalence ratio, steady-state heat exchanger exit temperatures, etc. Two of these parameters are shown in Fig. 41. For Schemes 1 and 2, the time required to proceed from steady-state conditions affecting the heat exchanger (flows, temperatures, and pressures) at the beginning of an increment to steady state conditions at the end of the increment was determined. The acceleration response time was defined as the sum of these incremental times. For Scheme 3, the mixer length and residence time required for 100 percent vaporization were calculated at each of the time increments and compared with the required length and residence time at Idle and SLTO.

Scheme 1

Heat exchanger performance calculations during the acceleration transient did not converge in some of the increments and the cumulative response time was not considered to be reliable. Previous studies had indicated that failure of the solution to converge was caused by the shape of the deposit formation vs. temperature curve shown in Fig. 13. Convergence was obtained by changing the shape of the curve to the modified and monotonic shapes and the cumulative response times depended on the selected curve. A summary of the results is shown in Table 15.

Incremental calculations were also made to determine the heat exchanger response time during engine deceleration. The engine power change that was chosen incorporated a range from maximum climb power to idle; such a variation could exist during an emergency shutdown. A constant heat exchanger gas-side inlet temperature of 1145 K was used as in the previously reported steady-state design calculation.

ENGINE ACCELERATION TRANSIENT

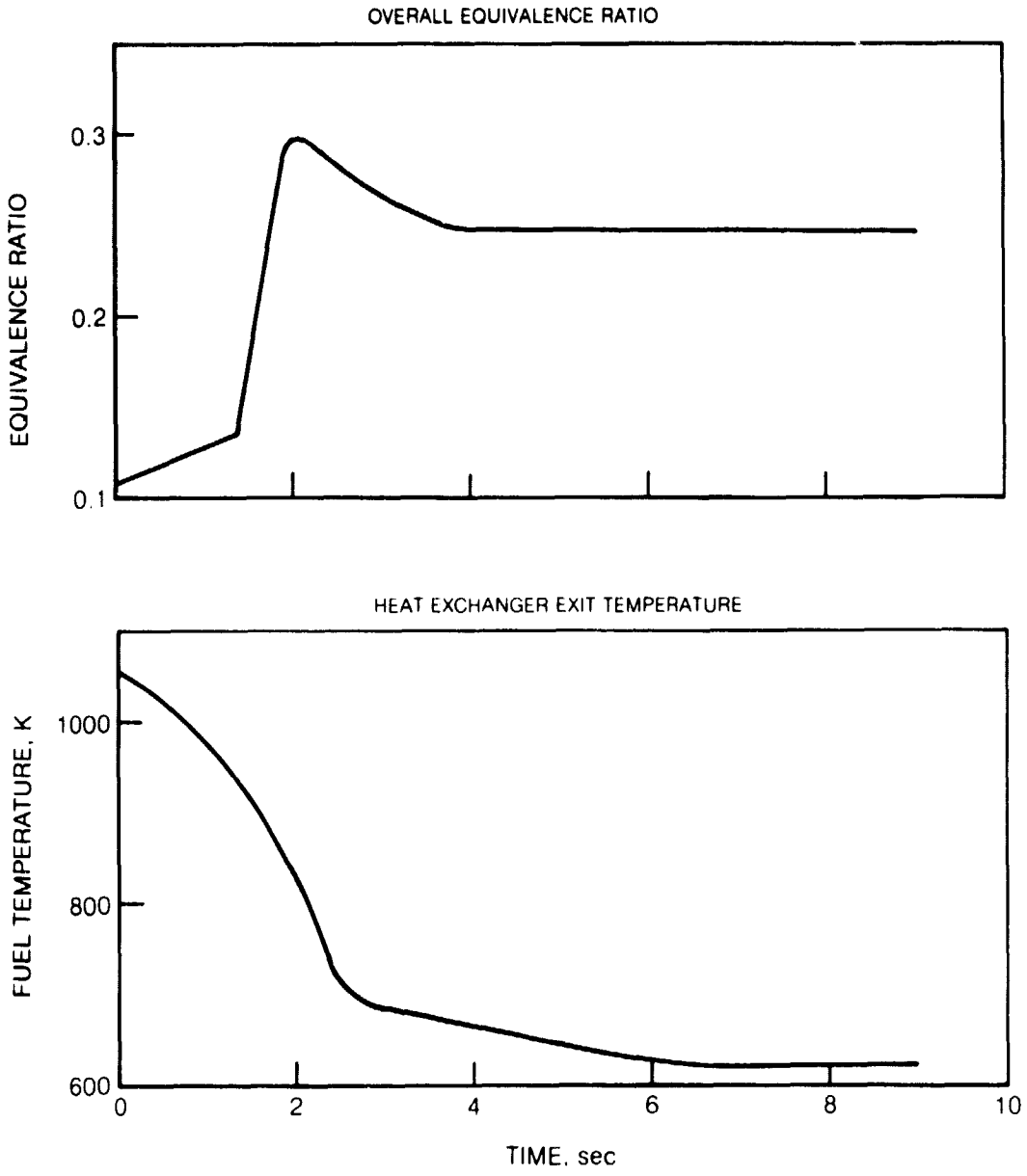

80-2-71-16

Table 15

RESPONSE TIME DURING ACCELERATION, SEC

Standard Coke Curve	4.5 (did not converge)
No Coke	1.8
Modified Coke Curve	
As-designed Heat Exchanger	4.1
100 Percent Larger	2.0
Monotonic Coke Curve	6.7

Two of the input parameters for the deceleration calculation are shown in Fig. 42. During deceleration, the standard deposit formation curve produced convergence and there was no need to vary the shape of the curve. The results of the deceleration study indicated that the sum of the incremental response times was 1.9 sec.

The absolute value of the heat exchanger response time should not be considered to be a simple addition to the engine acceleration and deceleration transients. For instance, Fig. 41 shows that the heat exchanger is actually cooled during acceleration and full engine power might be achievable even if the heat exchanger temperature is still in transient. The calculated response times can probably be considered as a maximum possible perturbation on the conventional engine transient response. The actual perturbation can only be determined using a calculation in which the vaporization system is integrated with other engine components during the transient.

Scheme 2

In Scheme 2, the heat exchanger in which the fuel is vaporized is the combustor wall and it was used for the calculation of the acceleration transient response time. In the first two time increments, the response time was reasonable; in subsequent increments, the response time was unacceptable. At some time increments, calculations indicated that the state of the fuel at the heat exchanger outlet was a vapor; but at other time increments, calculations indicated that liquid was present. The result of the calculations during acceleration are found in Table 16 where the incremental response time is shown for each of the increments.

FIG. 42

ENGINE DECELERATION TRANSIENT

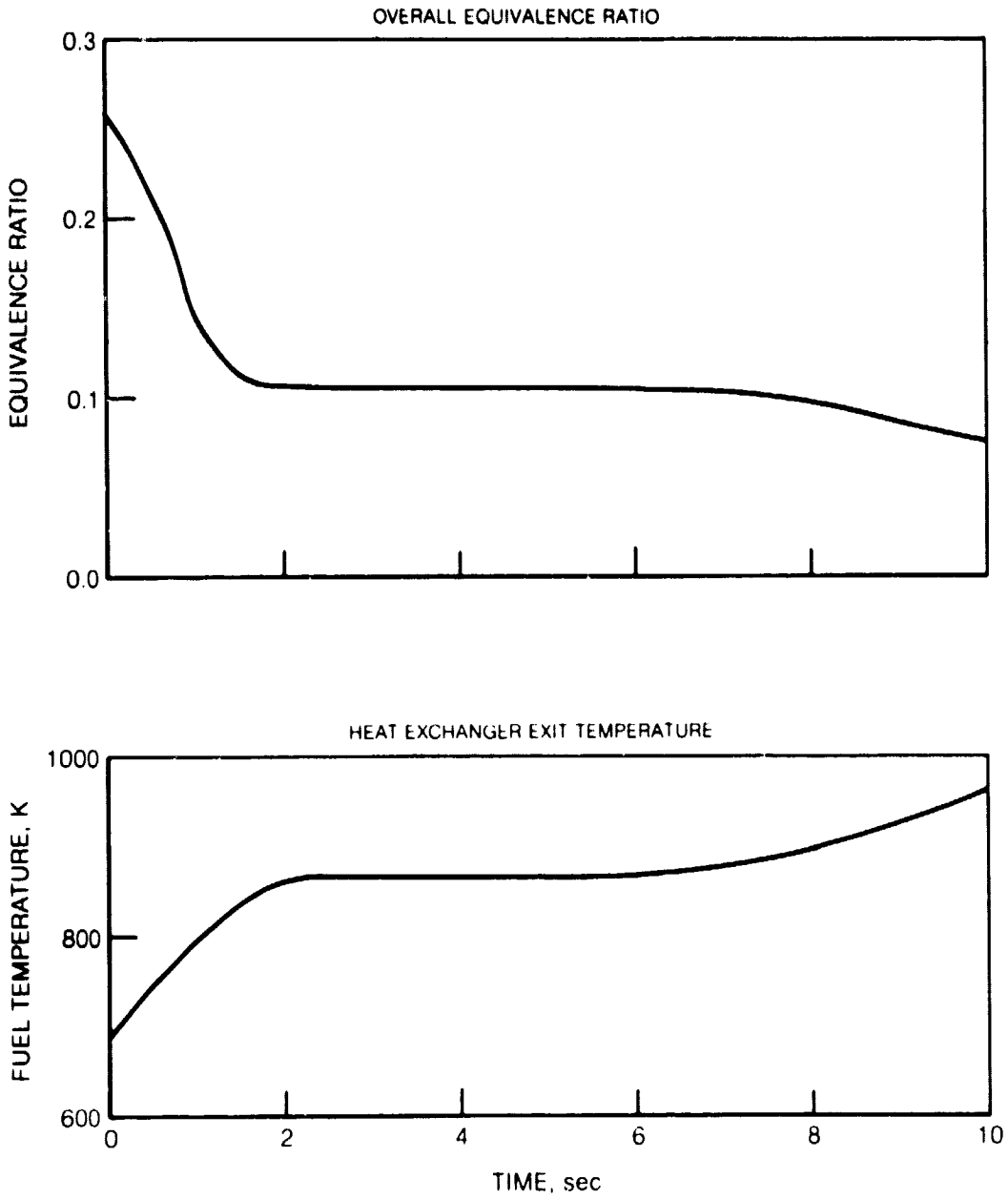

80-2-71-17

Table 16

SCHEME 2 ACCELERATION RESULTS

Time Increment, sec	Incremental Response Time, sec	Fluid State
0	--	Vapor
1.0	0.8	Vapor
1.5	0.4	Vapor
2.0	58	Liquid
3.0	27	Liquid
5.0	73	Liquid
7.0	27	Liquid

Engine acceleration with Scheme 2 is not feasible and considerable modification would be needed before a scheme of this type could be considered for external fuel vaporization.

Scheme 3

In Scheme 3, the fuel is vaporized by mixing it with a hot gas. By comparison with vaporization in a heat exchanger, where a change in wall temperature takes seconds, the process can be considered instantaneous. However, it is important that instantaneously, there is sufficient length and residence time to produce complete vaporization of the droplets. Droplet vaporization calculations were made during the acceleration transient and the results are shown in Table 17.

It can be seen that instantaneous performance at all the transient time increments used in the calculation can be accomplished by a slightly longer mixer than required for SLTO.

Table 17

SCHEME 3 MIXER REQUIREMENTS FOR 50 μ DROPLETS

Time Increment	Required Vaporizer Length, cm	Required Residence Time, msec
0 (Idle)	6.4	3.4
1.0	7.6	3.6
1.5	7.6	4.4
2.0	7.6	5.4
3.0	8.9	5.4
5.0	7.6	4.4
7.0	7.6	4.5
∞ (SLT	7.6	4.3

GROUND START AND ALTITUDE RELIGHT

It is desirable to start an LPP combustor on vaporized fuel because the addition of a liquid fuel startup system could compromise the combustor geometry, complicate the fuel distribution system, and add weight to the engine. The external vaporization system can produce vaporized fuel if there is a supply of air for the hot-side of the heat exchanger in Schemes 1 and 2 or mixer in Scheme 3 and if this air can be heated. Heating of the air in Schemes 1 and 3 which contain auxiliary burners is relatively straightforward in comparison with Scheme 2 where heat is supplied by the main engine combustor.

Ground Start

Startup on the ground with Schemes 1 and 3 can be accomplished with the components illustrated in Figs. 38-40. When the engine rotor is cranked by the starter, the fuel pump can provide sufficient flow to the auxiliary burner. Since air starters are often used for cranking, the air can be directed into the external vaporization system, first to the auxiliary burner and then to the heat exchanger. In Scheme 1, the air can be diverted overboard during startup if the pressure loss in the turbine cooling passages is prohibitive. In Scheme 3, the air pressure at the starter discharge must be sufficient to drive the mixture of air and vaporized fuel through the main engine fuel injectors.

With Scheme 2, the heat required for vaporization is normally supplied by the main engine combustor and special provisions must be made during startup to supply the heat. A possible approach is the use of an auxiliary burner for heating starter discharge air which is then directed to the hot-side of the preheater. If the preheater is correctly sized, the engine startup fuel flow can be vaporized in the preheater in Scheme 2.

Altitude Relight

At altitude relight, the fuel pressure is 0.34 atm and the dew point of the fuel is 495 K. In Scheme 1, a heat exchanger exit temperature of 585 K is required to produce a throttle exit fuel temperature equal to the dew point. Restart at altitude might be possible for Scheme 1 with the components in Fig. 38 if an adjustment in the predicted E^3 engine fuel flow is made. The predicted fuel flow is based on restart of a liquid-fueled burner which requires a high overall fuel-air ratio. A high fuel-air ratio strains the performance capability of the heat exchanger and requires a considerable increase in compressor bleed airflow as shown in Table 18 which contains the results of the heat exchanger analysis. Also shown in Table 18 is the effect of reducing the main combustor fuel flow to lower equivalence ratio values.

Table 18

SCHEME 1 FUEL TEMPERATURE AT ALTITUDE RELIGHT

Target Fuel Temperature = 585 K

Compressor Bleed, %	Engine Combustor Overall Equivalence Ratio	Temperature K
2.85	As Predicted	435
3.50	As Predicted	460
4.25	As Predicted	495
2.85	1.0	490
2.85	0.75	545
2.85	0.63	585

It appears that in Scheme 1, the required heat exchanger fuel flow can be obtained with a reasonable value of airflow and at a fuel flow that represents an acceptable engine combustor overall equivalence ratio.

In Scheme 2 which does not include a throttle valve, the required fuel temperature is equal to the dew point of the fuel which is 495 K. Scheme 2 at altitude, however, has no source of heat for restart. An auxiliary burner is required to heat the bleed air and permit the preheater to act as a vaporizer. During restart, the cold combustor walls must be bypassed because the fuel would be condensed in the cooling passages. Immediately upon restart, the fuel must be switched back to the combustor walls for cooling. The required switching of the fuel paths makes this restart method unacceptable because of its impact on engine reliability. A satisfactory method of altitude restart with Scheme 2 was not devised.

Restart at altitude should be possible for Scheme 3 with the components in Fig. 40. Calculations were made to determine droplet vaporization rates in the mixer using the airflow that corresponds to the velocity (37 m/sec) used in evaluating the mixer performance at the four steady-state E^3 conditions (Fig. 37). The fuel flow corresponds to the value that is predicted for the E^3 engine at altitude relight conditions. The results are shown in Table 19 along with the mixer performance at the SLTO design point.

Table 19

SCHEME 3 CALCULATED MIXER PERFORMANCE

	Altitude Relight	SLTO
Inlet Gas Velocity, m/sec	37	37
Airflow, %	5.3	2.86
Length, cm		
50μ	8.9	7.0
120μ	45.7	29.3
Residence time, msec		
50μ	9.7	3.8
120μ	52.5	17.8
Exit Temperature, K	535	735

The required mixer length and residence times at altitude relight conditions with predicted E^3 engine fuel flow are considerably greater than the SLTO design values. Length and residence time can be reduced by reducing fuel flow to a more reasonable value as shown in Fig. 43.

The calculations made to investigate altitude relight with Scheme 3 were based on using the auxiliary air pump to boost the bleed air pressure. The increased pressure is needed to make up the auxiliary burner pressure drop and the pressure drop of the fuel-air mixture passing through the main engine fuel injector. It is not known if the air pump can obtain shaft power during engine windmilling because of possible competition from other devices such as aircraft hydraulic pumps.

EFFECT OF FUEL FLOW ON SCHEME 3 MIXER AT ALTITUDE RELIGHT

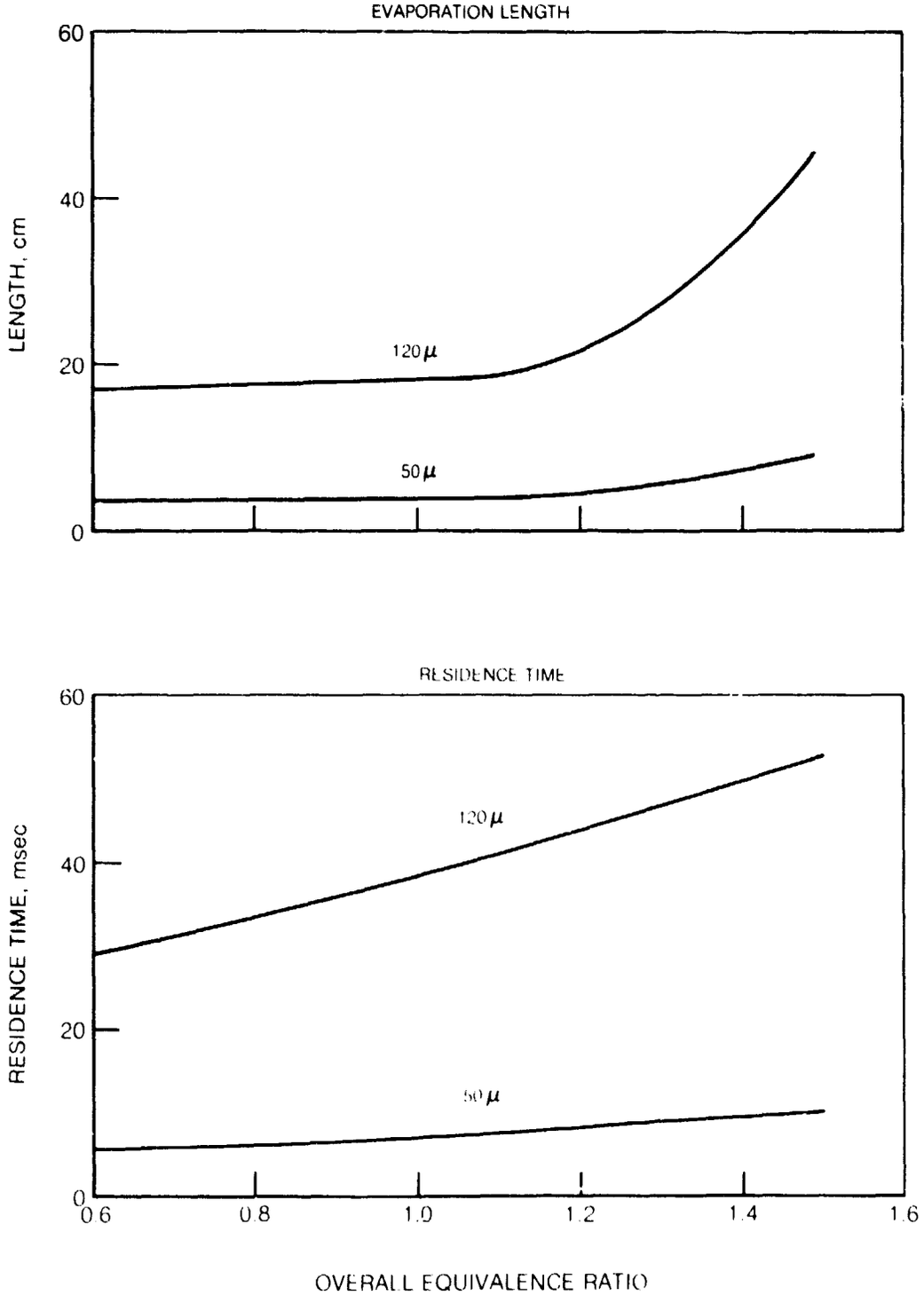

80-2-71-18

METALLURGICAL REQUIREMENTS

A review was made of reported data describing the effect of wall material on deposit formation. In references that appear in Appendix A, it was found that most of the data are in agreement, particularly regarding low deposit rates with aluminum, titanium, and nickel and high deposits with copper. Inconel 600, Hastelloy C, and type 316 stainless steel showed low deposits. The high deposit rate found with L-605 might have been due to the presence of large amounts of cobalt. Carbon steel produced high deposits, but the cause is not evident; perhaps surface impurities were a factor. One of the tests that was run with type 304 stainless steel showed high deposit levels while another had low levels. It is possible that the surface condition on one of the tests, perhaps resulting from a manufacturing process, was responsible for the high deposit rate. There was no mention of any inspection or cleaning procedure in the reports.

Because sulfur was found on the walls of tubes used in fuel vaporization experiments (Ref. 20), sulfur corrosion must be considered to be a potential problem. Early tests in that program appeared to show slight indications of intergranular attack in type 304 stainless steel tubes. Later data obtained when the air temperature was maintained at 920 K maximum, the fuel temperature at 750 K maximum and the wall temperature at 810 K maximum indicated that intergranular corrosion was not present. It appears that a 304 SS wall exposed to fuel at 810 K and cleaned with air at 920 K will maintain its structural integrity.

Carburization of the substrate can occur when fuel is passed over a hot metal wall containing chromium and chromium diffuses to the surface. The chromium is combined with carbon and when the layers of chromium carbide become thick enough, differential expansion that accompanies thermal cycling results in spalling. Fresh surfaces are then exposed and the chromium carbide formation can continue until the material is destroyed. Wall thinning, pitting, and complete failure were experienced in unreported tests (Ref. 22) with Inconel 600 and Inconel X (15.5 percent Cr) at wall temperatures between 1000 and 1400 K. It appears that the wall temperature must be kept below approximately 900 K to avoid carburization.

The heat exchanger calculations indicated that the wall temperature can be maintained at 800 K when the fuel temperature is 700 K and the deposit thickness is less than 0.003 cm. When the deposit thickness is allowed to grow to 0.02 cm, the wall temperature can exceed 1000 K. A temperature of 1000 K can be tolerated from the standpoint of material strength but to be safe from corrosion-erosion problems, the temperature limit is probably close to 800 K.

A candidate material for the vaporization system heat exchanger is Hastelloy X which is a nickel-base alloy containing 15.5% Cr and 16% Mo. This material has excellent high-temperature yield, rupture, and creep strength, and it can be welded and brazed using established procedures. A candidate tube braze is AMS 4777, a nickel-base material suitable for furnace, induction or resistance brazing. The brazing process for this material is AMS 2675 and the brazing temperature is 1310 K.

FIRE SAFETY

Fire safety requirements for an external fuel vaporization system were investigated by reviewing installation manuals for two wide-bodied aircraft and the Code of Federal Regulations covering airworthiness standards for transport aircraft and aircraft engines, and discussing fire safety with a PWA design engineer experienced in nacelle interface problems. It was determined that a typical wide-bodied aircraft has three sensors located at critical positions in the engine nacelle. Each sensor has two elements for redundancy and can sense a change in temperature of less than 20 K. Each engine has two fire bottles, each containing 3 Kg of Freon which can flood the pylon and engine cowling spaces. It appears that the current fire detection and extinguishing methods may be adequate for use with external fuel vaporization systems if suitable safety precautions are taken. Heat shields must be installed between components of the system carrying hot gases and the engine compressor and burner cases. These components include the vaporizer in Scheme 1 and the mixer in Scheme 3. All lines carrying fuel must be shrouded and the space between the lines and the shrouds must be vented overboard. Additional weight must be added to the values in Table 12 to account for these precautions.

MAINTENANCE

Some components of the external fuel vaporizer will require a rigorous maintenance schedule while others are not likely to require any significant maintenance. The components and their maintenance requirements are listed below:

Scheme 1

Auxiliary Burner - Inspection and repair at frequencies comparable to present liquid-fueled engine combustors.

Heat Exchanger - Cleaning of deposits at 100 hour intervals.

Throttle Valve - Cleaning of deposits at 100 hour intervals.

Engine Vapor Fuel Manifolds and Injectors - Same cleaning requirements as heat exchanger and throttle valves.

Scheme 2

Preheater - Cleaning of deposits at 100 hour intervals.

Engine Combustor Walls - Cleaning of deposits at 100 hour intervals. Rigorous mechanical inspection for cracks at frequent intervals.

Scheme 3

Intercooler - Inspection during engine overhaul.

Air Pump - Inspection during engine overhaul.

Auxiliary Combustor - Inspection and repair at frequencies comparable to present liquid-fueled combustors.

Mixer - Inspection during engine overhaul.

The principle maintenance problems are the cleaning of Scheme 1 and 2 heat exchangers and the inspection of the Scheme 2 fuel-cooled engine combustor which operates in a particularly hostile environment. Pyrolytic cleaning of fuel deposits with hot air has been demonstrated in the experimental program reported in Ref. 20. It is expected that cleaning can be done in-situ by supplying an external connection in the fuel system where hot air generated on the ground can be introduced.

The experimental program reported in Ref. 20 was carried out to measure the deposits obtained while heating and vaporizing No. 2 fuel oil. The tests were run using concentric stainless steel tubes, 2 m long by 0.65 and 1.6 cm dia, respectively. Number 2 fuel oil was pumped through the inner tube and heated by high-temperature air which flowed through the surrounding annulus. Upon exiting from the heated

tube, the gaseous fuel passed through an orifice that simulated an engine fuel injector, and was finally condensed in a water-jacketed, pressurized tank.

The basic test conditions included a hot air inlet temperature of 920 K and a fuel exit temperature of 760 K. The fuel flow rate was 2.3 kg/hr and the airflow rate was 11 kg/hr. The effectiveness of air in removing deposits was investigated by passing heated air over deposits already formed. Several tests were conducted, each with a separate heated tube and at different conditions, as shown in Table 20 below.

Table 20

HEATED TUBE EXPERIMENT
TEST CONDITIONS

Test Number	1	2	3	4	5	6
Mode	50 Hrs Heating	50 Hrs Heating Followed by 30 Hrs Cleaning	50 Hrs Heating	Cyclic	Cyclic	Cyclic
Heating Air Temperature, (K)	920	920	920	920	810	810
Fuel Exit Temperature, (K)	760	760	760	760	640	640
Fuel Pressure, atm	1	1	20	20	20	20
Cleaning Air Temperature, (K)	N.A.	920	N.A.	920	810	730

To study vaporizer performance under conditions representative of continuous engine operation, a test duration of 50 hrs was selected. The heated tube (Tube 1) was sectioned after testing and examined to determine the extent of fouling. A separate tube (Tube 2) was used for 50 hrs of vaporization time followed by 30 hrs of cleaning time. Heated air for cleaning flowed through the tube at a rate of 4.5 lb/hr. Tube 1 was examined after 50 hrs of operation at a fuel pressure of 1 atm. It was found to contain a black, hard, brittle deposit which gradually increased in thickness as the fuel progressed along the tube. The deposit thickness reached a maximum of 0.025 cm at approximately 80 percent of the tube length and then began to decrease. The composition of the deposit was analyzed using an electron microprobe, and the major elements were found to be carbon and sulfur. Iron, silicon, copper, and oxygen were among the minor constituents. Tube 2 was examined after the cleaning cycle was complete. Photomicrographs indicated that the deposit was removed and electron microprobe analysis showed that the major surface constituents were iron, silicon, copper, oxygen and chromium. Increasing the fuel pressure to 20 atm resulted in the formation of a black, soft, sooty deposit prior to cleaning (Tube 3). The amount of deposit accumulated appeared similar to that obtained on Tube 1; however, it could not be displayed by metallographic procedures because the deposit was smeared while the specimen was being mounted and polished. The orifice surface was also covered with a deposit.

Intermittent engine operation was studied by testing over 10 complete cycles consisting of a 6.5-hr vaporization period followed by a 0.5-hr cleaning period. This test resulted in the formation of a red deposit on the internal surface of the tube which subsequent analysis showed to be free of carbon and sulfur

(Tube 4). In addition, microscopic examination indicated that the orifice was free of these deposits. With the fuel exit temperature at 640 K and the cleaning air temperature reduced to 810 K, it was found that the surface (Tube 5) was free of carbon but a yellow deposit which contained sulfur could be seen on the surface. A further reduction in the temperature of the cleaning air to 730 K resulted in the reappearance of carbon in the deposit (Tube 6). Although sulfur was also a major element in the deposit, the quantity of sulfur removed from the fuel was negligible. The sulfur content of fresh fuel and the condensate were both determined and found to be approximately equal.

The results of the deposit formation and removal tests indicate that deposits will form on heated surfaces at a rate that will require frequent cleaning. Cleaning of Jet-A deposits must be done at intervals of approximately 100 hours. Deposits can be removed in a few minutes if the surface is heated to a temperature of approximately 800 K in the presence of a flowing airstream. Although the tests did not indicate any deleterious effects on the tubes, long time operation with deposit-cleaning cycles has not been demonstrated.

CONCEPT COMPARISON AND SELECTION

The three concepts were evaluated in terms of the important requirements imposed on an engine. The evaluation was made by assigning a scale value to each of the three concepts to cover individual engine needs and requirements. The scale generally covered the range 0 to 10. The scale limits had the following meaning:

Zero	Unacceptable
5	Good
10	Outstanding

The comparative performance of the three Schemes was reviewed and evaluated with the help of a number of consultants from PWA/CPD. The results of the evaluation are shown in Table 21.

Table 21

EXTERNAL VAPORIZER EVALUATION SUMMARY

Scheme	1	2	3
Engine Performance	10	10	3
Weight (including engine)	4	4	2
Controls	3	5	4
Startup	3	1	4
Dynamic Response	5	0	5
Engine Maintenance	2	1	4

Engine performance was evaluated with the assumptions that the E^3 engine core was fixed in size and the cooled air leaving the heat exchangers in Schemes 1 and 2 was effective in either reducing overall turbine cooling airflow requirements or increasing the combustor exit temperature. As a result, an increased thrust up to 10 percent, a reduced specific fuel consumption up to 0.9 percent, and an increased thrust/weight ratio up to 3.3 percent can be obtained with the proposed schemes.

These results indicate that the weight of components in Schemes 1 and 2 can be traded against reduced engine weight if the engine core is allowed to vary. Because of these possible improvements a weighting factor value of 10 in engine performance and 4 in weight were given to Schemes 1 and 2. In Scheme 3 the horsepower required to drive the air pump imposes a small reduction in engine performance and the weight of the vaporizer cannot be redeemed.

Ground startup with Scheme 2 is possible only by the addition of more components to either heat the compressor bleed air or facilitate a liquid fuel ignition capability in the lean premixed-prevaporized combustor. Altitude relight of Scheme 2 is considered to be impossible. Furthermore, it was determined that Scheme 2 is operable only at steady state conditions and engine acceleration is impossible without additional components. Therefore, Scheme 2 is not considered to be feasible for an aircraft engine.

Although Scheme 3 might appear to have some advantages over Scheme 1, the current need for reduced fuel consumption and the potential of Scheme 1 to provide substantial improvements in engine performance weighed heavily in the selection of the recommended appraoch. It was concluded from the performance reviews that if an external fuel vaporization system is needed to supplement a lean, premixed pre-vaporized combustion approach, the practical problems of startup, dynamic response, and engine maintenance could be overcome and are secondary to the projected improvements in specific fuel consumption. Scheme 1 is therefore the preferred concept for external fuel vaporization.

CONCLUSIONS

The results of this study indicate that an external vaporization system can be devised for an E^3-type engine with hardware of reasonable size. The hardware can be packaged without increasing the total engine volume and the system is not unduly complex. Potential gains were found in engine performance in terms of reduced specific fuel consumption and improved engine thrust/weight ratio. The thrust/weight improvement can be traded against vaporization system weight. However, the beneficial effects on engine performance are found in a vaporization system such as Scheme 1 which is subject to fouling with deposits formed at the walls exposed to heated fuel. These deposits can be removed by pyrolytic cleaning at reasonable temperatures but cleaning will increase the complexity and cost of aircraft maintenance.

Future effort should include the measurement of critical temperature and pressure for Jet-A and future aircraft fuels. The deposit forming tendency, including deposit rate and deposit thermal resistance of aircraft fuels undergoing heating to their critical temperatures and beyond, should be verified. Deposit cleaning requirements, including time and temperature, should be established for Jet-A and future aircraft fuels. Vaporizer system analysis should be continued to include the range of fuel properties anticipated for future fuels.

Altitude restart and dynamic response of the engine will also be affected by the characteristics of an engine with an external fuel vaporizer. Vaporizer model development effort must be expended to produce the required performance of the vaporizer itself and to assure that the engine meets the steady-state and dynamic requirements imposed by the aircraft. The analysis of engine performance should be continued in order to establish the tradeoffs between thrust, engine size, specific fuel consumption and Scheme 1 characteristics such as bleed airflow and component weights. Further study of dynamic response should be carried out to ascertain that either the limitations on the engine are minor or they can be removed in normal engine development. Altitude relight fuel flow requirements of a lean, premixed-prevaporized combustor should be reviewed to determine whether an external fuel vaporization system can supply the required fuel.

LIST OF SYMBOLS

C_p	Specific Heat, cal/g-K
f	Friction Factor
g	Gravitational Acceleration, m/sec^2, ft/sec^2
G	Mass Velocity, Kg/m^2-sec
h	Heat Transfer Coefficient, BTU/hr-ft^2-F
H	Heat of Vaporization, BTU/lb
K	Thermal Conductivity, BTU/hr-ft-F
Nu	Nusselt Number
P	Pressure, Newtons/m^2
ΔP	Change in Pressure, Newtons/m^2
Pr	Prandlt Number
Re	Reynolds Number
T	Temperature, K
ΔT	Temperature difference, K
x	Vapor Quality
ΔZ	Change in Axial Dimension, m
μ	Absolute Viscosity, lb/hr-ft
ρ	Density, Kg/m^3, lb/ft^3
σ	Surface Tension, lb/ft

Subscripts

B	Bulk
BP	Bubble Point
DP	Dew Point
EFV	Equilibrium Flash Vaporization
IBP	Initial Boiling Point
Iso	Isothermal
SAT	Saturation
T	Total, liquid plus vapor
V	Vapor
W	Wall

REFERENCES

1. Hirschfelder, J. O., C. F. Curtis, and R. B. Bird: Molecular Theory of Gases and Liquids. p. 380, John Wiley and Sons Inc. 1964.

2. Voecks, G. E. and D. J. Cerini: Application of Rich Catalytic Combustion to Aircraft Engines. Presented at Third Catalytic Combustion Workshop. October 4, 1978.

3. Henzel, H. J., H. Kostka, and A. Michel: Autothermal Gasification of Liquid Hydrocarbons by Partial Oxidation. Paper presented at ERDA meeting on Fuel Processing for Fuel Cell Power Generation. April 13, 1977.

4. Szetela, E. J.: Deposits from Heated Gas Turbine Fuels. ASME 76-GT-9. 1976.

5. Shelton, E. M.: Aviation Turbine Fuels, 1978. BETC/PPS-79/2. Bartlesville Energy Technology Center. May, 1979.

6. Coordinating Research Council (CRC) Aviation Handbook. Fuels and Fuel Systems. NAVAIR 06-5-504. May, 1967.

7. Technical Data Book - Petroleum Refining. Second Edition. American Petroleum Institute. 1970.

8. Faith, L. E., G. H. Ackerman, and H. T. Anderson: Heat Sink Capability of Jet A Fuel: Heat Transfer and Coking Studies. NASA CR-72951. July, 1971.

9. Edmister, W. C. and D. H. Pollock: Phase Relationships for Petroleum Fractions. Chem. Eng. Progress. Vol. 44, No. 12, p. 905. 1948.

10. Edmister, W. C.: Applied Hydrocarbon Thermodynamics, Vol 3. Gulf Publishing Co. Houston, Texas, Nov. 1961.

11. Nelson, W. L.: Petroleum Refinery Engineering, 4th Ed. McGraw-Hill Book Co. Inc., New York, 1958.

12. Segalman, I., P. Goldberg, and J. J. Nolan: Hydrocarbon Fueled Scramjet. Vol. V - Cooling Investigations. AFAPL-TR-68-146. June, 1969.

13. Moody, L. F.: Friction Factors for Pipe Flow. Trans. Amer. Soc. Mech. Eng. Vol. 66, p. 671, 1944.

REFERENCES (Cont'd)

14. Chen, J. C.: Correlations for Boiling Heat Transfer to Saturated Fluids in Convective Flow. I&EC Process Des & Dev. v. 5 No. 3 July, 1966.

15. Lockhart, R. W. and R. C. Martinelli: Proposed Correlation of Data for Isothermal Two-Phase, Two-Component Flow in Pipes. Chem. Eng. Progress Vol. 45, No. 1, p. 39. January, 1949.

16. Kays, W. M. and A. L. London: Compact Heat Exchangers. McGraw Hill. 1964.

17. Eckert, E. R. G. and R. M. Drake: Heat and Mass Transfer, McGraw Hill Book Co. Inc, 1959.

18. Lohmann, R. P., E. J. Szetela, and A. Vranos: Analytical Evaluation of the Impact of Broad Specification Fuels in High Bypass Turbofan Engine Combustors. NASA CR-159454. Dec. 1978.

19. Carlson, N. G.: Development of Hi-Temperature Subsystem Technology to a Technology Readiness State. Topical Report, Preliminary Combustor Design. United Technologies Power Systems Division. FE-2292-11 1977.

20. Spadaccini, L. J. and E. J. Szetela: Approaches to the Prevaporized-Premixed Combustor Concept for Gas Turbines. ASME GT-85. 1975.

21. Lay, J. E.: Thermodynamics. C. E. Merrill Publishing Company, 1963.

22. Szetela, E. J. and Vranos, A.: Deposits from Heated Fuel -- An Information Study. UTRC Report R75-214388-1. December, 1975.

APPENDIX A

Summary of Literature Survey

SUMMARY

A literature survey was conducted as part of the program. Information was sought regarding the properties of Jet-A fuel including thermodynamic and thermal stability data and heat exchanger design principles covering single phase and two-phase fluids. Sufficient information was found for the conceptual design and analysis of heat exchangers and to identify areas where additional data are needed. A summary of the survey included the physical properties of Jet-A fuel, fuel deposit formation and removal, two-phase fluid mechanics including heat transfer and dynamic stability, and heat exchanger design data.

DATA SOURCES

The literature survey was conducted mainly by a computerized retrieval from the files of the Lockheed DIALOG and the DOE RECON collections. The DIALOG files that were searched included NTIS, Engineering Index, ISMEC (Institute of Mechanical Engineers), and Chemical Abstracts. A number of bibliographies from documents and text books obtained though the retrieval were also searched. Additional searches were conducted in the published papers of the International Heat Transfer Conference, in Advances in Heat Transfer, and in the ASME Journal of Heat Transfer. Personal files of UTRC workers in the field of fuel deposit formation were also reviewed. Approximately 3000 citations were examined during the survey and about 150 were found to be informative.

PROPERTIES OF FUEL

Some useful tables of properties of Jet-A such as density, viscosity, thermal conductivity, vapor pressure, specific heat, and enthalpy are contained in Ref. 1.* Many useful properties of petroleum fractions and fuels are also contained in Refs. 2 and 3 and a very comprehensive, though dated collection of fuel properties was presented in Ref. 4. Measured fuel properties determined by ASTM procedures for a thorough statistical sampling of fuels are contained in Ref. 5 (issued annually) and the analysis of a few samples of fuel collected world-wide is found in Ref. 6. A comprehensive collection of calculation procedures, working curves, and nomograms is contained in Ref. 7 for the determination of thermodynamic and transport properties of liquid and vapor fuel including critical temperature and pressure, enthalpy, density, viscosity, thermal conductivity, vapor pressure, specific heat, and surface tension. A comparison of some of the common properties of fuel obtained from various sources is shown below.

Properties of Fuel

Reference	Fuel	Specific Gravity at 100 F (311 K)	Viscosity at 100 F (311 K) cs	Specific Heat at 100 F (311 K) cal/gr - K
1	Jet A	0.809	1.27	0.508
2	Jet A-1	0.810	1.02	-
2	JP-5	0.790	1.26	0.482
4	JP-5	0.811	1.34	0.485
5	Jet A	0.792	1.23	-
7	Jet A	0.795	1.20	0.500

Three distillation procedures, ASTM D86, TBP (True Boiling Point) and EFV (Equilibrium Flash Vaporization) are described in Ref. 8. They must be used with care because none of them fit the full boiling range in the external fuel vaporization process where the liquid is in equilibrium with all of the vapor produced in the heat exchanger. ASTM D86 distillation is carried out with continuous removal and condensation of vapor and the final boiling point is of no value to the external fuel vaporization problem. TBP distillation is performed with physical separation of a large number of fractions and neither the initial nor the final boiling points are pertinent. EFV is done with liquid in equilibrium with vapor but the initial boiling point is in error because it is not measured until considerable vapor has been produced.

---

* References for Appendix A begin on page A-13.

Typical values for the boiling point of Jet A at atmospheric pressure are as follows:

Comparison of Boiling Points

	ASTM D86		EFV	
	F	K	F	K
Initial Boiling Point	335	442	378	465
Final Boiling Point	512	540	455	508

A plausible approach to external fuel vaporization is the use of ASTM D86 for the initial boiling point and EFV for the final boiling point. They can be obtained by using the data of Ref. 5 in the procedures of Ref. 7.

Procedures for extrapolating some of the properties of fuel fractions as a function of pressure are found in Ref. 8-10. A relation between fuel surface tension and temperature is described in Ref. 11. Background information on the evolution of fuel specifications, fuel characteristics and fuel additives can be found in textbooks Ref. 12-16.

THERMAL STABILITY AND DEPOSITS

A number of sources contain deposit formation rates and deposit thickness measurements. Data from four of the sources which reported test durations of 4-100 hr are summarized below.

Deposit Formation Rates

Reference	Fuel	Temperature F	Temperature K	Deposit Rate $\mu g/cm^2$-hr
17	Jet A	500-700	533-644	20-350
1	Jet A	1000-1200	811-922	100
18	Jet A	700	644	100
19	JP-5	700	644	200
20	No. 2 oil	500-600	533-589	500

These and other data surveyed in a previous program are contained in Ref. 21 which was summarized in Ref. 22.

The process of deposit formation involves the oxygen present in the fuel as dissolved gas or in chemical form which enters into reactions with hydrocarbons to form radicals. These intermediates form higher molecular weight materials that usually contain carbon, hydrogen, oxygen, sulfur, and nitrogen. Although the exact mechanism has not been defined many of its aspects are discussed in Ref. 21 and 23. Further theoretical treatment can be found in Ref. 24-26.

Fuel decomposition rates and subsequent deposit formation rates are a function of temperature, pressure, velocity, composition, the physical state of the fuel, the nature of bounding surfaces, and the gradients of temperature, concentration, and velocity at phase boundaries. These variables affect not only reaction kinetics but other processes such as diffusion, coagulation, and ultimately, decomposition. Early evaluations of thermal fuel reactions are found in Ref. 27-32. The effect of temperature, which usually shows a peak value of deposit formation rate in the vicinity of 500-700 F (533-644 K) was reported in Ref. 1, 19, 20, 33 and 34. Pressure effects do not seem to be important with kerosene-type fuels including No. 2 oil that do not contain volatile constituents. However, JP-4 fuel showed a distinct increase in deposit formation at low pressure in the temperature region where boiling occurs (Ref. 35). Experiments were reported in Ref. 36-38 in which the extent of pyrolysis in liquid and vapor states was determined and oxidation products were identified for a hydrocarbon during vaporization and in the liquid state. Recent experiments reported in Ref. 39 showed that deposit formation rate was a function of Reynolds No. over the

range 600-10,000. These results indicate that diffusion is an important step in the formation of deposits. Additional effects of velocity were reported in Ref. 34 and in unpublished data that were reported in Ref. 21.

An increase in the concentration of dissolved oxygen in the fuel greatly increases the deposit formation rate (Ref. 1, 17, 29, 40, 41). Many sulfur, nitrogen, and oxygen compounds also increase deposit formation (Ref. 42-47). According to Ref. 47, thermal stability depends in part on the chemical nature of the hydrocarbons. Chain branching and alkyl substituents on rings were found to increase deposits while monocyclic hydrocarbons showed better behavior.

The effect of wall material was reported in Ref. 1, 23 and 34. Most of the data are in agreement, showing that copper causes high deposit formation rates while aluminum, titanium, and nickel produced low rates of formation. Deposit rates on stainless steel were usually low except for one case where a high rate was encountered. Such anomalies in published data indicate that it may be necessary to ascertain the condition of a surface (impurities, cleanliness) in order to produce reliable data on the effect of wall material.

Unpublished data that were reported in Ref. 21 indicated that metal contaminants in the fuel have a deleterious effect on thermal stability of fuel. A concentration of only 0.01 ppm of elemental copper substantially affected the results in a fuel coking test. Unfortunately, it was also found that when exposed to copper walls, JP-5 has a high attraction for elemental copper. A concentration of 0.08 ppm of elemental vandium degraded thermal stability while 1 ppm or organometallic vanadium as vanadium acetyl acetonate did not. Cadmium can migrate into the fuel from plated sheet stock and increase deposit formation rate. Concentrations of 0.5 ppm lead naphthanate and 1.5 ppm lead tetraethyl also increased deposit rate. Iron, nickel, and cobalt acetylacetonates in concentrations of 50 ppm produced a deposit increase of 40 times that of uncontaminated fuel in tests reported in Ref. 43. It was reported in Ref. 48 that most corrosion inhibitors caused no measurable increase in deposit formation rate but those containing phosphorus did increase deposit rate.

Deposits have been examined using scanning electron microscopy (Ref. 49) where particles measuring 1000 A were found. Recently, using both scanning electron and transmission electron microscopy, particle sizes as small as 15 A have been noted (Ref. 39). The particles are arranged in coiled, chain-like clusters and it is believed that deposits consist of layers of the clusters. Both authors agreed that the deposits are formed in the liquid fuel and subsequently accumulate on surfaces in randomly packed structures. An IR spectrum of a fuel deposit reported in Ref. 39 was characterized by peaks representing carbon-hydrogen bonds in both alkyl and aromatic configurations and by carbon-oxygen single and double bonds.

Deposit properties such as thermal conductivity and specific gravity can only be implied from other observations. Two values of thermal conducitivity were reported in Ref. 1, 0.11 and 0.55 BTU/hr-ft-F (0.19 and 0.95 w/m-C). Deposit density was reported to be 0.5-0.6 g/cm^3. The author of Ref. 17 felt that a thermal conductivity of 0.07 BTU/hr-ft-F (0.12 w/m-C) and a specific gravity of 1 g/cm^3 were representative of fuel deposits.

According to Ref. 50, improvements in fuel processing can improve the thermal stability of fuel. Three of the many patents for improving fuel by processing and by the use of additives for improving thermal stability are contained in Ref. 51-53. Additional patents covering the use of additives in fuel to improve oxidation resistance and thermal stability are listed in Ref. 54. Special fuels like JP-6 and JP-7 (Ref. 40) produce lower deposit formation rates by comparison with Jet A or JP-5.

Deposits can be removed by flowing hot air over the surface. The practice described in Ref. 17 for measuring deposit formation rate consisted of a flow of oxygen over a specimen contained in a furnace at 975 F (800 K). Eight minutes time was sufficient to remove the deposit. Cyclic experiments were reported in Ref. 20 during which a cycle consisted of 5.5 hours of vaporizing No. 2 oil and 0.5 hrs of flowing hot air. Electron microprobe results indicated that the surface was clean when the air was at a temperature of 1200 F (922 K), trace amounts of sulfur remained when the air temperature was 1000 F (811 K), and trace amounts of both sulfur and carbon remained when the air temperature was 850 F (728 K).

A large group of Russian literature has appeared during the past ten years. Some of it has been translated (Ref. 55) but most of it is still in Russian (Ref. 56-68). Although the titles do not necessarily correspond to the content, it does not appear likely that a great deal of new data can be found in the Russian literature.

TWO PHASE FLUID MECHANICS

The literature in two phase flow, which is very extensive, generally covers four subjects: flow patterns, heat transfer, pressure drop, and dynamic instability. Two excellent summaries of the principles and problems of forced-flow, once-through boiling are contained in Ref. 69 and 70. Comprehensive text-books on the subject of boiling and two phase flow are also available (Ref. 71-74). One important feature of once-through boiling which is pointed out in the literature is that complete thermodynamic equilibrium is not established at the exit. Instead, a small quantity of liquid is carried in slightly superheated vapor. Some attempts to dry the vapor have consisted of using swirl-inducing inserts to centrifuge the liquid to the wall (Ref. 75), a rotating boiler (Ref. 76) and cyclone centrifuge (Ref. 77).

When two phases flow through the same channel, the gas usually flows faster than the liquid. The liquid accumulates in the pipe and at some ratios of gas to liquid flow, the surface of the liquid can become disturbed and the nature of the flow can be affected. Observations were reported in Ref. 78 of many forms of flow such as bubble, slug, plug, annular, stratified, wavy, and spray. Boundaries between the various regimes were drawn in terms of the ratio of gas and liquid mass velocities and the physical properties of the two phases. An analysis was presented in Ref. 79 in which some of the boundaries between flow regimes were calculated using equations containing Froude and Weber Numbers in a form that was derived from forces acting on a typical liquid element.

A recent review of boiling heat transfer equations appeared in Ref. 80. For nucleate boiling in forced flow situations, the equation suggested in Ref. 81 was recommended. This equation contains two parts: one part with a modifying factor to a common grouping of dimensionless parameters describing macroscopic convection and another part covering the microscopic agitation of bubbles. Other equations that deserve consideration in nucleate boiling were reported in Ref. 82-84. When the heat flux becomes too high or the liquid mass velocity becomes too low to sustain nucleate boiling, a transition to film boiling occurs and the heat transfer coefficient is greatly reduced. Unfortunately, predictions of film boiling are not reliable at this time. It was stated in Ref. 85 that although work in this area has been going on for over 20 years and over 200 correlations have been proposed, the film boiling problem is still not resolved, even for relatively simple geometries.

Pressure loss during boiling is usually expressed (Ref. 86) as the sum of three terms, gravitational, inertial, and frictional. Frictional loss is frequently expressed in terms of the classic Martinelli parameter (Ref. 87). This dependence has been described in detail in Ref. 88 for various combinations of laminar or turbulent flow in the liquid and vapor. Both inertial and gravitational loss

equations require a knowledge of the void fraction which depends on the slip between the fast flowing vapor and the slower liquid. The calculation of void fraction has been treated in Ref. 89-93.

Pressure loss across abrupt area changes including sudden expansion and contraction was treated in Ref. 94 and 95. Calculations of pressure loss in sudden expansions by four methods were presented in Ref. 96. Measurements of slip in a venturi was described in Ref. 97. Experimental measurement of the pressure losses in manifolds including manifold-to-branch, branch-to-manifold and manifold-across-branch losses were reported in Ref. 98. Included in that reference are comparisons with single-phase manifold loss data.

A two-phase flow system has the hydrodynamic potential for instability because the system can exist in more than one state (mostly liquid or mostly vapor) and an external energy source is available (pressure drop) to account for frictional dissipation. An analogy is made in Ref. 73 to oscillation of a mechanical system using the following equivalents:

Mechanical System	Hydrodynamic System
Mass	Mass flow rate
Exciting force	Pressure drop
Spring	Voids

Flow instabilities occur in forced circulation regimes in various ways:

1. Because a shift from mostly liquid to mostly vapor can occur in a vaporizer over a range of flow rates, the pressure loss vs. flow curve has an S-shape which can have multiple intersections with pump characteristic lines. According to Ref. 99, flow excursions of this type can be eliminated by changing the head-flow characteristics of the system.

2. A large number of flow channels having common inlet and outlet plenums can have an instability in one or a few of the channels without a significant change in the overall pressure drop because the flow can be redistributed to a large number of other stable channels. It was concluded in Ref. 99 that the tendency for flow oscillations is reduced by an increase in the pressure drop in the non-boiling portion of the flow or by an increase in the system pressure level.

3. A single forced convection channel can exhibit two-phase flow oscillations that are not associated with the pumping mode. Density waves are described in Ref. 100 and they are characterized by a constant rate of vapor generation and alternate expulsion of vapor and liquid at the exit of the channel.

According to Ref. 101, an increase in pressure drop at the channel inlet and a decrease in pressure drop at the channel exit can have a stabilizing effect. A comprehensive treatment of density wave oscillations appeared in Ref. 102. Density waves accompanied by thermal oscillations were reported in Ref. 100 and they were stabilized by a heat flux reduction or flow rate increase. An increase in pressure drop at the inlet can eliminate thermal oscillations.

4. Chugging is a cyclic phenomena characterized by periodic expulsion of liquid from the channel, sometimes from both ends. Expulsion is followed by reentry of liquid and a period comprised of apparently normal behavior. According to Ref. 101, the conditions for the occurrence of chugging are not well understood. Nucleation characteristics, including wall properties, may lead to the existence of a critical value of wall superheat.

Two-phase flow instabilities have been studied by a number of investigators. Fundamental analyses are contained in Ref. 103-107. Experimental data that have been reported include the effect of inlet restrictions (Ref. 108), effect of exit restrictions and subcooling (Ref. 99, 109), measured flow oscillations in parallel channels (Ref. 110) and instabilities involving variations in the internal two-phase flow patterns (Ref. 106). Experimental data that agree with available models for two-phase flow dynamics were reported in Ref. 111. A general review of analyses and experimental data was presented in Ref. 112.

HEAT EXCHANGERS

There are two comprehensive texts (Ref. 113 and 114) which are devoted to methods for designing heat exchangers suitable for external fuel vaporization. Heat exchanger design data are also contained in Ref. 115 and 116, and general heat transfer texts that are useful in heat exchanger design are included in Ref. 117-120. Useful design data consisting of comprehensive tables that describe the characteristics of tubing and typical factors of fouling are contained in Ref. 121. Recent heat exchanger core data for a single row, double row, and triple row finned tube geometry are contained in Ref. 122. An analytical model for the design of parallel flow, multi-stream heat exchangers and multi-section, plate-fin exchangers was presented in Ref. 123. A new method of presenting heat transfer data using dimensionless plots of heat transfer performance vs. pumping power with a parameter called "flow length between major boundary layer disturbances" was discussed in Ref. 124. This method leads to the possibility of presenting all surface geometries on a single, idealized plot.

According to Ref. 125, the shell side of baffled heat exchangers leads to special design problems because the fluid mechanics includes a transition between flow across tubes (between baffles) and flow along tubes (in the baffle window). Leakage between the tubes and baffles and between the baffles and the shell add further complications. A comprehensive treatment of the problem was presented in Ref. 126 but this treatment relies on the availability of a large number of empirical constants. A simple treatment for heat transfer and pressure loss is contained in Ref. 120. However, a comparison which was reported in Ref. 125 between pressure loss and predictions made by four methods of calculation indicated that the simple method of Ref. 120 gave losses with liquids that were 2-10 times too high. The data comparison suggested that the method of Ref. 128 can be used to calculate baffled shell side pressure loss with reasonable accuracy. A presentation was made in Ref. 129 of shell side pressure drop in two-phase flow including separate measurements for cross flow and window pressure losses and some data on void fraction and flow patterns.

Heat exchanger performance deterioration because of longitudinal conduction was discussed in Ref. 130. The same author treated the problem of heat exchanger performance deterioration due to flow nonuniformity in Ref. 131. Heat exchanger fouling, the effect of fouling on performance, and the design of heat exchangers for fouling service were discussed in Ref. 132-134. Measurements of circular fin temperature measurements which were reported in Ref. 135 indicated that high heat transfer rates were present on the front half of the fins and poor rates on the rear half. The use of a fin efficiency in heat exchanger design was questioned because of the complex form of the measured temperature distribution along the fins. The effect of artificial roughness on heat transfer and pressure drop in bank of in-line tubes was reported in Ref. 136 and the effect of variations in shell-side physical properties on heat transfer to a bank of tubes was discussed in Ref. 137.

Equations for the calculation of fuel-side heat transfer coefficients in heat exchangers in cases of laminar or turbulent convection were presented in Ref. 1. General equations for nucleate boiling heat transfer coefficients were reported in Ref. 81 and for film boiling of fuel in Ref. 138. An equation for heat transfer coefficient in super-critical fuel was presented in Ref. 139 and a general treatment of heat transfer to near-critical fluids is contained in Ref. 140.

Heat Transfer Reviews and Bibliographies

The heat transfer literature is quite voluminous and it is fortunate that reviews of the literature are published regularly. Heat transfer reviews appeared annually in Industrial and Engineering Chemistry for the year 1953 (Ref. 141) to 1959 (Ref. 142). The annual review for 1960 was found in Mechanical Engineering (Ref. 143), and since that time, it has appeared in International Journal of Heat and Mass Transfer (Ref. 144). A bibliography of Soviet work appeared annually in International Journal of Heat and Mass Transfer from 1971 to 1975 (Ref. 145) under one author and it is now being written by different authors (Ref. 146). A bibliography of Japanese work was found under one author in 1972 (Ref. 147) and from 1973 to the present (Ref. 148) it has been presented by another author.

Approximately 76 reports were published from 1948 to 1971 at Stanford University on a number of subjects pertinent to the design of heat exchangers. The final report (Ref. 149) consists of a bibliography of these reports and many other reports and papers written on the subject of heat transfer at Stanford during that period.

FUEL GASIFICATION

There have been recent efforts to produce vaporized fuel using heat that is produced chemically rather than being transferred conventionally through a heat exchanger. Work has been reported in Refs. 150 and 151 on a fuel gasifier which uses gasoline and air in a partial oxidation reactor to produce a gaseous product containing hydrogen, carbon monoxide, minor amounts of methane, carbon dioxide and water, and nitrogen. Work was reported in Germany (Ref. 152-154) on an autothermal, catalytic gasifier that has used diesel fuel without soot formation at an equivalence ratio of 10. The term autothermal was chosen to describe a process in which exothermal reactions between fuel and oxygen that produce CO_2 and H_2O are balanced by endothermic reactions in which the fuel reacts with CO_2 and H_2O to produce CO and H_2. Marketing efforts have begun on a process for vaporizing fuel in which superheaced steam is mixed with diesel fuel (Ref. 155). The reformed products are claimed to have properties which permit their use with minor modification in gas turbines which are designed for natural gas.

CONCLUSIONS

The literature search produced approximately 3000 citations of which about 150 were considered to be informative. The results indicate that suitable data are available for the conceptual design and analysis of heat exchangers as required during the external fuel vaporization study. There are, however, some areas where additional data will be needed, particularly if the design and development of hardware is being considered. These areas are as follows:

1. Some of the detailed fuel properties required in various heat transfer equations were calculated by procedures recommended in the literature. These properties should be verified.

2. Many of the recommended heat transfer and pressure loss equations were obtained for single-component fluids. Since Jet-A contains many components, the design equations should be verified.

3. The estimated properties of deposits such as density and thermal conductivity are only approximate. They should be determined with greater precision.

4. Deposit formation rates have all been determined for clean tubes. Deposit formation for tubes that have been cleaned a number of times are unavailable.

BIBLIOGRAPHY

Properties of Fuel

1. Faith, L. E., G. H. Ackerman, and H. T. Anderson: Heat Sink Capability of Jet A Fuel: Heat Transfer and Coking Studies. NASA CR-72951. July, 1971.

2. Coordinating Research Council (CRC) Aviation Handbook. Fuels and Fuel Systems. NAVAIR 06-5-504. May, 1967.

3. Maxwell, J. B.: Data Book on Hydrocarbons. Van Nostrand. 1950.

4. Barnett, H. C., and R. R. Hibbard: Properties of Aircraft Fuels. NACA TN 3276. 1956.

5. Shelton, E. M.: Aviation Turbine Fuels, 1978. BETC/PPS-79/2. Bartlesville Energy Technology Center. May, 1979.

6. Bradley, R. P.: Kerosene Type Aviation Turbine Fuel Properties Survey. AFAPL-TR-74-7. Air Force Aero Propulsion Laboratory. April, 1974.

7. Technical Data Book - Petroleum Refining. Second Edition. American Petroleum Institute. 1970.

8. Edmister, W. C. and D. H. Pollock: Phase Relationships for Petroleum Fractions. Chem. Eng. Progress. Vol. 44, No. 12, p. 905. 1948.

9. Cox, E. R.: Pressure-Temperature Chart for Hydrocarbon Vapors. Industrial and Engineering Chemistry. Vol. 15, No. 6, p. 592. 1923.

10. Mullins, B. P.: The Vaporization of Fuels for Gas Turbines. Part 1. The Bubble-Points and Dew-Points of Liquid Hydrocarbon Fuels. J. Inst. Petroleum, Vol. 32, p. 703. 1946.

11. Solov'ev, A. N. and V. I. Blagovistnaya: General Relation Between Surface Tension of Jet Fuels and Temperature. (Russian Translation) Khimiya i Tekhnologiya Topliv i Masel. No. 3, p. 53. March, 1977.

12. Gruse, W. A. and D. R. Stevens: Chemical Technology of Petroleum. McGraw Hill, 1960.

13. Goodger, E. M.: Hydrocarbon Fuels. John Wiley & Sons. 1975.

14. Brooks, B. T.: Chemistry of Petroleum Hydrocarbons. Reinhold, 3 Vol. 1955.

15. Ragozin, N. A.: Jet Fuels. USAF Foreign Technology Div. AD637097 (Russian Transl.). 1966.

16. Considine, D. M. (Editor): Energy Technology Handbook. McGraw Hill. 1977.

17. Watt, J. J., A. Evans and R. R. Hibbard: Fouling Characteristics of ASTM Jet A Fuel When Heated to 700 F in a Simulated Heat Exchanger Tube. NASA TN D-4958. December, 1968.

18. Lohmann, R. P., E. J. Szetela, and A. Vranos: Analytical Evaluation of the Impact of Broad Specification Fuels in High Bypass Turbofan Engine Combustors. NASA CR-159454. Dec. 1978.

19. Taylor, W. F. and J. W. Frenkenfeld: Development of High Stability Fuel, EXXON Report GRV. 12GAHF.75. January, 1975.

20. Spadaccini, L. J. and E. J. Szetela: Approaches to the Prevaporized-Premixed Combustor Concept for Gas Turbines. ASME GT-85. 1975.

21. Szetela, E. J. and A. Vranos: Deposits from Heated Fuel - An Information Study. UTRC Report R75-214388-1. December, 1975.

22. Szetela, E. J.: Deposits from Heated Gas Turbine Fuels. ASME 76-GT-9. 1976.

23. Taylor, W. F.: The Study of Hydrocarbon Fuel Vapor Deposits, AFAPL-TR-69-77. September, 1969.

24. Emanuel, N. M. Editor: The Oxidation of Hydrocarbons in the Liquid Phase. Pergamon Press, p. 140. 1965.

25. Mayo, F. R., N. A. Kirshen, H. Richardson, and R. S. Stringham: The Chemistry of Fuel Deposits and Their Precursors. Stanford Research Inst. AD754459. December, 1972.

26. Mayo, F. R.: Accounts of Chemical Research 1. No. 7, p. 193. July, 1968.

27. Nixon, A. C. and H. B. Minor: Effect of Additives on Jet Fuel Stability and Filterability. I&EC Vol. 48, No. 10 October, 1956.

28. Nixon, A. C.: Autoxidation and Antioxidants, Lundberg, W. O., Ed., Vol. II, Chapter 17, Interscience Publishers. 1961.

29. McKeown, A. B. and R. R. Hibbard: Effect of Dissolved Oxygen on the Filterability of Jet Fuels for Temperatures Between 300 F and 400 F, NACA RM 55128. December, 1955.

30. Hatcher, J. B.: High-Flux Heat Transfer and Coke Deposition of JP3 Fuel Mixture, JPL CIT Progress Report No. 20-157. February, 1952.

31. Kennerly, G. W. and W. L. Patterson: Kinetic Studies of Petroleum Anti-oxydants. I&EC Vol. 48, No. 10. October, 1956.

32. Norton, C. T. and D. E. Drayer: Oxidation of Organic Compounds. Vol. 1, Advances in Chemistry Series No. 75, ACS. 1968.

33. Hazlett, R. N.: Progress Report on Advanced Hydrocarbon Fuel Development. Naval Research Laboratory. March, 1975.

34. Smith, J. D.: Fuel for the Supersonic Transport. I&EC Process Design and Development, Vol. 8, No. 3. July, 1969.

35. Bradley, R. P. and C. R. Martel: Effect of Test Pressure on Fuel Thermal Stability Test Methods. AFAPL-TR-74-81. April, 1975.

36. Vranos, A.: Decomposition of Vaporizing n-Hexadecane. Combustion & Flame, 30, No. 2, p. 151. 1977.

37. Vranos, A.: Oxidation and Pyrolysis Products from Vaporizing n-Hexadecane. ASME Winter Annual Meeting, Atlanta, Ga. 1977.

38. Vranos, A.: Liquid Phase Reactions of Vaporizing Hydrocarbon Fuel. Progress in Aeronautics and Astronautics, Vol. 62. 1978.

39. Vranos, A., P. J. Marteney, and B. A. Knight: Determination of Coking Rate in Jet Fuel. Presented at International Conference on Fouling of Heat Transfer Equipment at Rensselaer Polytechnic Institute. August, 1979.

40. Bradley, R., R. Bankhead and W. Bucher: High Temperature Hydrocarbon Fuels Research in an Advanced Aircraft Fuel System Simulator on Fuel. AFFB-14-70, AFAPL-TR-73-95. April, 1974.

41. Bagnetto, L.: Thermal Stability of Hydrocarbon Fuels, Progress Report No. 7, Phillips Petroleum Company Report 4236-65R. September, 1965.

42. Taylor, W. F.: Development of High Stability Fuel, EXXON Report GRUS. 11GAHF.73. July, 1973.

43. Taylor, W. F.: Mechanism of Deposit Formation in Wing Tanks, SAE Paper 680733. October, 1968.

44. Taylor, W. F.: Development of High Stability Fuel. EXXON Report GRX. 6GAHF.72. April, 1972.

45. Taylor, W. F. and J. W. Frendenfeld: Deposit Formation from Deoxygenated Hydrocarbons. Effects of Trace Nitrogen and Oxygen Compounds. Ind. Eng. Chem. Prod. Res. Dev. V17, No. 1, p. 86. November, 1978.

46. Bachman, K. C.: Heat Transfer Unit Evaluates Performance of Jet Fuels for Supersonic Aircraft, SAE 650803. October, 1965.

47. Smith, J. O., B. M. Faubuss, and L. I. Belenyessy: Evaluation of Hydrocarbons for High Temperature Fuels. Part II Fuel Evaluation and Property Correlation. Vol. I Correlation Studies, Thermal Stability, and Containment Effects. WADC TR 59-327, Pt II, Vol. 1. February, 1962.

48. Martel, C. R., R. P. Bradley, J. R. McCoy and J. Petrarca: Aircraft Turbine Engine Fuel Corrosion Inhibitors and Their Effect of Fuel Properties. AFAPL-TR-74-20. July, 1974.

49. Schirmer, R. M.: Morphology of Deposits in Aircraft and Engine Fuel Systems, SAE Paper 700258. April, 1970.

50. Lander, H. R. and C. R. Martel: Jet Fuel Thermal Stability Improvements Through Fuel Processing, AFAPL-TR-74-35. 1974.

51. U.S. Patent 3,666,656: Method for Inhibiting Fouling in a Refinery Process.

52. U.S. Patent 3,533,763: Process for Drying, Clarifying, and Stabilizing Hydrocarbon Liquids.

53. U.S. Patent 3,509,040: Process for Producing Jet Fuel.

54. Johnston, R. K. and E. L. Anderson: Review of Literature on Storage and Thermal Stability of Jet Fuels. Southwest Research Institute, RTD-TDR-63-4270. January, 1964.

55. Astaf'ev, V. A., V. D. Borisov, V. P. Logvinyuk, V. V. Malyshev, and A. A. Popov: Influence of Dissolved-Oxygen Concentration on Thermal-Oxidative Stability of Jet Fuels. Chem. and Technol. Fuels and Oils. Vol. 11, No. 7-8, p. 552 (Russian Transl.). July, 1975.

56. Kislitsyna, N. I., T. P. Vishnyakova, I. A. Golubeva, I. V. Rozhkov, B. A. Englin, I. F. Krylov, V. V. Sashevskii, V. V. Sher, and I. V. Shkhiyants: Effect of Metal Dialkyldithiocarbamates on the Oxidative Thermal Stability of Jet Fuels. Neftekhimiya, Issue 5, p. 777-82. 1975.

57. Tumar, N. V., O. P. Lykov, T. P. Vishnyakova, I. V. Derechinskaya, I. A. Golubeva: Increasing the Chemical Stability of Jet Fuels with the Use of Antioxidant Additives. Khim. Tekhnol. Topl. Masel, Issue 1, p. 13-16, 1976.

58. Bol'shakov, G. F., E. A. Glebovskaya, Z. G. Kaplan: Structure of Deposits Formed in Jet Fuels Studied by Spectral Analysis. Prikl. Spektrosk., Mater. Soveshch., 16th, Series 2, p. 55-60, 1969.

59. Chertkov, Ya. B., E. P. Seregin, T. I. Kirsanova, A. N. Romanov, T. A. Lifanova, G. B. Skovorodin: Relation of the Performance Characteristics of Jet Fuels to the Group Composition of Sulfur Compounds Contained in Them. Khim. Tekhnol. Topl. Masel, Issue 1, p. 49-52, 1976.

60. Astaf'ev, V. A., V. D. Borisov, V. P. Logvinyuk, V. V. Malyshev, A. A. Popov: Effect of the Concentration of Dissolved Oxygen on the Thermo-oxidative Stability of Jet Fuels. Khim. Tekhnol. Topl. Masel, Issue 7, p. 41-2, 1975.

61. Papok, K. K., V. A. Piskunov, P. G. Yurenya: New Approach to Evaluation of Carbon-Deposit Properties of Fuels. Ekspluat. Svoistva Aviats. Topl. Issue 2, p. 53-7, 1972.

62. Burtyshev, N. Ya. I. A. Aizen, N. D. Ryabova: Spectral Analysis of Deposits from Jet Fuels. Deposited Doc., Issue VINITI 1301-75, 11 pp., 1975.

63. Nagypataki, Gyula: Influence of Sulfur Compounds on the Thermal Stability of Jet Fuels. Banyasz. Kohasz. Lapok, Koolaj Foldgaz, Issue 2, p. 48-51, 1971.

64. Sablina, Z. A., A. A. Gureev, A. A. Kukushkin, N. I. Melent'eva, B. A. Englin, A. M. Fomina, A. Gryaznov: Changes in the High-Temperature Properties of Jet Fuels During Prolonged Storage. Khim. Tekhnol. Topl. Masel. Issue 12, p. 39-42, 1970.

65. Mardanov, M. A., S. M. Markhaseva, S. A. Samedova: Improving Fuel Thermal Stability With Complex Compounds. Ekspluat. Svoistva Aviats. Topl., Issue 2, p. 116-20, 1972.

66. Makhlitt, R., A. G. Sardanashvili: Increase in the Stability of Jet Fuel by a Continuous Adsorption Method. Khim. Tekhnol. Topl. Masel, Issue 5, p. 15-17, 1974.

67. Astaf'ev, V. A., V. D. Borisov, T. P. Vishnyakova, I. A. Golubeva, N. I. Kislitsyna, I. F. Krylov, V. V. Malyshev, G. M. Fukson: Mechanism of the Action of Additives Improving the Oxidative Thermal Stability of Jet Fuels. Khim. Tekhnol. Topl. Masel, Issue 8, p. 23-6, 1974.

68. Vishnyakova, T. P., I. A. Golubeva, N. Kislitsyna: Effect of Pehnols on the Thermal Stability of Jet Fuels. Neftepererab. Neftekhim. (Moscow). Issue 9, p. 1-3, 1974.

69. Stone, J. R., V. H. Gray, and O. A. Gutierrez: Forced-Flow Once-Through Boilers. NASA SP-369. 1975.

70. Poppendiek, H. F. and C. M. Sabin: Technology of Forced-Flow and Once-Through Boiling, A Survey. NASA SP-5102. 1975.

71. Hsu, Y. Y., and R. W. Graham: Transport Processes in Boiling and Two-Phase Systems. Hemisphere Publishing Corp. 1976.

72. Collier, J. G.: Convective Boiling and Condensation. McGraw Hill. 1972.

73. Tong, L. S.: Boiling Heat Transfer and Two-Phase Flow. Robert E. Kreiger Publ. Co. 1975.

74. Hsu, Y. Y. and R. W. Graham: Transport Processes in Boiling and Two-Phase Systems. Hemisphere Publishing Corp. 1976.

75. Owhedi, A.: Boiling in Self Induced Radial Acceleration Fields. Ph. D. Thesis. Oklahoma State Univ. 1966.

76. Marto, P. J. and V. H. Gray: Effects of High Accelerations and Heat Fluxes on Nucleate Boiling of Water in an Axisymmetric Rotating Boiler. NASA TN D-6307. 1971.

77. Lawler, M. T. and S. Ostrach: A Study of Cyclonic Two-Fluid Separation. Case Inst. Tech. FTAR-TR-65-2. AD621524. June, 1965.

78. Baker, O.: Simultaneous Flow of Oil and Gas. Oil Gas J. 53, p. 185. 1954.

79. Quandt, E.: Analysis of Gas-Liquid Flow Patterns. AICHE. Preprint 47. 6th National Heat Transfer Conference. 1963.

80. Hsu, Y. Y.: Boiling Heat Transfer Equations. Published in Two-Phase Flows in Nuclear Reactors. Von Karman Institute for Fluid Dynamics. Lecture Series 1978-5, Vol. 1. Rhode Saint Genese, Belgium. April, 1978.

81. Chen, J.: Correlation for Boiling Heat Transfer to Saturated Fluids in Convective Flow. I&EC Process Des. and Dev., Vol. 5, pp. 322-329. July, 1966.

82. Dengler, C. E. and J. N. Addoms: Heat Transfer Mechanism for Vaporization of Water in a Vertical Tube. Chem. Eng. Progress Symp. Series . Vol. 52 (18), p. 95. 1956.

83. Bennett, J. A. R., J. G. Collier, H. R. C. Pratt and J. D. Thornton: Heat Transfer to Two-Phase Gas-Liquid Systems. Trans. Inst. Chem. Engrs. 39, 113. 1961.

84. Schrock, V. E. and L. M. Grossman: Forced Convection Boiling in Tubes. Nuclear Science and Engineering 12, p. 474. 1962.

85. Bergles, A. E.: Future Directions of Research in Multi-Phase Flow and Heat Transfer. 2nd Multi-Phase Flow and Heat Transfer Symposium-Workshop. U. of Miami. April, 1979.

86. Stone, J. R. and T. M. Damman: An Experimental Investigation of Pressure Drop and Heat Transfer for Water Boiling in a Vertical-Upflow Single-Tube Heat Exchanger. NASA TN D-4057, July, 1967.

87. Martinelli, R. C. and D. B. Nelson: Prediction of Pressure Drop During Forced Circulation Boiling of Water. Trans. ASME, p. 695. August, 1948.

88. Lockhart, R. W. and R. C. Martinelli: Proposed Correlation of Data for Isothermal Two-Phase, Two-Component Flow in Pipes. Chem. Eng. Progress Vol. 45, No. 1, p. 39. January, 1949.

89. Levy, S.: Steam Slip-Theoretical Prediction from Momentum Model. Trans. ASME J. of Heat Transfer 83, p. 113. 1960.

90. Zuber, N. and J. A. Findlay: Average Volumetric Concentrations in Two-Phase Flow Systems. ASME Journal of Heat Transfer, p. 453. November, 1965.

91. Thom, J. R. S.: Prediction of Pressure Drop During Forced Circulation Boiling of Water. Int. Journal Heat and Mass Transfer. Vol. 7, p. 709. July, 1964.

92. Zivi, S. M.: Estimation of Steady State Void Fraction by Means of the Principle of Minimum Energy Production. ASME Trans., Vol. 86C, p. 247. 1964.

93. Marchaterre, J. F. and B. M. Hoglund: Correlation for Two-Phase Flow. Nucleonics 20, No. 8. 1962.

94. Husain, A., and J. Weisman: Two Phase Pressure Drop Across Abrupt Area Changes. US AEC Report COO-2152-15. January, 1975.

95. Janssen, E.: Two-Phase Pressure Loss Across Abrupt Contractions and Expansions, Steam-Water at 600 to 1400 PSIA. Third International Heat Transfer Conference. Vol. V, p. 13. August, 1966.

96. Lottes, P. A.: Expansion Losses in Two-Phase Flow. Nuclear Science and Engineering, 9, p. 26. 1961.

97. Adadev, I. T., S. V. Teplov and I. M. Pchelkin: Two-Phase Flows and Problems of Heat Exchange. FTD-MT-1023-71, AD-742697. February, 1972.

98. Kunz, H. R.: Experimental Investigation of Heat Rejection Problems in Nuclear Space Powerplants. Vol. 1. Manifold Pressure Loss and Flow Distribution. Pratt & Whitney Aircraft PWA-2227. 1963.

99. Gouse, S. A.: Two-Phase Gas-Liquid Flow Oscillations: Preliminary Survey. MIT DSR8734-5. July, 1964.

100. Stenning, A. H. and T. N. Veziroglu: Flow Oscillation Modes in Forced-Convection Boiling. Proceedings of 1965 Heat Transfer and Fluid Mechanics Institute. Stanford U. Press. June, 1965.

101. Bouré, J. A.: Oscillatory Two Phase Flows. Published in Two-Phase Flows With Application to Nuclear Reactor Design Problems. Von Karman Institute for Fluid Dynamics. Lecture Series 71. Rhode Saint Genese, Belgium. December, 1974.

102. Yadigaroglu, G.: Two-Phase Flow Instabilities and Propagation Phenomena. Published in Two-Phase Flows in Nuclear Reactors. Von Karman Institute for Fluid Dynamics. Lecture Series 1978-5. Vol. 2. Rhode Saint Genese, Belgium. April, 1978.

103. Van der Walle, F., C. L. Spigt, H. J. Lamein, and M. Bogaerdt: A Theoretical Study on Two-Phase Flow Characteristics. Proceedings of Symposium on Two-Phase Flows. Univ. Exeter, Devon, England. June, 1965.

104. Rudinger, G. and A. Chang: Analysis of Nonsteady Two-Phase Flow. Project Squid. Technical Report CAL-88-P. June, 1964.

105. Stenning, A. H. and T. N. Veziroglu: Semi-Annual Status Report on Boiling Flow Instability. U. of Miami N65-31037. May, 1965.

106. Hess, H. L., J. R. Hooper, and S. L. Organ: Analytical and Experimental Study of the Dynamics of A Single-Tube Counterflow Boiler. NASA CR-1230. February, 1969.

107. Meyer, J. E. and J. P. Rose: Application of Momentum Integral Model to the Study of Parallel Channel Boiling Flow Oscillations. Trans. ASME J. Heat Transfer 85, p. 1. 1963.

108. Berenson, P. J.: An Experimental Investigation of Flow Stability in Multitube Forced-Convection Vaporizers. ASME 65-HT-61. 1965.

109. Flow Stability in Multitube Forced-Convection Vaporizers. APL TDR64-117. October, 1964.

110. Gouse, S. A., R. G. Evans, C. W. Deane and J. C. Crowley: Two-Phase Gas-Liquid Dynamics: Part 1--Flow Oscillations in Transparent, Parallel, Vertical, Heated Channels. MIT DSR74629-1. November, 1967.

111. Possa, G. and J. B. van Erp: Measurement and Analysis of Two-Phase Flow Dynamics. Proceedings of Symposium on Two-Phase Flow. Univ. Exeter, Devon, England. June, 1965.

112. Bergles, A. E.: Review of Instabilities in Two-Phase Systems. Published in Two-Phase Flows and Heat Transfer. Vol. 1. Hemisphere Publishing Co., Washington. 1977.

113. Kays, W. M. and A. L. London: Compact Heat Exchangers. McGraw Hill. 1964.

114. The Design and Performance of Compact Heat Exchangers. Vol. I-III, Northern Research and Engineering Corp., Cambridge, Mass. 1965.

115. Fraas, A. P. and M. N. Ozisik: Heat Exchanger Design. John Wiley. 1965.

116. Afgan, N. H. and E. U. Schlunder: Heat Exchangers: Design and Theory Source book. McGraw Hill. 1974.

117. Kraus, A. D.: Extended Surfaces. Sparton Books, Inc. 1964.

118. Welty, J. R.: Engineering Heat Transfer. John Wiley. 1974.

119. Schank, I. A.: Industrial Heat Transfer. John Wiley. 1965.

120. Kern, D. Q.: Process Heat Transfer. McGraw Hill. 1950.

121. Standards of Tubular Exchanger Manufacturers Assoc. Tubular Exchangers Manufacturers Assoc., Inc. 1959.

122. Saboya, F. E. M. and E. M. Sparrow: Experiments on a Three Row Fin and Tube Heat Exchanger. ASME Trans. J. Heat Transfer, p. 520. August, 1976.

123. Chato, J. C., R. J. Laverman, and J. M. Shah: Analyses of Parallel Flow, Multi-Stream Heat Exchangers. Int. J. Heat Mass Transfer. Vol. 14, p. 1691. 1971.

124. LaHaye, P. G., F. J. Neugebauer, R. K. Sakhiya: A Generalized Prediction of Heat Transfer Surfaces. ASME Trans. J. of Heat Transfer. Vol. 96, p. 511. November, 1974.

125. Emerson, W. H.: Shell-Side Pressure Drop and Heat Transfer with Turbulent Flow in Segmentally Baffled Shell-and-Tube Heat Exchangers. Inst. J. Heat and Mass Transfer. Vol. 6, p. 649. 1963.

126. Tinker, T.: Shell-Side Characteristics of Shell and Tube Heat Exchangers. Trans. ASME, p. 36. January, 1958.

127. Whitely, D. L.: Calculating Heat Exchanger Shell Side Pressure Drop. Chem. Eng. Progress, Vol. 57, No. 9, p. 57. September, 1961.

128. Bell, K. J.: Exchanger Design Based on the Delaware Research Program. Petroleum Engr. 32(11), C26-36, C40a-40c. 1960.

129. Grant, I. D. R. and D. Chisholm: Two-Phase Flow on the Shell-Side of a Segmentally Baffled Shell-and-Tube Heat Exchanger. ASME Trans. J. Heat Transfer, p. 38. February, 1979.

130. Chiou, J. P.: The Effect of Longitudinal Heat Conduction on Crossflow Heat Exchanger. ASME Trans. J. Heat Transfer, p. 347. May, 1978.

131. Chiou, J. P.: Thermal Performance Deterioration in Crossflow Heat Exchanger Due to Flow Nonuniformity. ASME Trans. J. of Heat Transfer, p. 581. November, 1978.

132. Kern, D. Q.: Heat Exchanger Design for Fouling Services. Third International Heat Transfer Conference. Vol. 1, p. 170. August, 1966.

133. Watkinson, A. P. and N. Epstein: Gas Oil Fouling is a Sensible Heat Exchanger. Chem. Eng. Prog. Symp. Series, Vol. 65, No. 92, p. 84. 1969.

134. Watkinson, A. P. and N. Epstein: Particulate Fouling of Sensible Heat Exchangers. Fourth International Heat Transfer Conference, HE 1.6. 1970.

135. Neal, S. B. H. C. and J. A. Hitchcock: A Study of the Heat Transfer Process in Banks of Finned Tubes in Cross Flow, Using a Large Scale Model Technique. Third International Heat Transfer Conference. Vol. III, p. 291. August, 1966.

136. Groehn, H. G. and F. Scholz: Heat Transfer and Pressure Drop of In-Line Banks of Tubes with Artificial Roughness. Heat and Mass Transfer Sourcebook, p. 21, Scripta Publishing Co. 1977.

137. Preece, R. J., J. Lis, and J. A. Hitchcock: Effect of Gas-Side Physical-Property Variations on the Heat Transfer to a Bank of Tubes in Cross-Flow. Proc. Inst. Mech. Eng., Vol. 189, p. 69. November, 1975.

138. Glickstein, M. R. and R. H. Whitesides: Forced-Convection Nucleate and Film Boiling of Several Aliphatic Hydrocarbons. ASME 67-HT-7. 1967.

139. Segalman, I., P. Goldberg, and J. J. Nolan: Hydrocarbon Fueled Scramjet. Vol. V - Cooling Investigations. AFAPL-TR-68-146. June, 1969.

140. Hendricks, R. C., R. J. Simoneau, and R. V. Smith: Survey of Heat Transfer to Near-Critical Fluids. NASA TN D-5886. November, 1970.

141. Eckert, E. R. G.: Heat Transfer Review. Industrial and Engineering Chemistry. V. 46, p. 932. 1954.

142. Eckert, E. R. G., V. P. Hartnett, T. F. Irvine, Jr., and E. M. Sparrow: Heat Transfer Review. Industrial and Engineering Chemistry, Vol. 52, p. 327. 1960.

143. Eckert, E. R. G., T. F. Irvine, Jr., E. M. Sparrow, and W. E. Ibele: Heat Transfer Review. Mechanical Engineering. Vol. 83, No. 7, p. 34 and No. 8, p. 50. 1961.

144. Eckert, E. R. G., E. M. Sparrow, R. J. Goldstein, C. F. Scott, E. Pfender, S. V. Patankar, and J. W. Ramsey. Int. J. Heat Mass Transfer, Vol. 21, No. 10. October, 1978.

145. Luikow, A. V.: Heat and Mass Transfer Bibliography - Soviet Works. Int. J. Heat Mass Transfer, Vol. 18, p. 981. 1975.

146. Soloukhin, R. I. and O. G. Martinenko: Heat and Mass Transfer Bibliography-Soviet Works. Int. J. Heat Mass Transfer, Vol. 22, p. 157. February, 1979.

147. Sato, T.: Heat Transfer Bibliography, Japanese Works. Int. J. Heat Mass Transfer, Vol. 15, p. 2633. 1972.

148. Mori, Y.: Heat Transfer Bibliography - Japanese Works. Int. J. Heat Mass Transfer, Vol. 22, p. 151. January, 1979.

149. London, A. L.: Final Report, Stanford University-Office of Naval Research on Compact Heat Exchangers and Thermodynamic Investigations. Technical Report No. 76. November, 1971.

150. Houseman, J. and D. J. Cerini: On-Board Hydrogen Generator for a Partial Hydrogen Injection Internal Combustion Engine. SAE Paper 740600. August, 1974.

151. Voecks, G. E. and D. J. Cerini: Application of Rich Catalytic Combustion to Aircraft Engines. Presented at Third Catalytic Combustion Workshop. October 4, 1978.

152. Henzel, H. J., H. Kostka, and A. Michel: Autothermal Gasification of Liquid Hydrocarbons by Partial Oxidation. Paper presented at ERDA meeting on Fuel Processing for Fuel Cell Power Generation. April 13, 1977.

153. U.S. Patent 4,018,573: Reactor for the Catalytic Conversion of Hydrocarbons with a Gas Containing Oxygen to Form a Fuel Gas.

154. U.S. Patent 3, 897,225: Method and Apparatus for Generating a Gas Mixture to be Formed Through Catalytic Conversion of Fuel and Gas Serving as an Oxygen Carrier.

155. Caldwell, D., F. Elefers, and M. Frankhenel: The Vaporized Fuel Oil System. Chem. Eng. Prog., p. 66. November 1978.

APPENDIX B

ANALYTICAL PROCEDURES

All three of the external fuel vaporization schemes required the design of heat exchangers and one of the schemes required the design of a droplet vaporization device. The analyses were performed using the three computer codes listed below:

1. A steady-state heat exchanger program;
2. A transient response code based on (1);
3. A spray vaporization program.

The first two programs were applied to the heat exchangers employed in Schemes 1, 2, and 3. The spray vaporization analysis was used only for Scheme 3.

Steady-State Heat Exchanger Deck

The steady-state heat exchanger deck provides a means to calculate the fluid and wall temperatures, deposit formation, and pressure loss at various points in the heat exchanger. The analysis is used for heat exchangers in which one fluid behaves as a perfect gas while the other is assumed to be a distillate fuel. However, the procedure is capable of treating wide variations in heat exchanger geometry.

Methods of Solution

The geometry of each heat exchanger being analyzed consists of a macrostructure and microstructure. For describing the macrostructure, the device is divided into nodes of equal size as shown in Fig. B-1. The number of nodes in each direction is selected by the user on the basis of the expected thermal gradients from node to node. Within each node, conditions are assumed to vary slowly. The nodes are connected for each side (air or fuel) of the heat exchanger in one or more paths. (Two parallel air paths and one fuel path are indicated in Fig. B-1.) To describe the microstructure of the design, each node is treated as a miniature heat exchanger consisting of a tube bundle with external (air side) fins. Plain tubes can be simulated by setting an input value of fin area/total area to zero. The fuel may make multiple passes through the tube bundles. The overall heat transfer coefficients for both the air and fuel within the node are calculated from input tables and correlations. This microstructure defines for each node an equivalent single tube heat exchanger having

equivalent heat transfer coefficients for both the air and fuel sides. Using the concept of hydraulic diameter, the combustor wall utilized in Scheme 2 is thus seen as a limiting case to the microstructure concept.

The temperature distribution in both the air, fuel and tube walls of the heat exchanger is calculated using a relaxation approach. The average temperature for each fluid and the walls in each node estimated during the previous iteration is used to calculate the thermal properties of the fluids and wall, the amount of deposit, and the heat transfer coefficients of each fluid. These parameters are combined to yield an effective heat transfer coefficient h_{eff} (see below). Since for a finned tube bundle, the areas available for heat transfer on the air and fuel sides are not equal, this effective heat transfer coefficient is arbitrarily referenced to the air side. With subscripts A and F denoting the air and fuel sides respectively, then the steady-state heat transfer rate in the Kth node is:

$$\dot{Q}_K = h_{eff_K} \; A_{A_K} \left(\bar{T}_{A_K} - \bar{T}_{F_K} \right) \tag{1}$$

The average fluid temperatures are functions of the heat transfer rate between fluids. For example, the average air temperature is:

$$\bar{T}_{A_K} = 1/2 \left(T_{A_{IN_K}} - T_{A_{OUT_K}} \right) \tag{2}$$

and

$$T_{A_{OUT_K}} = T_{A_{IN_K}} + \frac{\dot{Q}_K}{\left(\dot{m}_A \, Cp_A \right)_K} \tag{3}$$

Necessarily, the inlet temperature for this node is the outlet temperature of the previous node (or the air supply temperature if this is the initial node) for the air path containing this node. Similarly for the fuel side,

$$\bar{T}_{F_K} = 1/2 \left(T_{F_{IN_K}} - T_{F_{OUT_K}} \right) \tag{4}$$

and

$$T_{F_{OUT_K}} = T_{F_{IN_K}} + \frac{\dot{Q}_K}{\left(\dot{m}_F \, Cp_F \right)_K} \tag{5}$$

It should be noted that the air in the air path containing the Kth node is generally not flowing parallel to the fuel in the fuel path containing the Kth node. In addition, thermal properties may be strong functions of temperature

especially if a deposit is formed or if the fuel partially or completely vaporizes (see next section).

At the beginning of each iteration, the outlet temperature for the last node in each path on each side of the heat exchanger are compared with those calculated during the previous iteration. If all outlet temperatures are within a specified tolerance (typically 10 F), the iteration is terminated. Otherwise the new average fluid temperatures together with the new wall temperatures are used as the basis of the next iteration.

In addition to calculating the fluid and wall temperature distributions, the program determines the amount of deposit formation and fuel vaporization as well as the pressure loss in each fluid path.

Effective Heat-Transfer Coefficient

The effective heat transfer coefficient (h_{eff}) consists of the thermal resistances of the air and fuel thermal boundary layers, the metal wall, and the deposit layer. Using the finned area on the air side as the reference area (and omitting the subscript K for convenience), then the effective heat transfer coefficient for the Kth node is:

$$h_{eff} = \left[\underset{\text{AIR}}{\frac{1}{\eta_o h_A}} + \underset{\text{WALL}}{\frac{t_W}{K_W\left(A_{W_{OD}}/A_A\right)}} + \underset{\text{DEPOSIT}}{\frac{t_C}{K_C\left(A_{W_{ID}}/A_A\right)}} + \underset{\text{FUEL}}{\frac{1}{h_F\left(A_{W_{ID}}/A_A\right)}} \right]^{-1} \qquad (6)$$

Four thermal resistances must be evaluated.

Air

For the air side of heat exchangers, tables have been prepared giving heat transfer coefficient correlations in terms of the Stanton, Prandtl and Reynolds numbers from which h_A is calculated as described in the previous section. The fin effectiveness (η_o) and the heat transfer area (A_A) are evaluated from geometric factors and the methodology found in Ref. 1.* For the special case of combustor walls, h_A is determined from a two-dimensional boundary layer analysis.

Wall

The wall thermal conductivity and thickness are evaluated from the inputs to the program. The wall area is the outer surface area of the tube bank.

---

* References for Appendix B begin on page B-11.

Deposit Layer

The deposit thermal conductivity is input to the program. The deposit thickness is evaluated from a correlation of deposit thickness and wall (metal) temperature. The heat transfer area is the inside (clean) surface area of the tube bank.

Fuel

The fuel side heat transfer area, $A'_{W_{ID}}$, is the inside area of the tube bank corrected for coke formation; i.e., the coke layer represents a reduction in tube hydraulic diameter. The fuel heat transfer coefficient is evaluated by one of several means depending upon the fuel quality and boundary layer state.

Tables of thermal properties as a function of fuel pressure, temperature and quality have been prepared for Jet-A from the curves described previously. If the fuel pressure exceeds the fuel critical pressure or if the current value of $\overline{T}_F$ is less than the fuel saturation temperature, then the fuel is a liquid and h_B is evaluated from Equation 2 or 3 of the main body of the report; the particular equation used will depend upon whether the pressure exceeds the critical pressure. If the fuel is a vapor (the fuel quality is unity), the heat transfer coefficient is evaluated from a table derived from data in Ref. 1.

If the fuel is a mixture of liquid and vapor, then it is assumed that h_B is essentially infinite, an assumption often made in boiling heat transfer problems and verified at typical heat exchanger conditions. There exists in the code an alternative procedure to calculate a weighted average of the contributions to h_B from the liquid and vapor portions of the mixture as discussed in the previous section; however, no essential differences in heat exchanger performance were produced using this procedure in comparison with the assumption that the fuel heat transfer coefficient for the mixture is infinite.

Transient-Response Deck

The previous discussion was concerned with the determination of heat exchanger performance for steady-state engine operating conditions. Changes in steady-state engine operating conditions require a finite amount of time to accomplish. Two factors are responsible for this time lag. First, inertial effects impose a lag. For example, during engine acceleration the torque imparted to the turbine by the hot gas stream is finite, and the change in rotational speed of the engine is not instantaneous. Second, constraints may be imposed on the engine fuel control to prevent the occurrence of certain adverse behavior. For example, during acceleration, the rate of increase of fuel flow must not be so large as to cause compressor stall.

With a fuel system incorporating the heat exchangers discussed in this report, an additional time lag may be introduced. For example, a finite amount of time is required for the heat transfer surfaces of the heat exchanger to adjust to each change in engine operating conditions during the transient. Since some fuel is always within the heat exchanger, the temperature of fuel and possibly the vapor quality delivered to the engine will vary from the desired conditions which will, in turn, affect the engine transient. Necessarily, this additional time lag must be sufficiently short.

The rigorous way to estimate the effect of the heat exchanger system on engine transient response is to incorporate models for the proposed fuel system schemes into an engine response analysis. This was not feasible under the scope and schedule of the present study. Instead, an alternative approach was used which was accomplished by an adaptation of the steady-state heat exchanger computer program. Snap acceleration and snap deceleration curves describing fuel flow and airflow in a typical advanced Pratt & Whitney Aircraft engine configuration were obtained and these were non-dimensionalized to simulate the E^3 engine. Discrete points during each transient were then selected. These points constituted a set of desired steady-state operating points during the transient. It was postulated that, for each time increment during the transient, additional time would be required for the heat exchanger to reach the new steady-state condition; that is, it was assumed that the engine could not reach the new operating point until the heat exchanger reached its new steady-state condition. The sum of all time lags due to the transient of the heat exchanger was called response time lag. This is a conservative view since the engine may be able to operate quite satisfactorily even if the heat exchanger has not reached its new steady-state condition.

The adaptation of the steady-state heat exchanger code to the transient response problem was based on the following analysis. It was assumed that the engine transient is divided into a sufficient number of time increments such that within each time increment conditions change in a step-wise manner. The Kth element in the heat exchanger at time t has an average wall temperature $\overline{T}_{W_K}(t_1)$. During the transient from time t_1 to the time t_2, the engine air flow and fuel flow are assumed to change instantaneously. Initially, the wall temperature remains at $T_{W_K}(t_1)$ but since the fluid conditions on either side of the wall have changed to the time t_2 conditions, there is a heat transfer imbalance, $\dot{Q}_{net_K}$, which will tend to change the wall temperature. Thus, at t_1

$$\dot{Q}_{NET_K}(t_1) = h_{A_K} A_{A_K}\left[T_{A_K}(t_2) - \overline{T}_{W_K}(t_1)\right] - h_{F_K} A_{F_K}\left[\overline{T}_{W_K}(t_1) - T_{F_K}(t_2)\right] \qquad (7)$$

Equation (7) is not exact since the average wall temperature is used whereas a wall temperature gradient exists. However, since the transient analysis used herein is only a first approximation to the more rigorous approach of integrating an engine response deck with the heat exchanger deck this simplification appears to be justified. At time t_2, the heat exchanger is assumed to be operating in the steady state so that:

$$\dot{Q}_{NET_K} \ (t_2) = 0 \tag{8}$$

Therefore, the average net heat transfer available for wall heating during the interval t_1 to t_2 is:

$$\overline{\dot{Q}_{NET_K}} = 1/2 \ \dot{Q}_{NET_K} (t_1) \tag{9}$$

For the heat exchanger as a whole, the total net heat transfer rate is:

$$\dot{Q}_{NET} = \sum_K \ \overline{\dot{Q}_{NET_K}} \tag{10}$$

The amount of heat absorbed by the walls of the Kth node in adjusting the wall temperature from the steady-state value at t_1 to the steady-state value at t_2 is:

$$q_{ABS_K} = m_K \ Cp_K \left[\overline{T}_{W_K} (t_2) - \overline{T}_{W_K} (t_1) \right] \tag{11}$$

For all nodes of the exchanger,

$$q_{ABS} = \sum_K \ q_{ABS_K} \tag{12}$$

Letting τ be the time lag in adjusting the heat exchanger steady-state from conditions at t_1 to conditions at t_2,

$$\tau_i \ \dot{Q}_{NET} = q_{ABS} \tag{13}$$

For the entire transient, therefore, the total time lag imposed by the heat exchanger system is $\Sigma \tau_i$.

Spray Vaporization Deck

To estimate the performance of the fuel evaporator designs considered in the Scheme 3 system in which the fuel spray and hot gas are in intimite contact with each other, the Spray Vaporization computer program was utilized. The details of the model used in the earliest version of this code have been reported previously (Ref. 2). In its application to the present problem, the current version of the code is not materially different from that earlier formulation. In the next subsection, a brief summary of the analysis is given. This is followed by a subsection describing the application of the model to the evaluation of the fuel evaporator.

Features of the Model

The model is applicable to both axisymmetric and two-dimensional (rectangular) flows in which the radial components of droplet velocity have become negligible. The flow field is divided into a number of streamtubes (the precise number is dependent upon the arbitrarily-chosen initial gas-phase and liquid-phase profiles). Within each streamtube, both the gas and liquid are treated in a one-dimensional manner. Mixing occurs among the streamtubes for both phases due to the turbulent exchange of mass, momentum and energy. The equations of motion include source (or sink) terms that provide for the mutual interaction of the phases. For example, the gas temperature will decrease as energy is extracted by the liquid phase for droplet heating and vaporization and vapor superheating; and, the vaporization rate will decrease as the vapor concentration in the gas phase increases. The effects of swirl and radial pressure gradients are neglected in the model but the effects of axial pressure gradients or changes in total cross sectional flow area are included.

If axial pressure gradients are ignored, then it is possible to write most of the equations of motion used in the analysis in the form:

$$\frac{d}{d_x}(\dot{m}\psi) = \dot{m}'(\psi' - \psi) + \dot{m}''(\psi'' - \psi) + S_\psi \qquad (14)$$

For the gas phase, the parameter ψ represents velocity, enthalpy, and specie mass fractions while $\dot{m}$ is the local gas phase flow rate. The quantities $\dot{m}'$ and $\dot{m}''$ are the mass exchange rates between this streamtube and the two adjacent streamtubes; these rates are evaluated from the velocity gradient and eddy viscosity. For the liquid phase, ψ represents either the droplet velocity or enthalpy and $\dot{m}$ is the local liquid phase flow rate. The exchange rates for

the liquid are assumed to be proportional to the gas phase rates and the droplet number density. For either phase, S_ψ is the source (or sink) of ψ.

The equations of motion are solved using a simple forward marching procedure. The integration step-size (Δx) is chosen to assure overall conservation of mass, momentum and energy. The computer program includes conservation checks (and other tests) to determine whether the step-size can be increased as the solution marches downstream.

The source terms, S_ψ, represent the effects of droplet vaporization, heating, and drag. The equations for droplet heat and mass transfer are essentially those developed for single droplets (Ref. 3); however, the droplet mass transfer equation has been modified to include the effect of the gas phase vapor concentration on the vaporization rate. The vaporization rate and the heat transfer rate require specification of a mass transfer coefficient and a heat transfer coefficient, respectively. These are evaluated from correlations developed by Ranz and Marshall (Ref. 4). The drag on the droplets is estimated using drag coefficient correlations developed by Dickerson and Schuman (Ref. 5).

Throughout a typical computation, the thermal properties of both phases vary. The properties of the gas phase (such as its thermal conductivity, molecular viscosity, and heat capacity) are functions of both temperature and specie concentration; typically, a mixture of air and fuel vapor are considered. These properties are evaluated for both the bulk gas and the film surrounding each droplet in a manner similar to the recommendation of El Wakil, et. al (Ref. 6). The liquid thermal properties are evaluated as a function of the liquid temperature. For certain liquids representing a mixture of physically similar components, a somewhat more elaborate procedure exists for calculating the vapor pressure. For example, certain distillate fuel oils whose distillation curves are known with some precision may be treated in this manner.

Evaluation of Fuel Vaporizers

In evaluating the fuel vaporizers considered for Scheme 3, a number of simplifying assumptions were made. These assumptions are justifiable since the results are adequate enough for comparing alternative designs, and, in any case, component performance is only one factor in determining the best system.

It was assumed that the flow of both the gas and liquid phases were one-dimensional and that the axial pressure gradient was negligible. (Independent calculations indicated that the pressure gradient in the evaporator is small.) Fuel properties were obtained from the literature for Jet-A. The fuel vapor pressure was assumed to be a function of liquid fuel temperature only using initial boiling point data obtained at various pressures. The use of the

more elaborate vapor pressure model described above did not seem warranted due to the large variation in reported distillation data for Jet A.

Several calculations were made with the computer program. These calculations covered a range of hot gas temperature and velocity, evaporator diameter, and fuel-air ratio. Three outputs of the analysis were of primary concern. The first parameter was the length required to achieve complete vaporization. The second was the mixed flow exit gas temperature decrement from the initial gas temperature. Finally, the residence time within the evaporator was of interest since this must be short in comparison to the autoignition time for the mixture.

LIST OF SYMBOLS

A	Area
Cp	Heat capacity
h	Heat transfer coefficient
K	Thermal conductivity
m	Mass
Q,q	Heat transfer
S	Source (sink)
t	Thickness
T	Temperature
X	Axial position
η	Effectiveness
τ	Time
ψ	Conserved quantity

Subscripts

A	Air
ABS	Absorbed
c	Coke
eff	Effective (overall) value
F	Fuel
ID	Inside diameter
IN	Quantity flowing into element
K	Index
NET	Net amount
OD	Outside diameter
OUT	Quantity flowing out of element
w	Wall
1,2	Successive time steps
$\bar{(\ )}$	Average
$\dot{(\ )}$	Time rate of change
( )', ( )"	Adjacent streamtube values

REFERENCES

1. Kays, W. M. and A. L. London: Compact Heat Exchangers. McGraw-Hill Book Co. Inc. 1958.

2. Chinitz, W.: A Theoretical Model of the Spray Vaporization Process. United Technology Research Center Report R76-110750-1, February, 1976.

3. Preim, R. J. and M. F. Heidmann: Propellant Vaporization as a Design Criterion for Rocket-Engine Combustion Chambers, NASA TR R-67 (1960).

4. Ranz, W. E. and W. R. Marshall, Jr.: Evaporation from Drops, Part I., Eng. Prog. Vol. 8, No. 3, March 1952, pp. 141-146.

5. Dickerson, R. A. and M. D. Schuman: Rate of Aerodynamic Atomization of Droplets, J. Spacecraft and Rockets, Vol. 2, No. 1, Jan-Feb, 1965, pp. 99-100.

6. El Wakie, M. M., O. A. Uyehara, and P. S. Myers: A Theoretical Investigation of the Heating-Up Period of Injected Fuel Droplets Vaporizing in Air, NACA TN 3179, Appendix B, May 1954.

FIG. B-1

EXAMPLE OF MACROSTRUCTURE FOR HEAT EXCHANGER COMPUTER PROGRAM

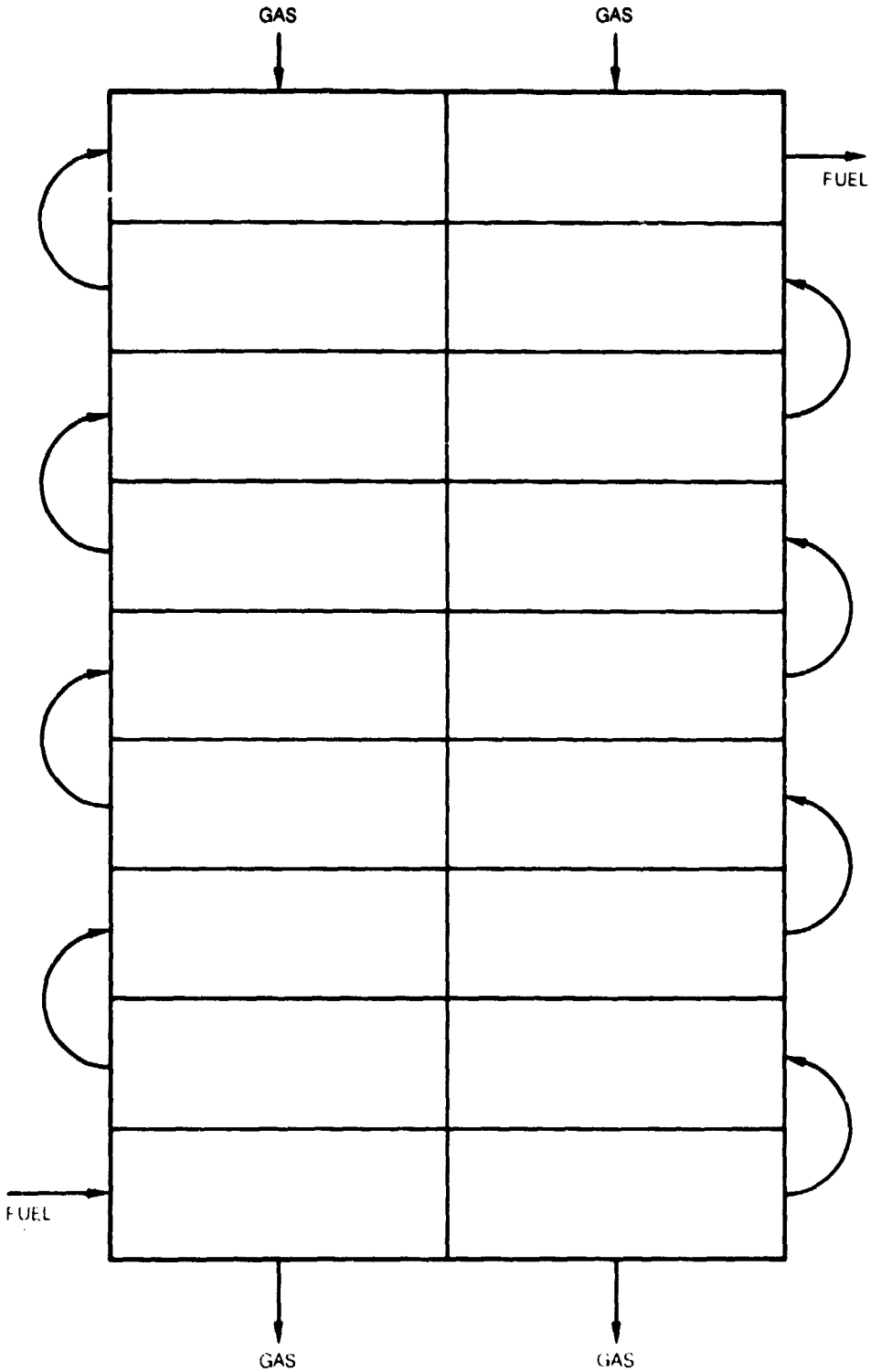

80-2-71-1